Feedback Control of Instabilities in Hydrodynamic Systems

FEEDBACK CONTROL OF INSTABILITIES IN HYDRODYNAMIC SYSTEMS

By

MD. SHAH NOOR

A THESIS
SUBMITTED IN PARTIAL FULFILLMENT OF THE
REQUIREMENTS FOR THE DEGREE OF
MASTER OF SCIENCE
AT
MCMASTER UNIVERSITY
HAMILTON, ONTARIO
SEPTEMBER 2005

MCMASTER UNIVERSITY

DEGREE:	Master of Science, 2005
DEPARTMENT:	Mathematics and Statistics, Hamilton, Ontario
UNIVERSITY:	McMaster University
TITLE:	FEEDBACK CONTROL OF INSTABILITIES IN HYDRODYNAMIC SYSTEMS
AUTHOR:	MD. SHAH NOOR, B.SC., M.SC. (SHAH JALAL UNIVERSITY OF SCIENCE & TECHNOLOGY, BANGLADESH)
SUPERVISOR:	Dr. Bartosz Protas
PAGES:	xv, 109

MCMASTER UNIVERSITY
DEPARTMENT OF
MATHEMATICS AND STATISTICS

The undersigned hereby certify that they have read and recommend to the Faculty of Graduate Studies for acceptance a thesis entitled "FEEDBACK CONTROL OF INSTABILITIES IN HYDRODYNAMIC SYSTEMS" by MD. SHAH NOOR in partial fulfillment of the requirements for the degree of **Master of Science**.

Dated: September 2005

Supervisor: _____
Dr. Bartosz Protas

Readers: _____
Dr. Stanley Alama

_____
Dr. Dmitry Pelinovsky

_____
Dr. Nicholas Kevlahan

Dedicated to

..... the reminiscences of my loving father whose
sincere support and relentless encouragement
have led me to higher studies, my mother whose
inspiration and lovely affection have
given me the way of light, my honorable
teachers to whom I am indebted forever,
and my family members.....

Acknowledgments

First of all I would like to extend my heartfelt thanks and gratitude to my supervisor Dr. Bartosz Protas. His patience, generous guidance, and unrestricted friendship are deeply appreciated and will be remembered forever.

Special thanks are due to my honorable supervisory committee members Dr. Stanley Alama, Dr. Dmitry Pelinovsky, and Dr. Nicholas Kevlahan for their instructive suggestions and kind consent for serving as my committee members.

Sincere thanks go to my friends, fellows, colleagues, and teachers both in home and abroad whose encouragement has made me enthusiastic in the area of research.

I am very much grateful to the Department of Mathematics and Statistics at McMaster University for supporting me and for giving me the opportunity to pursue my graduate studies.

With due humbleness I would like to express my eternal gratitude and reverence to my deceased father, Md. Saef Ullah and to my mother Teraban Begum, for their unconditional love and sincere support for my higher studies. Finally, I would like to conclude this session by waving my deep affections and tender regards to my brothers and beloved younger sisters, Rahima and Fatema. In particular, my sisters' inartificial love for me, I should say, deserves a distinct appreciation.

Hamilton, Ontario — Md. Shah Noor

September 19, 2005

Abstract

This dissertation is concerned with the development of a linear control strategy for stabilization of unstable solutions of the 1D Kuramoto-Sivashinsky equation in a periodic domain. This equation serves as a simple model for hydrodynamic system. The Kuramoto-Sivashinsky equation is solved using a spectral method in both steady and unsteady regime, which is described. Computational results show the existence of several families on steady solutions, some of which are unstable. The unstable solutions are stabilized using the Linear-Quadratic-Gaussian algorithm. The feedback operators are determined by solving the matrix Riccati equation. In the thesis we also analyze computationally the effectiveness of the feedback stabilization algorithm depending on various parameters.

List of Figures

Contents

Chapter 1

Introduction

1.1 Motivation

As we know that infinite dimensional systems (i.e., *PDEs*) model many important physical phenomena such as traffic signal, weather prediction, hydrodynamics, transport in porous media, geomechanics, aerodynamics, biological and molecular dynamics, and charged particle transport emphasizing the linking of quantum, statistical and fluid mechanical states to name a few. In practice, steady solutions of a PDE have many good properties, such as turbulence vs. small drag, fluctuations in laminar flows etc., that unsteady solutions don't have. However, steady solutions are often unstable. Hence, they need to be stabilized in order to better understand the behavior of the physical phenomena that the PDE governs. For stabilization of unstable solutions of the PDE system we need to apply the well known mathematical tools called *control theory*. We will use the *linear control theory*, the simplest approach in control theory. In this project our aim is to study the instabilities that arise in the hydrodynamic systems such modeling the turbulence in fluid mechanics. We know that the Navier-Stokes equation (*NSE*) is the governing equation in hydrodynamics. This is a highly nonlinear PDE system. So far now it does not have any analytical solutions.

Therefore, we need to investigate its numerical solutions. Nevertheless, the complete numerical investigation of NSE is often very complicated. In order to alleviate this difficulty for studying this equation numerically we consider some of its ideal cases.

Motivated by this goal we have considered the Kuramoto-Sivashinsky Equation (*KSE*), a simple nonlinear partial differential equation as will be given in section 1.5. This equation is a good model for the NSE. Its solutions have multiscale, chaotic, and pattern forming behavior in periodic domains. Moreover, this equation has similar type of nonlinearity(energy-preserving) that the NSE has. Thus this equation has gained a rapid popularity from scientists and engineers. The steady solutions of KSE for different ranges of the parameter contained in it have good properties but they are unstable. Therefore we need to stabilize its steady fixed point (i.e. stationary) solutions. This requires to simplify the nonlinear infinite dimensional KSE system into a linear infinite dimensional system using the transformation of the solution $u(x,t)$ of KSE of the form $u(x,t) = \tilde{u}(x) + \varepsilon v(x,t)$ where $\tilde{u}$ is the stationary solution of KSE and $v(x,t)$ is some arbitrary perturbation from $\tilde{u}$. However, in practice the implementation of linear control theory for an infinite dimensional system is inconvenient. Therefore to avoid this difficulty we further need to project the infinite dimensional solution space of KSE into a finite dimensional solution space. This means that we need to discretize the infinite dimensional KSE system using some standard numerical techniques such as spectral Galerkin method and eventually we get the finite dimensional system. Hence the motivation of our present study arose from the necessity of stabilizing the steady but unstable solution of KSE.

Another motivation of our present study came from Armaou et al. [1] and Christofides et al. [2]. They stabilized the unstable laminar (zero solution) solution of KSE using various feedback law. In our present study we want to analyze different properties of the feedback

gain operator that is responsible for stabilizing the system.

1.2 The Idea of Feedback Control

Control mechanisms have widespread application in nature as well as in our every day life. For examples, organs in our body use control mechanisms to keep the essential biological variables, for instance, cholesterol levels, blood sugar levels and body temperature at certain points. Such mechanisms are systematically studied by a discipline called *control theory*. This subject develops a bridge between the real world problem and the mathematical theory. It has a wide variety of applications in science, engineering, and commerce such as in the design of robotic systems, the flight of spacecrafts, the satellite communications, the regulation of chemical and biological systems, manufacturing companies, and financial markets to name a few.

Control theory can be studied in different aspects. Among them are *the classical control theory* and *modern control theory*. Classical control theory is one that limits its discussion on the transfer functions and frequency domain approach. It deals with the systems that are linear and with constants coefficients. In practice there are very few physical phenomena that can be modeled by such a linear constant coefficient systems except for some ideal cases. Therefore, for studying those systems we need to study another branch of control theory called modern control theory. The modern control theory originates on the state-space approach. In this approach a higher order ordinary differential equation, or a partial differential equation representing a physical model is being written as dynamical system with respect to the state variables involved. Therefore some differences between the classical and modern control theory are in order. The former handles with only linear, constant coefficient system where the transfer functions can be easily computed but the later one

can be more easily extended to nonlinear, time-varying systems which cannot be easily described by transfer functions (see E. D. Sontag [3], & W. L. Brogan [4]). In addition to the above, another advantage of modern control theory over the classical one is that it ensures optimality and robustness of solutions to the problem under consideration.

Mathematical control theory is a branch of applied mathematics that deals with the analysis and design of a control system together with its implementation. It develops sophisticated theories to efficiently handle the control problems that arise in practice. The main purpose of *controlling* an object is to influence its behavior in order for it to achieve certain properties. For controlling the object under consideration these influences can be implemented in different ways. For examples mathematician implement these influences using various mathematical techniques designed for the respective mathematical models while engineers do them building devices, such as electric heating pad, automobiles, industrial robots and airplane autopilots, that incorporate various mathematical techniques. Briefly, we can say that the objective of control is to manipulate the available inputs of a dynamical system to cause the system to behave in a more desirable manner than the one without control. For instance, every movement that our body makes is the result of application of a control algorithm. Most of them can be characterized as the feedback control of different means. This idea of control can easily be generalized to our physical world (see E. D. Sontag [3], & K. T. Lee [5]).

There are two major types of control namely *open-loop control* and *closed loop control.* In an open-loop control system, there is no information path (or control loop) from the system, say $\mathbf{X}$, to the control input, say $\mathbf{u}(t)$. The control input, $\mathbf{u}(t)$, is generated by some dynamic processes without regard to the measured or estimated output, say $\mathbf{y}(t)$, external to the system itself and then is applied to the system. The input, or the control, $\mathbf{u}(t)$ is selected

based on the particular goals one needs to achieve for the system and all available a priori information about the system. There is no direct or indirect influence on the input by the measured output of the system. Fig. 1.1 depicts a general representation of how an open-loop control system works. It is to be noted that when unexpected noise or disturbances act upon an open-loop system, or when its behavior is not understood completely, then the output of the system may behave unexpectedly.

Mathematically an open-loop control is constructed using *optimization method*. This is why optimal design and control of systems in industrial processes has long been of concern to the applied scientists and engineers. The practical attainment of an optimum control design for a physical system is generally the result of the combination of mathematical analysis, empirical information, and the subjective experience of the scientist and engineer. The formulation of a dynamic process or control system design is done by using a trial and error procedure, in which primarily some measurements or estimates are made and then information is sought from the system to determine its improvements. Throughout this process if a sufficient mathematical characterization of the system is achieved, then one can conclude about the effect of changes about a preliminary design (see M. M. Denn [6], & W. L. Brogan [4]).

Properties of open-loop control are:

- The effects of *only* known disturbances can be mitigated.
- Once the controlled system is stable, it remains stable for ever.
- The controller does not care about the output of the system rather it drives the system in a very specific way.

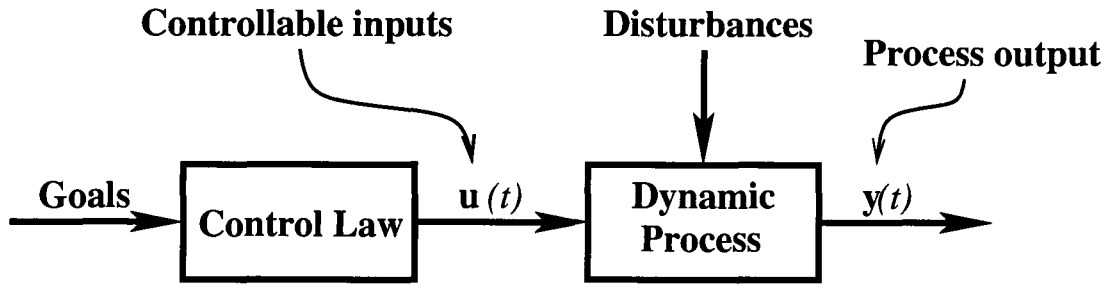

Figure 1.1: *An open-loop control system. For a certain goal, a specific input* $\mathbf{u}(t)$*, determined, for instance, by an optimization procedure, is applied to the system, resulting in a response* $\mathbf{y}(t)$*. Note that noise and/or system uncertainties may alter this output.*

Another kind of control systems is termed as the *closed-loop* control system about which we are particularly interested in order to apply into our present problem. Fig. 1.2 depicts the idea of how a closed-loop system does its functioning. In closed-loop system there is always an information path (or control loop) from the system, **X**, to the control input, $\mathbf{u}(t)$. In this system, the input or control $\mathbf{u}(t)$ is modified via this control loop from the information about the behavior of the measured or estimated system output. A closed-loop system is better adjustable with the unexpected disturbances and uncertainties about the dynamic behavior of the system (see W. L. Brogan [4]). This type of control is referred to as *feedback* control since the outputs, after some suitable transformations, are fed back to the input and then compared with the desired response. The resulting error, for instance the error between the measured output and the desired response, is the basis for the application of the control to the system. The controller generates the control signal on the basis of the error thus computed. If a mechanical signal has to be applied to the system, it is generated by an actuator from the output of the controller. In this arrangement, the control signal takes the actual controlled variable into account including noise or disturbances if any. The system is then driven (by the control signal) until the error is reduced to a certain tolerable limit. The procedure thus illustrated is called the feedback control law in which feedback

is negative (see G. P. Rao [7]).

There are many reasons why a feedback control rule is preferable to that of an open-loop control. For instance, one can see that sometimes a feedback rule is simpler in comparison to an open-loop scheme in that it may require a fair amount of computation and complex implementation. Moreover a feedback can automatically adjust to unforeseen system changes or to unexpected system noise/disturbances and thus can increase the stability of the system dynamics (see W. L. Brogan [4] & K. T. Lee [5]). Feedback control law can be divided into two categories such as *Linear* and *nonlinear* feedback law. For practical application a linear feedback control is widely used due to its simplicity. However in rigorous cases nonlinear feedback control may be used.

General advantages/properties of feedback control are:

- closed loop operation done with negative feedback
- applicable in the presence of noise and/or system uncertainties
- provide an adjustable degree of robustness, i.e. stabilize the system in the presence of noise and/or system uncertainties
- optimality, attain the above goal with the least effort possible.

Linear feedback control is again of two kinds, namely *state feedback control* and *output feedback control*. When *all* the state variables of a system are available to form its output signals, then the state feedback control is applied to such a system. In this case the input is constructed by multiplying the states by an operator (matrix), generally called feedback operator, and then is supplied to the system as a new input. On the other hand, output feedback control is applied based on incomplete information about the state of the

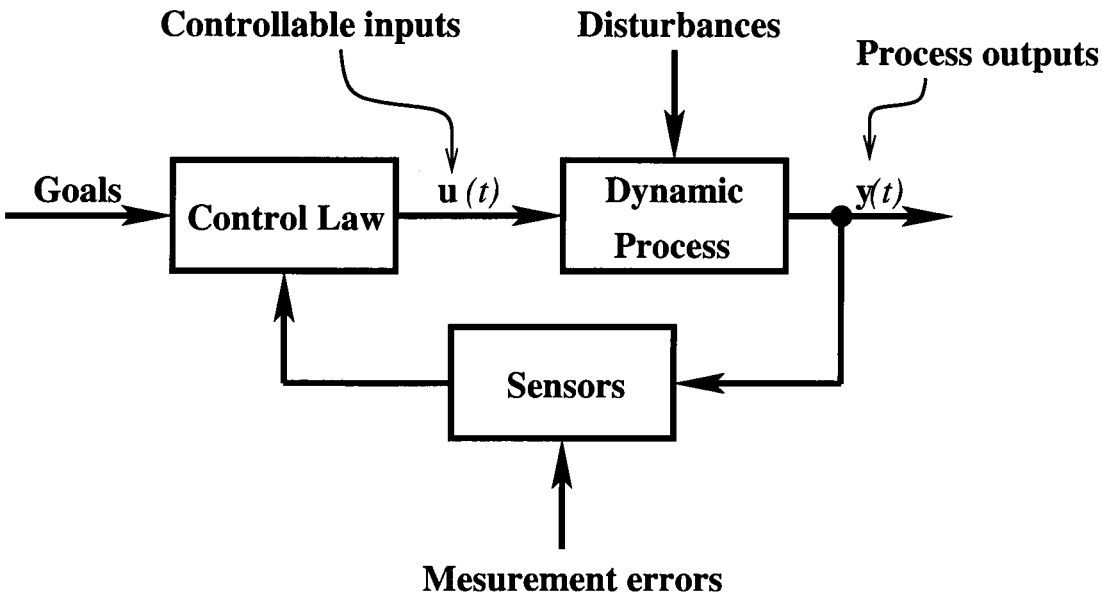

Figure 1.2: *A closed-loop control system. For certain goal some input* $\mathbf{u}(t)$*, determined by a control law, is applied to the system, even in the presence of some disturbances, and produces some response* $\mathbf{y}(t)$ *which is measured by some sensors and then this is again applied to the system as an input unless the desired response is achieved.*

system obtained through some observation operator. In this case the input is constructed by multiplying the outputs by an operator (matrix), called feedback operator as before, and then is fed back to the system as the new input. It is to be noted that the state variable feedback serves only the academic interest because the outputs are only the signals that are accessible to the system. State feedback in contrast to output feedback has the following advantages:

(i) The state contains all available information about the system under consideration. Thus a feedback can be obtained from the available state information for stabilizing the unstable solutions of the system if any.

(ii) Often there are some situations for which the state variables are all measurable. In this case the state variables can be used to form the output.

(iii) Many optional control rule can take the form of a state feedback control law.

(iv) There are efficient ways to reconstruct or measure the state variables from the available control inputs and control outputs.

We will present a more formal discussion with the appropriate mathematical setting regarding the control theoretic issues so far mentioned in Chapter 2.

In our study we are interested in infinite dimensional system, i.e., partial differential equations (*PDEs*). Control theory exists for both finite and infinite dimensional systems. Infinite dimensional formulation is possible (see Lions [8]) but implementation is very difficult which needs discretization of an infinite dimensional operator equation. This difficulty leads us to apply an alternative approach. In this approach we project the solution of the PDE from an infinite dimensional solution space to a finite dimensional space. In other words, we discretize the PDE using some standard numerical techniques and then apply the finite dimensional theory. However an obvious question may arise regarding the discretization issues. Does the solution obtained in the discrete case approach, for increased resolution, the infinite-dimensional solution? This is an important question, but is *very* difficult to answer. Later we will provide some numerical characterization that will partially answer this question.

We often encounter *the infinite dimensional systems* modeled by partial differential equations and delay differential equations or *finite dimensional systems* modeled by ordinary differential equation that come from real world problems. In such cases to serve our practical purposes we need to investigate the stability, or well-posedness of the solution. In

those cases efficient application of control strategy may play a vital role. A mathematical model representing a physical phenomenon may appear to be a linear, nonlinear, deterministic, or stochastic differential equations. Different mathematical models lead scientist to develop different controls strategies. For instance, a nonlinear mathematical model of a robotic system leads to apply linear and/or nonlinear control; incorporating models for uncertainty expressed in probabilistic or statistical terms leads to *stochastic models*, a subject which require much research activity. Another area of control theory is *robust control* which is mathematically different but closely related to *stochastic model.* Robust control deals with the design of control laws which are guaranteed to perform in the presence of disturbances and uncertainties. The area of *adaptive control*, which differs from robust control interms of the mathematics employed, deals with the control of partially unknown systems (see E. D. Sontag [3]).

Thus, the consequences of the continued practical, theoretical, and philosophical interests have been the development of the aforementioned control including many other such as statistical control, optimal control, sampled data control, multivariable control etc. Among all other controls *linear feedback control* has received a special attention in the literature and in applications because it is comparatively easy to implement into the system linearized about a state. Therefore in our present model we concentrate only to apply linear feedback control for stabilization purposes.

1.3 An Example

In order to explain the mechanism how the feedback control strategy is applied to a system to achieve a more desirable goal, let us consider one of the simplest problems in robotics, namely, that of controlling the position of a single-link rotational joint using a motor placed

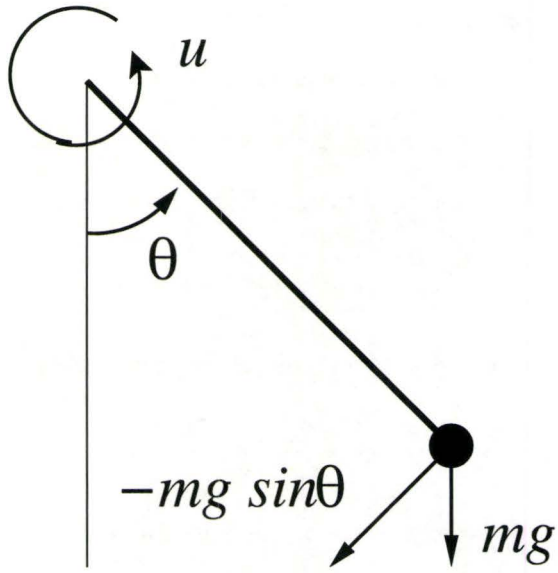

Figure 1.3: *A Pendulum. A torque $u(t)$ is applied at the pivot that makes an angular displacement $\theta(t)$ from the equilibrium position of the pendulum.*

at the pivot. This example is taken from [3]. In mathematical terms, this problem can be considered as a pendulum to which one can apply a torque as an external force $u(t)$ to control the arm position of the pendulum (see Fig. 1.3).

For simplicity, let us assume that there is no friction acting on the system, a mass m is attached to the end of a rod of unit length, g denotes the acceleration due to gravity, and θ denotes the angular displacement in counterclockwise direction of the arm of the pendulum with respect to the vertical. Then from the Newton's law for rotational motion, we obtain the following second-order nonlinear differential equation:

$$m\ddot{\theta}(t) + mg\,sin\theta(t) = u(t), \tag{1.1}$$

where $u(t)$, called the *input* or *control* function, denotes the value of the external torque at time t.

Note that the vertical stationary position $(\theta = \pi, \dot{\theta} = 0)$ represents an equilibrium point in the absence of the control (i.e., when $u \equiv 0$), however, a small deviation from the equilibrium position will result in an unstable motion. Now assume that we want to apply torques (external forces $u(t)$) as needed to correct for such deviations. But for small $\theta - \pi$, we have

$$sin\theta = -(\theta - \pi) + o(\theta - \pi).$$

where the "little-o" notation: $o(x)$ defined for some function $f(x)$ for which

$$\lim_{x \to 0} \frac{f(x)}{x} = 0.$$

Dropping the nonlinear term $o(\theta - \pi)$, and assuming $\phi := \theta - \pi$ as our new variable, equation (1.1) reduces to the following linear differential equation

$$\ddot{\phi}(t) - \phi(t) = u(t), \tag{1.2}$$

which is an *open-loop* equation.

Our aim is now to force ϕ and $\dot{\phi}$ to zero, for any nonzero $\phi(0)$, $\dot{\phi}(0)$ in equation (1.2) so that it takes least control efforts. Now if we are to the left of the vertical (see Fig. 1.4), that is, if $\phi = \theta - \pi > 0$, then we want to move to the right, and therefore, we apply a negative torque. Similarly if we are to the right, we apply a positive(i.e. counterclockwise) torque. In other words, we want to apply the following *proportional feedback*

$$u(t) = -\alpha\phi(t), \tag{1.3}$$

where α is some positive real number, called the *feedback gain.*

Now we can form the obtain the *closed-loop* equation after the control given by equation (1.3) into the *open-loop* equation (1.2), i.e.,

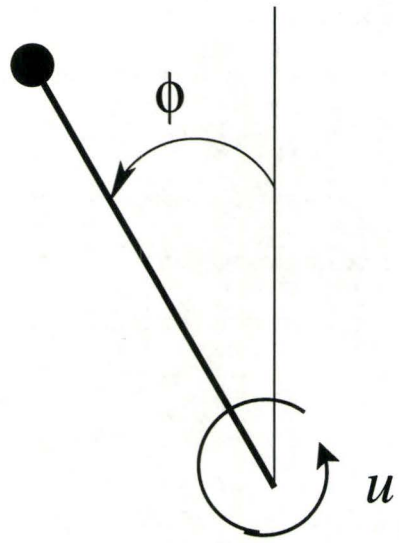

Figure 1.4: *An Inverted pendulum. A small deviation $\phi(t)$ from the equilibrium position causes an unstable motion of the pendulum.*

$$\ddot{\phi}(t) + (\alpha - 1)\phi(t) = 0. \tag{1.4}$$

For this closed-loop system, the associated characteristic equation is given by

$$r^2 + \alpha - 1 = 0 \tag{1.5}$$

whose solution can be written as

$$r = \pm\sqrt{1-\alpha}.$$

Note that if $\alpha < 1$, then all of the solutions of the above closed-loop equation except for those with

$$\dot{\phi}(0) = -\phi(0)\sqrt{1-\alpha}$$

diverges to $\pm\infty$, if $\alpha > 1$, the solutions are oscillatory, since $r = \pm i\sqrt{\alpha - 1}$, and finally if

$\alpha = 1$, then each set of initial values with $\dot{\phi}(0) = 0$ is an equilibrium point of the closed-loop system. Therefore, none of the three cases guarantees the desired configuration. This shows that proportional control does not work for the linearized model, and hence for the original nonlinear equation (1.1). These behavior of the closed-loop system can be explained physically in the following manner. For $\alpha < 1$, let us consider the initial condition as $\phi(0) = k$ where $k > 0$ but small real number, and $\dot{\phi}(0) = 0$. Then the solution of (1.4) becomes

$$\phi(t) = \frac{k}{2}\left(e^{\sqrt{1-\alpha}t} - e^{-\sqrt{1-\alpha}t}\right),$$

and thus the pendulum moves away with time t, rather than toward, the vertical position. When $\alpha > 1$, the solution then is

$$\phi(t) = k\cos\sqrt{\alpha - 1}\, t,$$

which shows that even though the torque is being applied in order to mitigate the instability of the pendulum, but this feedback produces much inertia. As a result when the pendulum is close to $\phi(0) = 0$ but moves with a relatively large speed, the controller (1.3) starts pushing toward the vertical, and thus overshoot and finally oscillation result.

In order to remedy these problem we take $\alpha > 1$ and modify the controller (1.3) so that it has a control over the velocities, i.e., we need to add a damping or diffusion term to the system which results the following *proportional-derivative(PD)*, feedback law,

$$u(t) = -\alpha\phi(t) - \beta\dot{\phi}(t), \tag{1.6}$$

where $\alpha > 1$ and $\beta > 0$. In practice, implementation of such a controller require measurement of both the angular displacement and the velocity of the system. However, for

instance, if only the angular displacement is available, then to implement the control algorithm one needs to estimate or measure the velocity which gives an idea of *observer* that is a means of performing such an estimation. Therefore, considering $\dot{\phi}$ is measurable, the resulting closed-loop system with the above PD controller can be simplified as

$$\ddot{\phi}(t) + \beta\dot{\phi}(t) + (\alpha - 1)\phi(t) = 0. \tag{1.7}$$

whose auxiliary equation has the following roots

$$r = \frac{-\beta \pm \sqrt{\beta^2 - 4(\alpha - 1)}}{2},$$

both of which have negative real parts. Therefore all the solutions of equation (1.2) converges to zero. Hence the system has been *stabilized* under feedback law (1.6). To avoid the oscillatory behavior of the solutions if any we further can impose the following condition

$$\beta^2 > 4(\alpha - 1), \tag{1.8}$$

which kills the oscillations and thus the solutions have only decaying properties.

We therefore conclude from the above discussions that through a suitable choice of the controller gains α and β one can achieve the desired behavior for the linearized model of the given nonlinear problem. But even though most control systems are designed and implemented using linear feedback strategies, there are lot of cases in which the nonlinearities of the system must be taken into account to get a better result for the application of control approach, for example, in the automatic control of spacecraft attitude or in the design of autonomous robots. However, the design and analysis of nonlinear control systems requires more sophisticated mathematical tools than are typically used for linear systems.

That is why nonlinear control theory draws on a wide variety of topics, including dynamical systems theory, differential geometry, the study of Lie algebras, and Lagrangian and Hamiltonian systems. Research aspects in this field involves questions of stability, output-stability and detectability for nonlinear systems, primarily focusing on the notion of input to state stability (see E. D. Sontag [3]).

1.4 Mathematical and computational challenges in control theory

It is well recognized that there is an increasing demand for the application of control theory in our real world problem. This widespread demand has led researchers in control community to develop many sophisticated theories for use in control. However there are many technical problems when one needs to implement them in practice. For solving the practical problems it has been found that even though the theories exist but often they become very difficult to apply. Most physical phenomena that are to be controlled are modeled by infinite dimensional system such as partial differential equations (*PDE*). Since implementation of many control theories that are developed for the infinite dimensional problems is inconvenient, therefore, practically we solve such problems using some standard numerical approach, i.e., by some finite dimensional formalism. Therefore a very natural question is in order – does the solution of the finite dimensional control problem (based on the discretization of a PDE) converge to a solution of the continuous problem? There is some evidence that for certain classical systems this is not the case (see E. Zuazua [9]). Hence, the formulation of a finite dimensional problem to ensure that the above hold is a challenge for the implementation of the control theory in practice.

In another study by E. Lauga et al. in [10] has provided numerical evidence that in a

finite-dimensional discretization of a PDE controllability is systematically lost as numerical resolution is refined. These are some numerical evidences that address some challenging mathematical and computational issues of control theoretic applications.

1.5 KSE as a model system

In this study our aim is to develop an algorithm for stabilizing the unstable solutions of a partial differential equation that exhibits chaotic behavior by using the feedback control strategy. Therefore we have selected the Kuramoto-Sivashinsky Equation (*KSE*), a simple nonlinear dissipative partial differential equation with first order in time but fourth order in space, that exhibits a very rich nontrivial dynamical behavior which is temporally complex/chaotic but spatially coherent patterns. This equation has been considered as a model problem for simulating the development of turbulence in physical systems. Moreover extensive numerical simulations for this KSE system has been done by a number of researchers and have shown the existence of periodic cellular patterns. It can be written in many different forms depending on the normalization of the parameter involved. Here we have chosen the one that is used by Hyman et al. [11]:

$$\partial_t v + \nu \partial_x^4 v + \partial_x^2 v + (\partial_x v)^2 = 0, \qquad x \in \Omega, \qquad t \in [0,T] \tag{1.9}$$

subject to the periodic boundary conditions

$$\partial_x^i v(0,t) = \partial_x^i v(L,t), \qquad t \in [0,T], \qquad i = 0,\ldots,3, \tag{1.10}$$

and the initial condition

$$v(x,0) = v_0(x), \qquad x \in \Omega, \tag{1.11}$$

where the subscripts t and x denote the time and the space derivative, respectively, ν, sometimes called the instability parameter, is positive, the solution $v(x,t) \in H_p^2(\Omega)$ represents the state of the system, $H_p^2(\Omega)$ denotes the Hilbert space of functions with square-integrable second derivatives that satisfy the boundary conditions of equation (1.9) (i.e. $H_p^2(\Omega) = \{v \in H^2(\Omega) : \partial_x^i v(0,t) = \partial_x^i v(L,t),\ i = 0,\ldots,2\})$, $v_0(x) \in H_p^2(\Omega)$, H^2 denotes the sobolev space of functions with square-integrable second derivatives and $\partial_x^i \triangleq \frac{\partial^i}{\partial x^i}$. For simplicity we assume that $\Omega \triangleq [0,L]$ where $L = 2\pi$ is the length of a typical pattern cell and v_0 is an L-periodic spatial function.

Kuramoto-Sivashinsky equation (KSE) has been derived by many scientists to model different physical phenomena such as it appeared to model the Belousov-Zhabotinskii reaction patterns in the aspect of angular-phase turbulence for reaction-diffusion systems, thermal instabilities with diffusion in laminar frame fronts, interfacial instabilities between two viscous fluid systems, the perturbations of a Poiseuille flow of a film layer down on a vertical or inclined plane, among others (see Greene et al. [12] & Kevrekidis et al. [13] and the references therein). This equation is widely studied by the researchers as a prototype due to its chaotic and pattern-forming behavior to forecast the spatio-temporal complexities that exist in the dynamical system.

As in [11] introducing the renormalized dimensionless natural bifurcation parameter $\tilde{L} = L/(2\pi\sqrt{\nu})$, normalizing the KSE in an interval of length $L = 2\pi$, setting the incipient instability parameter $\nu = 4$ as proposed by Sivashinsky, and hence introducing the new bifurcation parameter $\alpha = 4\tilde{L}^2$, where L is the size of a cell forming a typical pattern along spatial coordinates, we can write (1.9), (1.10), and (1.11) as

$$\partial_t v + 4\partial_x^4 v + \alpha\left(\partial_x^2 v + (\partial_x v)^2\right) = 0, \qquad x \in \Omega, \qquad t \in [0,T] \tag{1.12}$$

subject to the periodic boundary conditions

$$\partial_x^i v(0,t) = \partial_x^i v(2\pi,t), \qquad t \in [0,T], \qquad i = 0,\ldots,3, \tag{1.13}$$

and the initial condition

$$v(x,0) = v_0(x), \qquad x \in \Omega, \tag{1.14}$$

where the new time scaling is defined as $\partial_t := \frac{1}{\alpha}\partial_t$

Now integrating the above system over Ω in the light of [14], the evolution of the mean of v can be simplified as $\partial_t \int_0^{2\pi} v dx = -(\alpha/2)\int_0^{2\pi}(\partial_x v)^2 dx \neq 0$. That is why, it is often convenient to transform the given system into a different form which is obtained by first differentiating it with respect to x and then re-expressing it in terms of a new variable $u = \partial_x v$ such that the new system becomes:

$$\partial_t u + 4\partial_x^4 u + \alpha\left(\partial_x^2 u + u\partial_x u\right) = 0, \qquad x \in [0,2\pi], \qquad t \in [0,T] \tag{1.15}$$

subject to the periodic boundary conditions

$$\partial_x^i u(0,t) = \partial_x^i u(2\pi,t), \qquad t \in [0,T], \qquad i = 0,\ldots,3, \tag{1.16}$$

and the initial condition

$$u(x,0) = u_0(x), \quad x \in [0, 2\pi] \tag{1.17}$$

where $u(x,t)$ is continuous and periodic with the same period as $v(x,t)$, and $u_0(x) = \partial_x v_0(x)$.

Now integrating $u(x,t) = \partial_x v(x,t)$, and using the boundary condition (1.13) for $i = 0$, we obtain

$$\int_\Omega u(x,t)dx = 0, \quad \forall t. \tag{1.18}$$

One can observe here that $u(x,t) = C$, a constant, satisfies (1.15). Again $C = 0$ due to (1.18). Moreover $u(x,0) = u_0(x)$ is 2π periodic for all $x \in \Omega$, and $< u_0 >= \frac{1}{2\pi}\int_\Omega u_0(x)dx$ represents the mean value of the initial solution and hence integrating (1.15) over the domain Ω yields,

$$\frac{d}{dt}\int_\Omega u(x,t)dx = 0, \quad i.e., \quad \frac{1}{2\pi}\int_\Omega u(x,t)dx =< u_0 > .$$

It follows from (1.18) that $< u_0 >= 0$. This shows that the mean of the solution remains conserved with respect to time. In other words, we can say that the "dynamics" of $u(x,t)$ satisfying (1.15) are centered around the mean value of the initial data. Therefore, we can assume the following conditions

- the solution $u(x,t)$ is periodic on Ω, with the periodic initial condition $u(x,0) = u_0(x)$
- $\int_\Omega u_0(x)dx = 0$.

The system of equations (1.15)- (1.18) is our final version of the Kuramoto-Sivashinsky Equation (KSE) which we want to study in terms of control-theoretic tools. Here it is worth mentioning that the fourth derivative term is responsible for damping, the second

derivative term is responsible for instabilities, and the nonlinear term redistributes energy across wave numbers through mode coupling, and the parameter α has a similar meaning to the Reynold's number in fluid dynamics. It is clear from the expression $\alpha = 4\tilde{L}^2$ that α increases with the periodicity length L. The flow of energy in the system can be easily understood in terms of the spatial Fourier harmonics of the solution. Taking the Fourier transform of (1.15) we see that the fourth order spatial derivative term is proportional to the fourth power of the wave number and second order spatial derivative term is proportional to the square of the wave number. This suggests that short wave modes lose energy to sinks outside the model but the long wave modes are driven. Then the energy in the long wavelength modes propagates to the short wavelength modes through the nonlinear coupling. Through this nonlinear interaction, energy balance of each mode can be reached, which leads to nontrivial steady states.

1.6 Organization of Dissertation

1.6.1 Objectives

In this study our main objective is to develop an algorithm for stabilizing the unstable solutions of Kuramoto-Sivashinsky equation applying the idea of linear control theory. In order to do this we need a systematic presentation of the underlying mathematical procedures. The major accomplishment of this thesis can be categorized as:

- Implementation of unsteady and steady KSE simulations
- Analysis of multiplicity of steady state solutions, and
- Development and implementation of a linear feedback stabilization strategy.

1.6.2 Organization of the Dissertation

We have organized this dissertation as follows. In Chapter 1 we introduce the problem, in particular present:

- motivation of our research problem
- underlying idea of control theory

In Chapter 2 we discuss the numerical methods used in our computational study of the Kuramoto-Sivashinsky equation, in particular

- derivation and properties of spectral methods
- implementation of spectral Galerkin methods for both unsteady and steady KSE
- time discretization of KSE using Euler scheme
- Newton's method for solving finite dimensional nonlinear steady KSE obtained upon discretization
- results of steady and unsteady KSE

In Chapter 3 we introduce concepts of the control theory and computational results, in particular

- introduction to Linear Quadratic Regulator problem
- formulation of controlled KSE using actuator applied both in physical and Fourier space
- derivation of matrix Riccati equation for KSE

- some useful results concerning the solution of matrix Riccati equation
- important results that we have obtained for feedback stabilization of KSE

Finally in Chapter 4 we provide conclusions.

Chapter 2

Computational Characterization of Kuramoto-Sivashinsky Equation (KSE)

In this study our model equation is an infinite dimensional partial differential equation, namely Kuramoto-Sivashinsky Equation(KSE). We want to solve this system numerically. However as we know that the solution of an infinite dimensional problem by a numerical technique is impossible. Therefore we consider here the corresponding finite dimensional approximation of the solutions of KSE. We want to solve the KSE by a fairly common numerical method, known as the *Spectral method*. Hence in this chapter we will present some key material that is the basis of this method.

2.1 Mathematical Framework, Basic definitions and Useful Theorems

This section is devoted to introduce some background materials to work with when studying the spectral methods (see R. Peyret [15]) for the solution of KSE.

2.1.1 Spectral Methods

In this section our aim is to present the background material for constructing a finite dimensional approximation of the solution to a continuous problem. The *Spectral method* that lies in the general class of weighted residuals methods is one of the very well known numerical methods that best suits for the problems with smooth solutions on a periodic and bounded domain. In this method the approximation is defined as a truncated series expansion in terms of polynomials that are orthogonal with respect to some weight, so that some quantity (usually referred to as residual or error) which should be exactly zero is forced to be zero only in an approximate sense. The principal advantage of this method is the exponential decay rate, called *spectral* or *infinite* accuracy, of the error between the exact solution and the calculated one when the degree of the polynomials is increased. Due its very high accuracy it allows one to consider problems which would require a large number of mesh points by finite differences discretization, with very much fewer degrees of freedom. Often spectral method is useful to model the flow with shock waves or fronts.

Now consider a set $B = \{\phi_k(x)\}_{k=0}^{\infty}$ of functions defined on an interval $\Omega = [a, b]$. Then the set B is said to be a basis for a function space $H^2(\Omega)$ (e.g., Hilbert space) if the span of B is dense in $H^2(\Omega)$. The most convenient basis functions are those which are orthogonal to each other. The set B of basis functions is said to be orthonormal if the norm of the basis functions is normalized to unity, i.e., $(\phi_m, \phi_n)_w = 1$ where $w(x)$, defined on Ω, is the weight associated with the orthogonality of the basis functions in B. The set $B = \{e^{2\pi ikx}\}$, for example, forms an orthonormal basis for of the complex space $L^2([0, 1])$. This is fundamental to the study of Fourier series. B is said to be orthogonal with respect to the weight $w(x)$ defined on Ω if

$$(\phi_k, \phi_l)_w = c_k \delta_k^l, \tag{2.1}$$

where $(\phi_k, \phi_l)_w = \int_a^b \phi_k \phi_l w dx$ denotes the inner product of $\phi_k(x)$ and $\phi_l(x)$, c_k denotes some constant, and δ_k^l denote the Kronecker delta.

Now assume that a function $u(x)$ defined on Ω can be approximated by a truncated series of the form

$$u_N(x) = \sum_{k=0}^{N} \hat{u}_k \phi_k(x), \quad x \in \Omega, \tag{2.2}$$

where $\phi_k(x)$ are some basis functions and $\hat{u}_k$ are some unknown coefficients. Basing on the choice of basis functions and their domain we obtain different approximation series as follows:

- If the chosen basis functions are $\phi_k(x) = e^{ikx}$ $(i = \sqrt{-1})$ on $\Omega = [0, 2\pi]$, then the resulting spectral method is called Fourier spectral method or simply Fourier method.
- If the basis functions are Chebyshev polynomials defined on the bounded domain $\Omega = [-1, 1]$, the method is called Fourier Chebyshev method with respect to the weight $w(x) = (1 - x^2)^{-\frac{1}{2}}$.
- If the basis functions are Legendre polynomials defined on the bounded domain $\Omega = [-1, 1]$, the method is called Fourier Legendre method and the weight in this case is $w(x) = 1$.
- In a similar fashion other Fourier methods such as Fourier Bessel method, Fourier Laguerre method etc. are defined.

Later on we will state some theorems regarding the accuracy of representation of equation (2.2) in some special cases. Now if $u_N(x)$ is a finite dimensional approximation to $u(x)$, the residual is defined as

$$R_N(x) = u - u_N$$

Analogously the residual for a differential equation $Lu = f$, for instance, can be defined as

$$R(x) = f - Lu_N.$$

where L is a differential operator.

The weighted residual method can be constructed by canceling the residual R_N in an approximate sense, i.e., setting the inner product

$$(R_N, \psi_n)_{w_\star} := \int_\Omega R_N(x)\psi_n(x)w_\star(x)dx = 0, \quad n \in I_N, \tag{2.3}$$

where $\psi_n(x)$ are the test (or weighting) functions, I_N is some finite index set, and $w_\star$ is the weight related to the method and trial functions. Depending on the test functions $\psi_n(x)$ and the associated weights $w_\star$, we can define the following weighted residuals methods:

- The Galerkin method obtained by setting

  $$\psi_n = \phi_n \text{ and } w_\star = w, \tag{2.4}$$

  where $\phi_n(x)$ are the basis functions and $w(x)$ is the weight for which the basis functions $\phi_n(x)$ are orthogonal.

- The collocation method obtained by setting

$$\psi_n = \delta(x - x_n) \text{ and } w_\star = 1, \tag{2.5}$$

where x_n, $n = 1, 2, \ldots, N$ represent the collocation points defined on Ω, and δ represents the Dirac delta-function.

Using equation (2.3) in (2.5) we obtain the following identity characterizing the collocation methods

$$R_N(x_n) = 0. \tag{2.6}$$

Therefore, basing on the construction of these two approximation methods we may conclude that in collocation method, the residual is exactly zero at the collocation points whereas in the Galerkin-type method the residual is zero in the mean with respect to some weights. Thus we can say that collocation method gives rise to interpolation method whereas Galerkin method gives rise to an approximation method — a more typical classification.

2.1.2 Approximation of a given function using Galerkin approach

Galerkin method consists of setting in equation (2.4) the basis function $\phi_n(x)$ as the trigonometrical functions $\{e^{ikx}\}_{k=1}^{N}$, called *Fourier* basis, and the weight $w(x) = 1$ as the associated weight for the Fourier basis functions. If $u_N(x)$ is an approximation to $u(x)$, then the residual

$$R_N(x) = u - u_N = u - \sum_{k=0}^{N} \hat{u}_k \phi_k \tag{2.7}$$

is forced to zero via (2.3)

$$(R_N, \phi_n)_w = \int_\Omega \left(u - \sum_{k=0}^{N} \hat{u}_k \phi_k \right) \phi_n w dx = 0, \quad n = 0, \ldots, N. \tag{2.8}$$

Note that we have considered the index set $I_N = \{0, \ldots, N\}$ to calculate the $N+1$ coefficients u_k that are present in (2.8). These coefficients can be explicitly calculated by using the so-called orthogonality relation (2.1):

$$\hat{u}_k = \frac{1}{c_k} \int_\Omega u \phi_k w dx, \quad k = 0, \ldots, N. \tag{2.9}$$

2.1.3 Approximation of a given function using the Collocation approach

In the collocation method the residual $R_N = u - u_N$ is made equal to zero at the $N+1$ collocation points x_n, $n = 0, \ldots, N$, so that $I_N = 0, \ldots, N$ and

$$u_N(x_n) = u(x_n), \quad n = 0, \ldots, N, \tag{2.10}$$

This relation indicates that the collocation method is an interpolation method. But we know that $u_N(x) \equiv \sum_{k=0}^{N} \hat{u}_k \phi_k(x_n)$, so we have

$$\sum_{k=0}^{N} \hat{u}_k \phi_k(x_n) = u(x_n), \quad n = 0, \ldots, N. \tag{2.11}$$

It is a system of $N+1$ algebraic equations with $N+1$ unknowns $\hat{u}_k$, $k = 0, \ldots, N$ which has a unique solution provided that $\det\{\phi_k(x_n)\} = 0$. Alternatively one can also solve this system using a discrete orthogonality property of the trial functions ϕ_k associated to set of collocation points $\{x_n\}$ which is equivalent to the evaluation of a numerical integral in equation (2.9) by the Gauss formula.

2.1.4 Fourier Spectral Method

This is a very popular method and is extensively used for approximating the solution of a periodic problem. This is constructed by considering the trigonometric functions as the basis functions. *Such a basis is adapted to periodic functions.* Thus, if the initial and boundary conditions of partial differential equation (*PDE*) on a bounded domain are periodic then we can apply the spectral method to compute the solutions of the PDE. However, if the initial and boundary conditions of a PDE are not periodic, then we have a different problem and therefore a different method should be used. In this new problem the initial and boundary conditions of the PDE are made homogeneous using some transformations so that they are satisfied by the basis functions ϕ_k of the approximation of the solutions of the PDE. In such cases it is guaranteed that the solutions of the PDE can be approximated by a series of the form (2.2).

However if it is not possible to make the initial and boundary conditions of the PDE homogeneous, then still the traditional Galerkin method may be applied by constructing, from the orthogonal basis functions $\{\phi_k\}$, a new basis $\{\psi_k\}$ satisfying the boundary conditions; this can be done generally by defining ψ_k as a linear combination of some ϕ_k's. But still there might be a problem that the new basis functions are not orthogonal. In such a case it is inconvenient to use the Galerkin method. Therefore, to avoid this complexity, a new method, called the *"tau method"*, is developed. This is a modification of the Galerkin method that allows the use of trial functions not satisfying the homogeneous initial and/or boundary conditions.

Now suppose we want to approximate a function $u(x)$ defined on a domain $\Omega = [a, b]$ by Fourier spectral method. If the function is not periodic and/or not continuous, then Fourier spectral method can, in principle, still be applied. But, in this case the convergence of

the associated series becomes nonuniform near the boundaries and the Gibbs oscillations may contaminate the whole domain. That is why to use this method we impose some restrictions that the functions to be approximated should be smooth enough and periodic. In this respect we assume for simplicity that our function $u(x)$ is 2π-periodic defined on the interval $\Omega = [0, 2\pi]$.

2.1.5 Calculation of Fourier coefficients using spectral Galerkin technique

Now we consider the above function $u(x)$ is real valued and is represented by a finite trigonometric series instead of (2.2) as

$$u_N(x) = \sum_{k=-N}^{N} \hat{u}_k e^{ikx}, \tag{2.12}$$

which contains $2N+1$ unknown complex coefficients $\hat{u}_k$. The complex form (2.12) is useful for applying the *Fast Fourier Transform (FFT)*. Obviously $\hat{u}_0$ is real and since $u(x)$ is real valued, so the following complex conjugacy relation holds for every two Fourier coefficients, with an opposite value of k, that is to say,

$$\hat{u}_{-k} = \overline{\hat{u}}_k, \tag{2.13}$$

where $\overline{(.)}$ denotes the complex conjugate.

Therefore using (2.13) we need to compute only $2N+1$ unknown *real coefficients* of (2.12). Now using the Galerkin-type method as in section 2.1.2 and the orthogonality property for the complex exponential functions

$$\int_0^{2\pi} e^{i(k-n)x}dx = \begin{cases} 2\pi & \text{if } k=n \\ 0 & \text{if } k\neq n, \end{cases} \tag{2.14}$$

we obtain the following expression for the Fourier coefficients

$$\hat{u}_k = \frac{1}{2\pi}\int_0^{2\pi} u(x)e^{-ikx}dx, \quad k=-N,\ldots,N. \tag{2.15}$$

In practice, the complex coefficients $\hat{u}_k$ are calculated for $k=0,1,\ldots,N$ and the remaining coefficients are obtained from (2.13).

2.1.6 Calculation of Fourier coefficients using Collocation technique

Here we want to compute the discrete Fourier coefficients $\hat{u}_k$ present in Fourier series expansion (2.12) by using the collocation technique as discussed before. To do this let us denote the two end points of the domain of definition of $u(x)$ by $x_0=0$ and $x_M=2\pi$, then the collocation points associated with the Fourier series are defined by

$$x_n = \frac{x_M - x_0}{M}n = \frac{2\pi n}{M}, \quad n=0,\ldots,M, \tag{2.16}$$

Since $u(x)$ is assumed to be periodic, so it satisfies $u(x_0)=u(x_N)$ and similar equalities for its derivatives. The collocation coefficients are now computed by setting the residual $R_N(x)=u(x)-u_N(x)$ to zero at the collocation points, i.e.,

$$R_N(x_n) = u(x_n) - u_N(x_n) = 0, \quad n=1,\ldots,M, \tag{2.17}$$

or

$$\sum_{k=-N}^{N} \hat{u}_k e^{ikx_n} = u(x_n), \quad n = 1, \ldots, M. \tag{2.18}$$

But since $u(x)$ is real, so as before, this equation contains $2N+1$ real unknowns instead of $2N+1$ complex unknown coefficients. In order to calculate them we must have $2N+1$ equations, in other words, we set $M = 2N+1$. Note that one can show that the matrix $\mathcal{M}$ associated with the system (2.18) is unitary up to the factor M, i.e., $\mathcal{M}^{\star}\mathcal{M} = M\mathbb{I}$ (where $\mathcal{M}^{\star}$ is the conjugate transpose of $\mathcal{M}$ and $\mathbb{I}$ is the identity matrix) so that its determinant satisfies $|det\mathcal{M}| = M^{M/2}$. This suggests that $\mathcal{M}$ is invertible and hence the system (2.12) has a unique solution. Therefore, with the aid of discrete orthogonality relation

$$\sum_{n=1}^{M} e^{i(k-l)\frac{2\pi n}{M}} = \begin{cases} M \text{ if } k-l = mM, \ m = 0, \pm 1, \pm 2, \ldots, \\ 0 \text{ otherwise.} \end{cases} \tag{2.19}$$

we obtain the following discrete Fourier transform

$$\hat{u}_k = \frac{1}{M} \sum_{n=1}^{M} u(x_n) e^{-ikx_n}, \quad k = -N, \ldots, N. \tag{2.20}$$

2.1.7 Some convergence results of the spectral method

For approximating a function using this method it is required that the Fourier coefficients should have sufficient decay properties. Therefore it is essential to present some results on the convergence of this method. Assume that the function $u(x)$ defined on $[0, 2\pi]$ is periodic, continuous including its derivatives $u^{(p)}$ up to the order $m-1$ and with the m-th derivative absolutely integrable, the well known result of the decay of Fourier coefficients (R. Peyret [15]) is given by

$$\hat{u}_k = O(|k|^{-m}) \text{ for } k \to \infty. \tag{2.21}$$

When the total variation of the m-th derivative is bounded, the above result reduces to

$$\hat{u}_k = O(|k|^{-m-1}) \text{ for } k \to \infty. \tag{2.22}$$

These results show that the convergence of the spectral method depends on the regularity of the function $u(x)$ under consideration. In other words, we can say that the more regular is the function u, the more rapid is the convergence toward zero of its Fourier coefficients when $k \to \infty$. The error estimate based on the $L^p(0, 2\pi)$-norm of the convergence of the approximation u_N is given by [15]

$$||u - u_N||_{L^p(0,2\pi)} \leq CN^{-m}||u^{(m)}||_{L^p(0,2\pi)}, \tag{2.23}$$

where $1 < p < \infty$ and C is an arbitrary constant independent of N. For $p = 1$ or $p = \infty$, the above inequality holds for a constant $C(1 + logN)$ instead.

Therefore from (2.23) we may conclude that for an infinitely differentiable function, the approximation error is smaller than any integral power of $1/N$, i.e., the convergence is exponential. This decay property is commonly called *" spectral"* or *"infinite"* accuracy. However, it should be mentioned that in the presence of singularity, the rate of convergence of the Fourier series approximation to a function is only algebraic (R. Peyret [15]).

Relation between Galerkin and Collocation coeffi cients that gives rise to aliasing error

If we analyze the continuous and discrete orthogonality relation given by (2.14) and (2.19) which are respectively,

$$\int_0^{2\pi} e^{i(k-n)x}dx = \begin{cases} 2\pi & \text{if } k=n \\ 0 & \text{if } k\neq n \end{cases}$$

and

$$\sum_{n=1}^{M} e^{i(k-l)\frac{2\pi n}{M}} = \begin{cases} M \text{ if } k-l=mM, \ m=0,\pm1,\pm2,\ldots, \\ 0 \text{ otherwise.} \end{cases}$$

we observe that the former one is not zero for $k-l=0$, while the later on is not zero for $k-l=mM, \quad m=0,\pm1,\pm2,\ldots$. This is an error that arises from discretization and is closely related to the question of sampling. This distinction shows that two trigonometrical functions with different frequencies, e^{ik_1x} and e^{ik_2x}, are equal at collocation points $x_n = 2\pi n/M$ when $k_2-k_1=mM, \quad m=0,\pm1,\pm2,\ldots$. Therefore, the same set of values at collocation points may represent either e^{ik_1x} or $e^{i(k_1+mM)x}$. This phenomenon is known as *"aliasing"*.

An interesting question, however, may arise if a smooth signal (or function) $u(x)$ defined on $[0,2\pi]$ is sampled as $u(x_n)$ at discrete collocation points $x_n = 2\pi n/M$, where $n=1,\ldots,M$. To investigate the answer of this question let us denote the Galerkin-type coefficients by $\hat{u}_k^g$ as defined by the integral (2.15) and by $\hat{u}_k^c$ the collocation-type coefficients given by the sum in (2.20). For convenience let us repeat (2.15) and (2.20) which are in turn:

$$\hat{u}_k^g = \frac{1}{2\pi}\int_0^{2\pi} u(x)e^{-ikx}dx, \quad k=-N,\ldots,N. \tag{2.24}$$

and

$$\hat{u}_k^c = \frac{1}{M}\sum_{n=1}^{M} u(x_n)e^{-ikx_n}, \quad k=-N,\ldots,N. \tag{2.25}$$

Consider the infinite Fourier series expansion of $u(x)$ as

$$u(x) = \sum_{k=-\infty}^{\infty} \hat{u}_k^g e^{ikx}. \tag{2.26}$$

Now substituting the value of $u(x_n)$ obtained after evaluating the sum (2.26) at the discrete collocation points $x_n = 2\pi n/M$, $n = 1, \ldots, M$, in (2.25) we obtain

$$\begin{aligned}
\hat{u}_k^c &= \frac{1}{M} \sum_{n=1}^{M} \left(\sum_{p=-\infty}^{\infty} \hat{u}_p^g \, e^{ipx_n} \right) e^{-ikx_n}, \quad k = -N, \ldots, N, \\
&= \frac{1}{M} \sum_{p=-\infty}^{\infty} \hat{u}_p^g \left(\sum_{n=1}^{M} e^{i(p-k)x_n} \right), \quad \text{assuming the series is absolutely convergent} \\
&= \hat{u}_k^g + \sum_{m \in \mathbb{Z} \setminus \{0\}} \hat{u}_{k+mM}^g, \quad k = -N, \ldots, N, \quad \text{using the relation (2.19)}
\end{aligned} \tag{2.27}$$

where the sum

$$\sum_m \hat{u}_{k+mM}^g, \quad k = -N \ldots N$$

that characterizes *the aliasing error* through the difference between the coefficients $\hat{u}_k^c$ and $\hat{u}_k^g$, is called *"alias"*. Its presence is a consequence of the sampling phenomenon mentioned before. It is noticed that the modes appearing in the alias term correspond to frequencies larger than the cut-off frequency N. Therefore, the discrete mode k collects all the energy from all the periodic images of mode k in the continuous spectrum. This is the reason it is important that the wave amplitudes decay rapidly, and that we have a large enough value of M: if both of these are true, then the contribution from the other periodic modes is extremely small. However, if $u(x)$ is not a smooth enough function, or M is not large enough, then modes for small values of k will contain energy from higher modes. This is called *aliasing error"*. More precisely, it can be shown that the L_2-norm of the aliasing error (R. Peyret [15])

$$E_A = \sum_{k=-N}^{N} \left(\sum_m \hat{u}^g_{k+mM} \right) e^{ikx} \tag{2.28}$$

is bounded by $CK^m ||u^{(m)}||_{L_2(0,2\pi)}$.

2.2 Steady and unsteady solutions

It has been illustrated [11] that the dynamics of KSE (1.15) is equivalent to the dynamics of a low- dimensional system and the solutions of KSE transition to chaos for different ranges of the parameter α. Hyman et al. in [11] numerically integrated the KSE in time for a given periodic initial condition and then categorized different behavior of the solutions including laminar (trivial), periodic, chaotic. Analysis of chaotic behavior of KSE by different researchers is briefly summarized in (J. M. Greene et al. [12]).

However, the study of the steady states of KSE and their stability play a vital role for the foundation of understanding the underlying dynamics of the system (J. M. Greene et al. [12]). In addition the study of the unsteady states of KSE gives an understanding of the solutions about the transition to chaos. Hence it is interesting to consider both the steady and unsteady problems of KSE. The solutions of an ordinary or partial differential equation which do not depend on time are usually termed as *steady* while those which depend on time are called *unsteady*. Therefore, the unsteady solutions of KSE are obtained by solving equation (1.15) subject to the boundary conditions (1.16) and the initial condition (1.17) whereas the steady solutions of KSE are obtained by solving the equation (1.15) after setting $\partial_t u(x,t) = 0$. Note that the former problem is a parabolic problem which can be solved by any numerical time integration scheme but the later one is an elliptic problem having only the boundary conditions. Therefore, this problem has to be solved by an iterative method such as Newton' method.

2.3 Discretization of KSE and the solution method

2.3.1 Discretization of unsteady KSE

The behavior of the solution of KSE is quite varied and complicated due to the presence of both second and fourth order spatial derivative terms. The second derivative term $\alpha\partial_x^2 u$ is antidissipative (or antidiffusive) and it maintains the excitation in the absence of any external excitation. Hence this term introduces energy into the system and therefore has a destabilizing effect. In addition, the nonlinear term $\alpha u\partial_x u$ transfers energy from low to high wave numbers where the stabilizing fourth derivative viscosity term $4\partial_x^4 u$ dominates. In fact, the presence of the nonlinear term in KSE ensures the boundedness of the solution $u(x,t)$ as $t \to \infty$. Now linearize the KSE (1.15) about the laminar state $\tilde{u} \equiv 0$ we obtain

$$\partial_t u + 4\partial_x^4 u + \alpha\partial_x^2 u = 0 \tag{2.29}$$

The eigenfunctions (Fourier modes) of the solution $u(x,t)$ of (2.29) are given by e^{ikx}, $k \in \mathbb{Z}$ and the the corresponding eigenvalues are given as $\lambda_\alpha(k) = k^2(\alpha - 4k^2)$, for $k \in \mathbb{N}$. The typical distinction between small and large wave numbers is illustrated by the dispersion relation for the linear KSE (2.29) as shown in the Fig. 2.1.

From the eigenvalue analysis of this linear part of KSE it is clear that the laminar solution $\tilde{u} \equiv 0$ is stable if $\sqrt{\alpha/4} < 1$, and the two new degenerate unstable modes appear at every successive integer of $\sqrt{\alpha/4}$. Hence we conclude that the new branches bifurcate at the integer values of $\sqrt{\alpha/4}$ and the eigenvectors of the bifurcated modes at $\sqrt{\alpha/4} = n$ as given above are e^{ikx}, $k \in \mathbb{Z}$. Therefore the set of these eigenvectors can be written as $\{\cos kx, \sin kx\} = \{\cos nx, \sin nx\}$ (since at the bifurcation points $k = \pm\sqrt{\alpha/4}$).

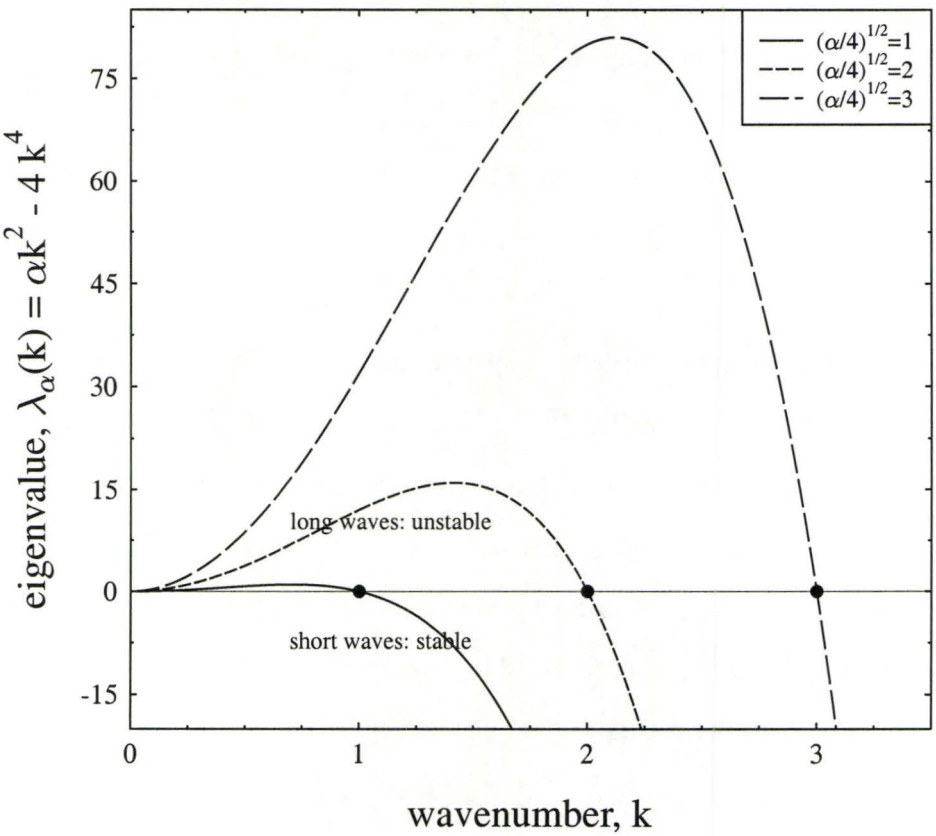

Figure 2.1: *Dispersion relation for the linear part of the KSE. From the graph we notice that if* $k < 1$ *(or equivalently if* $\sqrt{\alpha/4} < 1$*), then the laminar solutions of KSE are stable. If* $k = 1$ *(or equivalently* $\sqrt{\alpha/4} = 1$*), then the eigenvalues of linearized matrix about laminar states are zero. If* $k > 1$ *(or equivalently* $\sqrt{\alpha/4} > 1$*), then the laminar solutions are unstable. Therefore, laminar solutions change stability and hence bifurcate at* $\sqrt{\alpha/4} = 1$.

Now before the discretization of the KSE (1.15) we need to say few words about the truncation of Fourier series approximation of the solution. Since the closure of the Fourier basis with respect to the topology induced by the L_2 norm contains all the 2π-periodic functions, so the solution to the KSE for fixed time can be approximated, at least in the L_2 sense, to any accuracy by a Fourier series. Again due to the presence of a strong diffusion term for higher wave numbers, a rapid convergence of the Fourier series is expected , and hence the truncation of the Fourier series to a finite set of coordinates is reasonable. Besides here we assume that the solution of KSE is smooth and the initial data is spatially periodic with period 2π which also support the representation of the solution by a truncated Fourier series.

The existence, uniqueness, regularity, and the nonlinear stability for all time t of the solution of KSE system (1.15)- (1.18) are well understood and are studied by R. Temam in [16]. The author in his book proved that the solution $u(x,t)$ of KSE system remains bounded for all time. This mathematical result validates the finite dimensional representation of the solution of the KSE by truncation of higher frequencies. The appropriate size of the truncation can be determined by numerical study of the decay rate of the associated Fourier coefficients. Therefore, we can now approximate the solution $u(x,t)$ of our model KSE system as $u_N(x,t)$ by the following truncated Fourier series

$$u_N(x,t) = \sum_{k=-N}^{k=N} \hat{u}_k e^{ikx}, \tag{2.30}$$

where the expansion coefficients $\hat{u}_k = \hat{u}_k(t)$ are functions of time t, $t \in [0,T]$. By the conservative nature of KSE (1.15), $\hat{u}_0(t)$ remains constant, i.e.,

$$
\begin{aligned}
\frac{d}{dt}\hat{u}_0(t) &= \frac{1}{2\pi}\frac{d}{dt}\int_0^{2\pi} u(x,t)dx \\
&= \frac{1}{2\pi}\int_0^{2\pi} \partial_t u(x,t)dx \\
&= -\frac{1}{2\pi}\int_0^{2\pi} (\alpha u\partial_x u + \alpha\partial_x^2 u + 4\partial_x^4 u)dx, \text{ since } u(x,t) \text{ is } 2\pi\text{-periodic} \\
&= 0
\end{aligned} \tag{2.31}
$$

But in fact, $\hat{u}_0(t) = 0$ as we see from the straightforward calculation that

$$\hat{u}_0 = \frac{1}{2\pi}\int_0^{2\pi} u(x)dx = 0,$$

since $u(x) = \partial_x v(x)$ and $v(x)$ is periodic with period 2π.

Denoting the residual of the solution by $R_N(x,t)$ defined on the domain $[0,2\pi]\times[0,T]$ we have

$$R_N = \partial_t u_N + \alpha(u_N\partial_x u_N + \partial_x^2 u_N) + 4\partial_x^4 u_N \tag{2.32}$$

The Galerkin method consists of setting to zero the scalar product

$$(R_N, \psi_n)_w = \int_0^{2\pi} R_N \psi_n w dx$$

where $\psi_n = e^{inx}$, $n = -N, -N+1, \ldots, N-1, N$, form the Fourier basis and $w(x) = 1$ is the weighting function associated with the orthogonality of the basis functions ψ_n, both of which are defined on the given spatial domain $\Omega = [0,2\pi]$. Therefore we have the following Galerkin conditions

$$(R_N, e^{inx}) = 0, \tag{2.33}$$

where $n = -N, \ldots, N$

Now the Fourier series expansion of the nonlinear product

$$P_N := P_N(x,t) = u_N(x,t)\partial_x u_N(x,t)$$

can be written as

$$\begin{aligned} F_N &= \sum_{q=-N}^{N} \hat{u}_q(t) e^{iqx}\, \partial_x \sum_{p=-N}^{N} \hat{u}_p(t) e^{ipx} \\ &= i \sum_{p,q=-N}^{N} p\hat{u}_p\hat{u}_q e^{i(p+q)x} \\ &= i \sum_{k=-2N}^{2N} \sum_{\substack{p,q=-N \\ p+q=k}}^{N} p\hat{u}_p\hat{u}_q e^{ikx}, \end{aligned} \tag{2.34}$$

where $\hat{u}_p = \hat{u}_q = 0$, for $|p|, |q| > N$

Using (2.34) in (2.32) and expressing different terms of (2.32) by their corresponding Fourier series, and then substituting (2.32) in (2.33), we have

$$\begin{aligned} \sum_{k=-N}^{N} (\dot{\hat{u}}_k + 4k^4\hat{u}_k - \alpha k^2\hat{u}_k) \int_0^{2\pi} e^{i(k-n)x} dx \\ + \alpha i \sum_{k=-2N}^{2N} \sum_{p,q=-N}^{N} p\hat{u}_p\hat{u}_q \int_0^{2\pi} e^{i(k-n)x} dx = 0, \end{aligned} \tag{2.35}$$

where $n = -N, -N+1, \ldots, N-1, N$, and $\hat{u}_r = 0$, for $|r| > N$. Finally, due to the orthogonality relation (2.14) we obtain the Galerkin equations

$$\dot{\hat{u}}_k + (4k^4 - \alpha k^2)\hat{u}_k + \alpha\hat{w}_k = 0, \quad k = -N, -N+1, \ldots, N-1, N \tag{2.36}$$

where

$$\hat{w}_k = i \sum_{\substack{p,q=-N \\ p+q=k}}^{N} p\hat{u}_p\hat{u}_q$$

To describe the time integration method, let us first discretize the equation (1.15) in space, and then in time with a very simple semi-implicit scheme. If we denote by u_N^n the Fourier series approximation u_N of the solution of KSE (1.15) at time $t_n = n\Delta t$, $n = 0, 1, \ldots$, where Δt is the time steps, then the equation (1.15) first discretized in space, and then in time so that the residual R_N becomes

$$R_N = \frac{u_N^{n+1} - u_N^n}{\Delta t} + \alpha(\partial_x^2 u_N^{n+1} + u_N^n \partial_x u_N^n) + 4\partial_x^4 u_N^{n+1} \tag{2.37}$$

where we considered

- the nonlinear term explicitly to avoid costly iterations
- the linear terms implicitly to allow one to mitigate the stability restrictions on the time step Δt that arises from the discretization of equation (1.15)
- the first-order accurate explicit/implicit Euler scheme just to make the discretization simpler.

Therefore after the obvious implementation of the time discretization the Galerkin equations (2.36) then take the form

$$\hat{u}_k^{n+1} = (\hat{u}_k^n - \alpha\Delta t \hat{w}_k^n)/\{1 + \Delta t(4k^4 - \alpha k^2)\}, \quad k = -N, -N+1, \ldots, N-1, N \tag{2.38}$$

where

$$\hat{w}_k^n = i \sum_{\substack{p,q=-N \\ p+q=k}}^{N} p\hat{u}_p^n \hat{u}_q^n$$

Note that in system (2.38) $\hat{u}_k^n$ is the approximation of $\hat{u}_k$ at the time $n\Delta t$. Therefore knowing the initial value $\hat{u}_k^0$, which is the Fourier transform of the initial condition (1.17), we can compute the solution $\hat{u}_k^n$ directly from (2.38) without any iteration.

However an interesting question may appear regarding the evaluation of the convolution sum $\hat{w}_k^n$ which must be computed as efficiently as possible. This is obtained through the so-called *"pseudospectral technique"*. This technique consists of performing the differentiations in the spectral space (the space of coefficients $\hat{u}_k^n$, $k = -N, \ldots, N$) and the products in the physical space (the space of the values $u_N(x_j)$ at the collocation points $x_j = 2\pi j/M$, $j = 1, \ldots, M = 2N+1$). Note that the calculation of $\hat{w}_k^n$ in Fourier space requires $O(N^2)$ operations, but the transition between the two spaces is made by the *FFT* (*Fast Fourier Transform*) which costs *"only"* $O(Nlog(N))$ operations. The algorithm is then given as follows:

1. calculate (using inverse *FFT*) $u_N^n(x_j)$, $j = 1, \ldots, M$ from $\hat{u}_k^n$, $k = -N, \ldots, N$,
2. calculate (using inverse *FFT*) $\partial_x u_N^n(x_j)$, $j = 1, \ldots, M$ from iku_k^n, $k = -N, \ldots, N$,
3. calculate the product $w_N^n(x_j) = u_N^n(x_j)\partial_x u_N^n(x_j)$, $j = 1, \ldots, M$
4. calculate (using *FFT*) $\tilde{w}_k^n$, $k = -N, \ldots, N$ from $w_N^n(x_j)$, $j = 1, \ldots, M$

where because of the *aliasing phenomenon* the quantity $\tilde{w}_k^n$ is different from

$$\hat{w}_k^n = i \sum_{\substack{p,q=-N \\ p+q=k}}^{N} p\hat{u}_p^n \hat{u}_q^n$$

However there is an efficient way to remove the aliasing error that arises in the spectral discretization of the product of two functions. The rule of aliasing removal is called *3/2-rule*. To discuss this approach let us consider two 2π-periodic functions

$$a_N(x) = \sum_{k=-N}^{N} \hat{a}_k e^{ikx}, \qquad b_N(x) = \sum_{k=-N}^{N} \hat{b}_k e^{ikx}$$

Then after simplification the coefficient of the product $w(x) = a(x)b(x)$ are found to be

$$\tilde{w}_k = \hat{w}_k + \sum_{\substack{p,q=-N \\ p+q=k+M}}^{N} \hat{a}_p \hat{b}_q + \sum_{\substack{p,q=-N \\ p+q=k-M}}^{N} \hat{a}_p \hat{b}_q,$$

where $\hat{w}_k$ are the coefficients of the convolution sum that we want to obtain only. Then the following algorithm addresses the issue of aliasing removal.

1. Extend the spectra $\hat{a}_k$ and $\hat{b}_k$ to $\hat{a}'_k$ and $\hat{b}'_k$ according to

$$\hat{a}'_k = \begin{cases} \hat{a}_k & \text{if } |k| \le N \\ 0 & \text{if } N < |k| \le N' \end{cases} \qquad \hat{b}'_k = \begin{cases} \hat{b}_k & \text{if } |k| \le N \\ 0 & \text{if } N < |k| \le N' \end{cases}$$

   where $N' = 3N/2$.

2. Calculate(via FFT) a_N and b_N in real space on the extended grid $x'_n = 2\pi n/M$, $n = 1,2,\ldots,M = 2N'+1$:

$$a_N(x'_n) = \sum_{k=-N'}^{N'} \hat{a}'_k e^{ikx'_n}, \qquad b_N(x'_n) = \sum_{k=-N'}^{N'} \hat{b}'_k e^{ikx'_n}$$

3. Multiply $a_N(x'_n)$ and $b_N(x'_n)$:

$$w(x'_n) = a_N(x'_n) b_N(x'_n), \quad n = 1,2,\ldots,M.$$

4. Calculate(via FFT) the Fourier coefficients of the product $w'(x'_n)$:

$$\tilde{w}'_k = \frac{1}{M} \sum_{n=1}^{M} w(x'_n) e^{-ikx'_n}, k = -N',\ldots,N'.$$

Taking the later quantity for $k = -N,\ldots,N$ gives an expression for the convolution sum free of aliasing errors (R. Peyret [15]).

2.3.2 Discretization of steady KSE

The steady KSE which is obtained by simply setting $\partial_t u = 0$ in the time dependent equation (1.15) is

$$\alpha(\partial_x^2 u + u\partial_x u) + 4\partial_x^4 u = 0, \quad x \in [0, 2\pi] \tag{2.39}$$

where $u = u(x)$ and $u \in H_p^2(0, 2\pi)$ (the associated solution space is defined in section 1.5). Approximating the solution of equation (2.39) by the truncated Fourier series as in the previous section, except that here the expansion coefficients are constants, rather than function of time, we have the following discretized steady state equation:

$$F_k := (4k^4 - \alpha k^2)\hat{u}_k + \alpha i \sum_{p=-N}^{N} p\hat{u}_p\hat{u}_{k-p} = 0, \quad k = -N, \ldots, N \tag{2.40}$$

where $F_k : \mathbb{C}^{N+1} \to \mathbb{C}$.

It has been noticed that the expansion coefficient for the zeroth mode $\hat{u}_0$ is indeterminate from the equation (2.40), but we deduced as before that $\hat{u}_0 = 0$. Hence, using the complex conjugate relation (2.13), we obtain the following system of M (letting $N - 1 = M$) nonlinear equations

$$\mathbf{F}_k(\hat{u}_1, \ldots, \hat{u}_M) = 0, \qquad k = 1, 2, \ldots, M, \qquad |k + p| \leq M \tag{2.41}$$

where $\mathbf{F}_k = [F_1 \;\; F_2 \;\; \ldots \;\; F_M]^T$,

$$F_k = (4k^4 - \alpha k^2)\hat{u}_k + \alpha i \sum_{p=1}^{k-1} p\hat{u}_p\hat{u}_{k-p} + \alpha i \sum_{p=k+1}^{M} p\hat{u}_p\bar{\hat{u}}_{p-k} - \alpha i \sum_{p=1}^{M} p\bar{\hat{u}}_p\hat{u}_{k+p}$$

provided that $\hat{u}_{k+p} = 0$, for $k+p > M$. The equation (2.41) represents a system of M nonlinear equations in M expansion coefficients $\hat{u}_1, \ldots, \hat{u}_M$ to be determined.

There are many well established numerical methods to solve such a nonlinear system of equations. Among them *Newton's method* is an attractive possibility because it is fairly straightforward to implement and has good convergence properties. The formula for solving the system of equations (2.41) is given by

$$\hat{\mathbf{u}}^{n+1} = \hat{\mathbf{u}}^n - [\mathbf{F}'_k(\mathbf{u}^n)]^{-1}\mathbf{F}_k(\mathbf{u}^n)$$

where n denotes the iteration count, $\mathbf{u}^0 = [\hat{u}_1^0, \ldots, \hat{u}_M^0]^T$ is an initial guess of the solution to the given system, $[\mathbf{F}'_k(\mathbf{u}^n)]^{-1}$ is the inverse of the Jacobian matrix $\mathbf{F}'_k(\mathbf{u}^n)$ computed at the n-th iteration, and $\mathbf{F}_k(\mathbf{u}^n)$ is the value of the vector function at the present iteration under certain assumptions. The convergence rate of this method is quadratic.

Now in order to solve the above system using the Newton's method we need to compute the Jacobian of the system evaluated at every iteration. Note that the vector function $\mathbf{F}_k : \mathbb{C}^M \to \mathbb{C}^M$ is a complex valued function and contains the conjugate of every complex variable $\hat{u}_1, \ldots, \hat{u}_M$. Because of the presence of complex conjugates, the function $\mathbf{F}_k$ is not formally differentiable, therefore Jacobian cannot be defined properly. This necessitates transformation of the above system into a form for which $\mathbf{F} : \mathbb{R}^{2M} \to \mathbb{R}^{2M}$ is differentiable and the Jacobian can be defined, where $\mathbf{F}_k^r$ and $\mathbf{F}_k^i$ are real and complex part of $\mathbf{F}_k$ respectively, and $\mathbf{F} := [\mathbf{F}_k^r \;\; \mathbf{F}_k^i]^T$

This can be done by using the substitution $\hat{u}_k = \xi_k + i\eta_k$, $k = 1, 2, \ldots, M$ in equation (2.41), using the complex conjugate relation for the real valued solution, and finally splitting real and complex parts of the original system. Hence after simplification we obtain the following system of $2M$ nonlinear algebraic equations in terms of real variables ξ_k and η_k for $k = 1, \ldots, M$

$$\begin{bmatrix} \mathbf{F}_k^r \\ \mathbf{F}_k^i \end{bmatrix} = 0, \quad k = 1, 2, \ldots, M \tag{2.42}$$

where

$$\mathbf{F}_k^r = \mathbf{F}_k^r([\xi_1 \ \ldots \ \xi_M \ \eta_1 \ \ldots \ \eta_M]^T)$$

and

$$\mathbf{F}_k^i = \mathbf{F}_k^i([\xi_1 \ \ldots \ \xi_M \ \eta_1 \ \ldots \ \eta_M]^T)$$

are explicitly given by

$$\begin{aligned}
\mathbf{F}_k^r : &= (4k^4 - \alpha k^2)\xi_k - \alpha \sum_{p=1}^{k-1} p(\xi_p \eta_{k-p} + \xi_{k-p}\eta_p) \\
&\quad + \alpha \sum_{p=k+1}^{M} p(\xi_p \eta_{p-k} - \xi_{p-k}\eta_p) + \alpha \sum_{p=1}^{M} p(\xi_p \eta_{k+p} - \xi_{k+p}\eta_p) \\
\mathbf{F}_k^i : &= (4k^4 - \alpha k^2)\eta_k + \alpha \sum_{p=1}^{k-1} p(\xi_p \xi_{k-p} - \eta_p \eta_{k-p}) \\
&\quad + \alpha \sum_{p=k+1}^{M} p(\xi_p \xi_{p-k} + \eta_p \eta_{p-k}) - \alpha \sum_{p=1}^{M} p(\xi_p \xi_{k+p} + \eta_p \eta_{k+p})
\end{aligned} \tag{2.43}$$

provided that $\xi_{k+p} = \eta_{k+p} = 0$, for $k + p > M$.

The corresponding Jacobian matrix $\mathbf{J}$, calculated at some fixed point (ξ_k, η_k), having dimension $2M$ for the system of equations (2.42) is

$$\mathbf{J} = \begin{bmatrix} \frac{\partial \mathbf{F}_k^r}{\partial \xi_q} & \frac{\partial \mathbf{F}_k^r}{\partial \eta_q} \\ \frac{\partial \mathbf{F}_k^i}{\partial \xi_q} & \frac{\partial \mathbf{F}_k^i}{\partial \eta_q} \end{bmatrix} \tag{2.44}$$

where each entry of $\mathbf{J}$ is a block matrix of size $M \times M$ and they are respectively given by

$$
\begin{aligned}
\frac{\partial \mathbf{F}_k^r}{\partial \xi_q} &= (4k^4 - \alpha k^2)\delta_q^k - \alpha k \eta_{k-q} - \alpha k \eta_{k+q} + \alpha k \eta_{q-k}, \\
\frac{\partial \mathbf{F}_k^r}{\partial \eta_q} &= -\alpha k \xi_{k-q} + \alpha k \xi_{k+q} - \alpha k \xi_{q-k}, \\
\frac{\partial \mathbf{F}_k^i}{\partial \xi_q} &= \alpha k \xi_{k-q} + \alpha k \xi_{k+q} + \alpha k \xi_{q-k}, \\
\frac{\partial \mathbf{F}_k^i}{\partial \eta_q} &= (4k^4 - \alpha k^2)\delta_q^k - \alpha k \eta_{k-q} + \alpha k \eta_{k+q} + \alpha k \eta_{q-k},
\end{aligned}
\tag{2.45}
$$

where $k, q = 1, 2, \ldots, M$. Note that we have obtained the equations (2.45) after applying the complex conjugacy relations for $\hat{u}_k = \xi_k + i\eta_k$, $k = 1, 2, \ldots, M$. Therefore we will compute (2.45) where $k, q = 1, 2, \ldots, M$ and $0 < k - q \leq M$ and $0 < q - k \leq M$.

2.4 Bifurcation Patterns for the Steady Solutions

In our investigation we want to study stabilization of different solutions at the same value of the parameter α in the KSE model which requires some knowledge about bifurcation. For better presentation we would like to mention the definition of bifurcation along with some examples.

Bifurcation is

- the phenomenon of the change of the type of a solution of a nonlinear problem and
- related to existence and appearance of multiple solutions of the same nonlinear problem.

In particular, interest centers on how to detect, calculate and classify points where there is a change in the type of solution of the nonlinear problem. In other words, bifurcations occur for dynamical systems if the phase portraits undergo some topological qualitative

changes. More briefly, there is no continuous deformation of the curves of one phase portrait to the curves of the other phase portrait. All local bifurcations are related to non-hyperbolic critical points but the global bifurcations are not so related. Let us discuss them by the following two examples:

Example 1 *Consider the following vector field:*

$$y' = g(y,\lambda) = \lambda y - y^2, \quad y \in \mathbb{R}, \quad \lambda \in \mathbb{R} \tag{2.46}$$

Note that $g(0,0) = 0$ and $\partial_y g(0,0) = 0$. The equilibrium points of (2.46) are given by $y = 0$ and $y = \lambda$. But $\lambda = 0$, $y = 0$ is the only nonhyperbolic equilibrium point. If $\lambda < 0$, the equilibrium point $y = 0$ is stable but $y = \lambda$ is unstable. If $\lambda = 0$ then the two equilibrium points coincide and hence there is a change in stability. If $\lambda > 0$, the solution $y = 0$ is unstable and $y = \mu$ is stable. Therefore, there occurs a bifurcation at $\lambda = 0$, called the trans-critical bifurcation.

Now consider the second example:

Example 2 *Suppose the vector field is given by*

$$y' = g(y,\lambda) = \lambda - y^3, \quad y \in \mathbb{R}, \quad \lambda \in \mathbb{R} \tag{2.47}$$

Obviously, $g(0,0) = 0$ and $\partial_y g(0,0) = 0$, and the only nonhyperbolic equilibrium point is $y = 0$, at $\lambda = 0$. But in this case the dynamics of the equation (2.47) remains same when $|\lambda| > 0$ and hence there is no bifurcation at the nonhyperbolic point $(0,0)$.

The study of the bifurcation points of a vector field helps us in understanding the dynamical behavior of the vector field. This means that a small perturbation of a vector field at a bifurcation point characterizes all possible dynamical behavior of the system under consideration in a small neighborhood of the bifurcation point. Bifurcations are divided into two categories, namely, *local* and *global*. Local bifurcations can be studied analytically whereas global bifurcations are very difficult to deal with analytically. The former

ones can be determined by studying the eigenvalues and the Taylor series expansion but the later ones can not be determined in this way (see S. Wiggins [17]).

2.5 Computational results for steady state

The steady solutions are obtained by Newton's method. In this method an initial solution is iterated until it converges to a solution up to certain accuracy. The converged solution is then considered as a steady state solution of the KSE system. In Fig. 2.2(a) we summarized the convergence of the steady state results as the resolution is refined. As a reference point we have chosen $\alpha = 12$. From this figure we observe that the more we refine the resolutions the smoother steady states we have. The long dashed line represents the solution for $N = 8$, the dotted line represents solution for $N = 16$, the dashed line represents the solution for $N = 32$, the dashed spaced line represents the solution for $N = 64$, and finally the solid line represents the solution for $N = 128$. A magnification of Fig. 2.2(a) is provided in Fig. 2.2(b).

An account of the decay of the solution error in Newton's method for the steady states is portrayed in Fig. 2.3. From the stability analysis of the linear problem

$$\alpha \frac{d^2u}{dx^2} + 4\frac{d^4u}{dx^4} = 0$$

defined on $x \in [0, 2\pi]$ obtained after linearizing the nonlinear steady KSE about the laminar state $\tilde{u} = 0$ we know that at every integer point of $\sqrt{\alpha/4}$ there is a bifurcation. Since at every bifurcation point the stability matrix $\mathbf{J}$ has at least one vanishing eigenvalue, so the matrix $\mathbf{J}$ is singular there and hence its inverse does not exist. Therefore, as the bifurcation parameter α approaches its bifurcation value, the conditioning of the Jacobian $\mathbf{J}$ deteriorates and therefore finding solution of the problem becomes more difficult. This is reflected in Fig. 2.3. For example, $\alpha = 4$ and $\alpha = 16$ are two bifurcation points of the laminar state

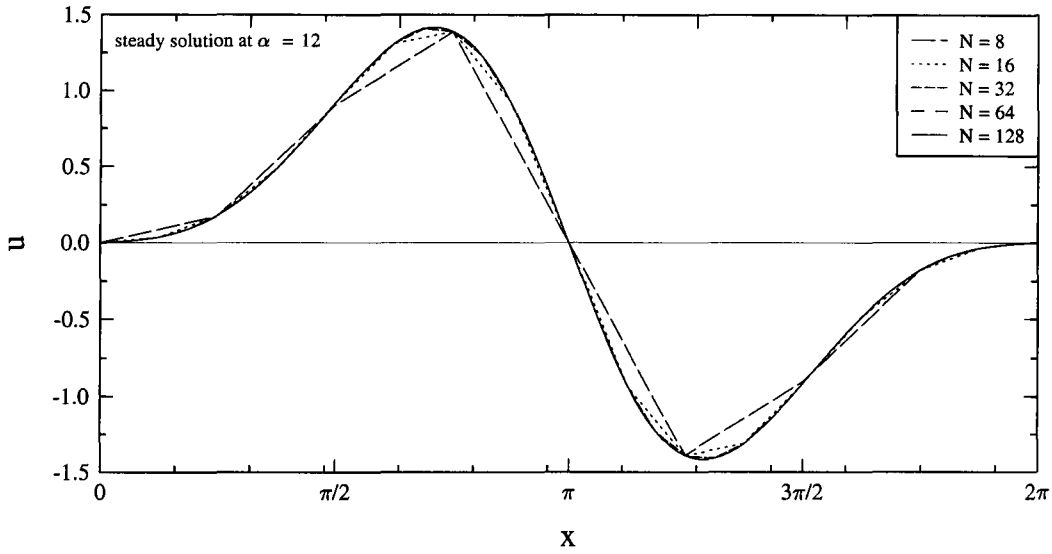

(a)

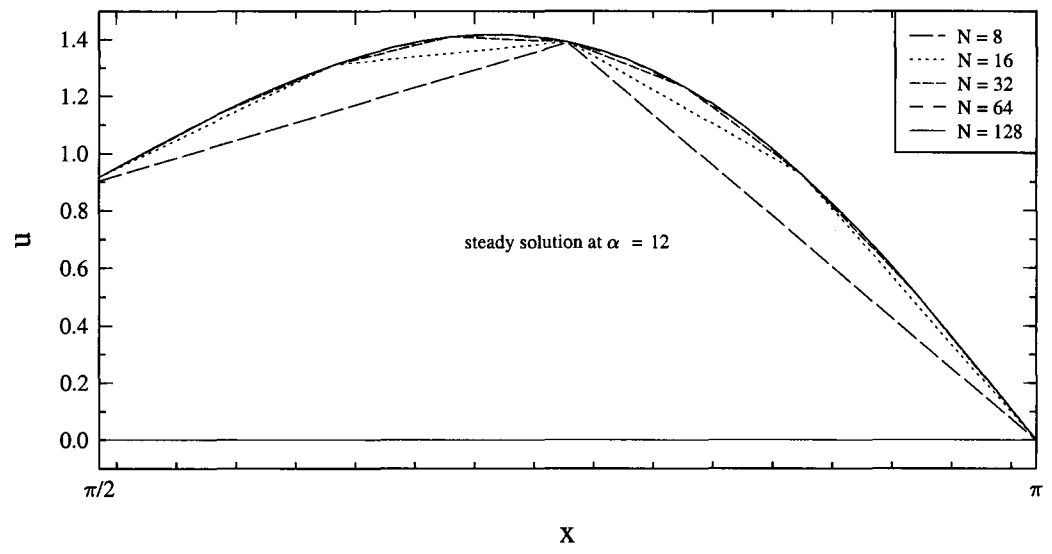

(b)

Figure 2.2: *Steady state u as a function of x. (a) Display of convergence of the steady state results as discretization is refined. (b) A magnification of Fig. 2.2(a). Display of convergence of the steady state results as discretization is refined.*

and $\alpha = 8$ is far from bifurcation points. The convergence of Newton's iteration is much faster when the solution is calculated at point α far from its bifurcation values.

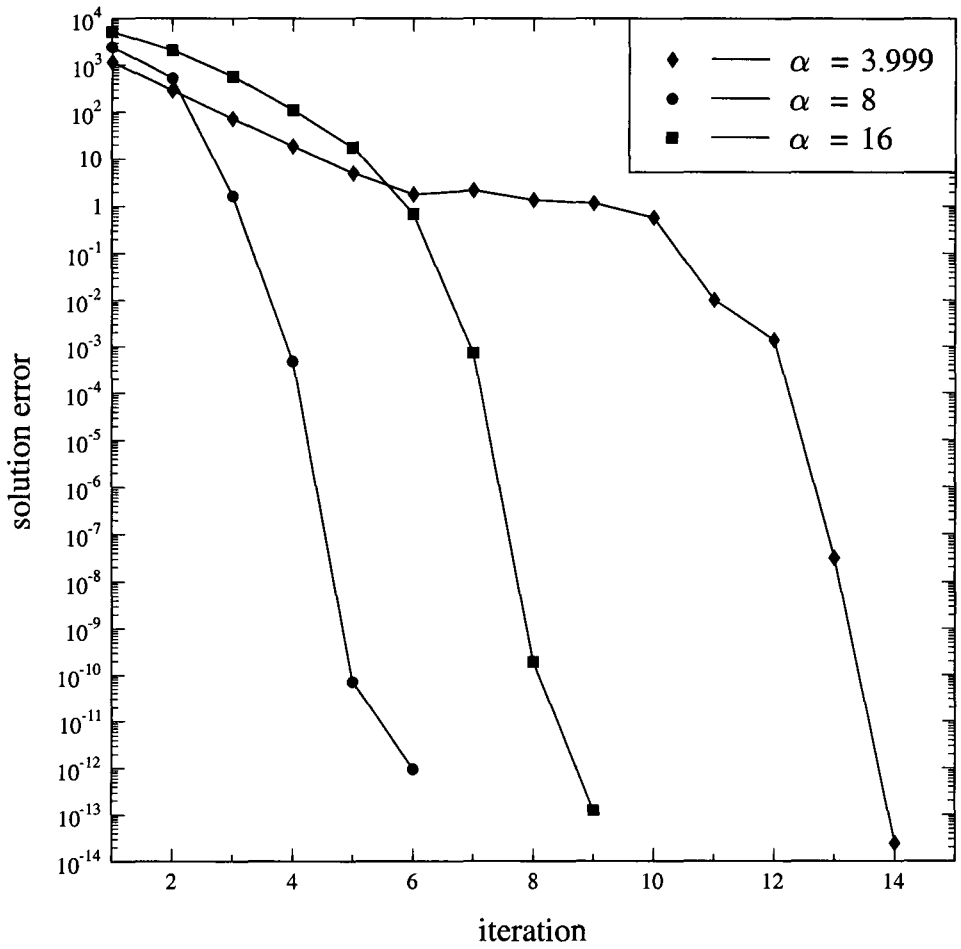

Figure 2.3: *Solution error as a function of Newton's iteration. The diamond line shows solution error for* $\alpha = 3.999$. *The circled line shows solution error for* $\alpha = 8$ *and the squared line shows solution error for* $\alpha = 16$.

We define energy of the steady state KSE (2.39) as

$$E := ||u(x)||_{L_2}^2 = \frac{1}{2\pi}\int_{\Omega} u^2(x)dx = \sum_{k=-N}^{N} |\hat{u}_k|^2$$

where $\hat{u}_k$ represents the k-th Fourier mode of the Fourier series expansion of $u(x)$ over the interval $\Omega = [0, 2\pi]$. Since a steady state bifurcates at every integer $\sqrt{\alpha/4} = n$, therefore the new state at bifurcation consists of the eigenvectors $\cos nx$ and $\sin nx$. We call the steady state that bifurcates at $\sqrt{\alpha/4} = n$ an n-cell state.

The calculated solutions are found to be extremely sensitive to the choice of initial guess. Since we are interested in the periodic solutions of KSE, so the preferred initial guess is also assumed to be periodic. We have chosen the initial guess (IG) as a sine function with adjustable frequency. By numerical observations we have developed an empirical relation between the amplitude and the angular frequency of the IG. For computing an n-cell steady state of KSE the best IG is chosen to be $A_n \sin nx$ where $A_n = 2n + 1$ (empirical formula). When a converged solution is found by the Newton's method for a given α, we then increase or decrease the parameter α successively to obtain a complete branch of steady states. We call this procedure a continuation technique. For $\sqrt{\alpha/4} = n < 1$ the laminar solution is stable and for any choice of initial guess we have numerically shown that the converged solution is a trivial solution. Therefore we call this branch a trivial branch as shown in Fig. 2.4. The n-cell branch of steady states exists for $n \geq 1$.

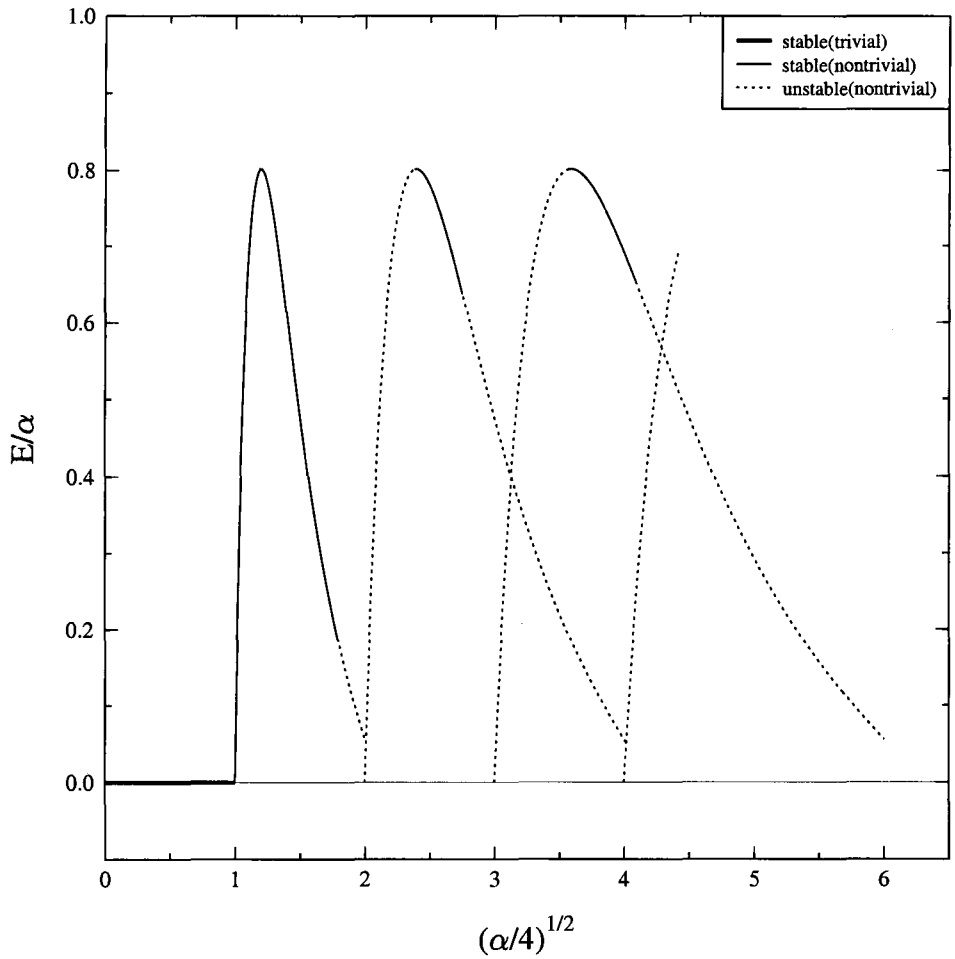

Figure 2.4: *Energy of steady states KSE as a function of the bifurcation parameter* $\sqrt{\alpha/4}$. *The bold solid line is a trivial solution, the solid and dotted lines are n-cell solutions. The solid line accounts for stable branches and the dotted line accounts for unstable branches.*

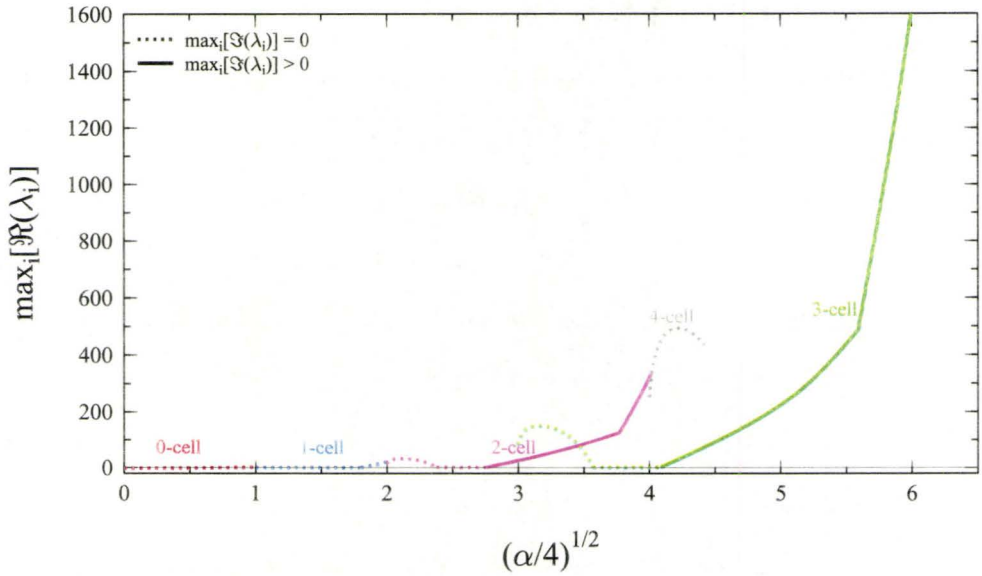

(a)

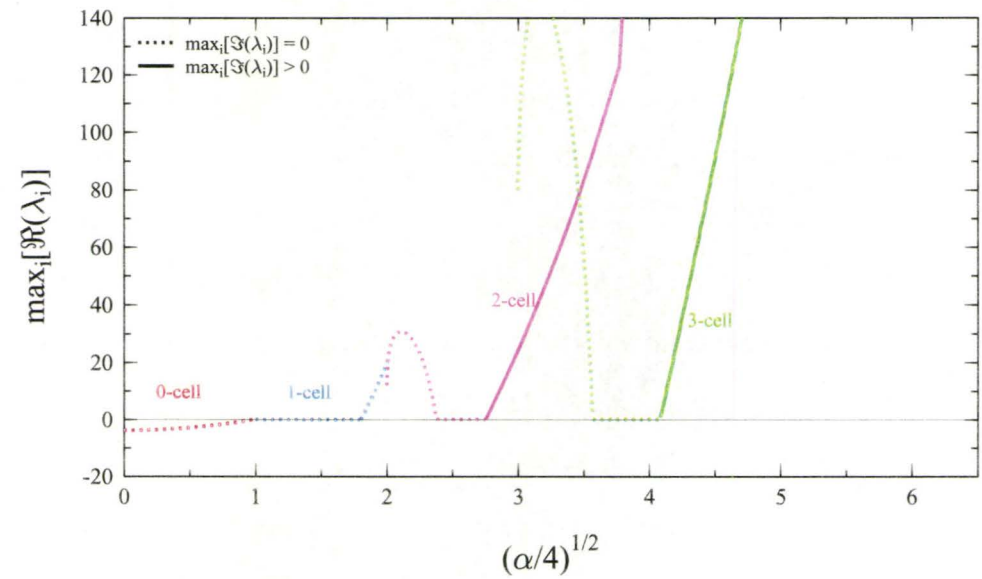

(b)

Figure 2.5: *Maximum real parts of eigenvalues is plotted as a function of bifurcation parameter* $\sqrt{\alpha/4}$. *(a) The bold solid line indicates all those eigenvalues with maximum real parts for which the eigenvalues with maximum imaginary parts is nonzero. The dotted line indicates all those eigenvalues with maximum real parts for which the eigenvalues with maximum imaginary parts is very close to zero. (b) A magnification of Fig. 2.5(a).*

First we have computed different branches of steady states of KSE reproducing the investigation done in [11], [12], and [13]. The resolution here we have taken is N = 128. We have presented the n-cell steady states in details in Fig. 2.4 by plotting energy E of the steady states as a function of the bifurcation parameter α. Since the laminar state bifurcates at every integer value of $\sqrt{\alpha/4}$, for better presentation we have labeled the horizontal axis as $\sqrt{\alpha/4}$. Similarly after scaling energy E by α we have labeled the vertical axis as E/α. In Fig. 2.4 we have plotted trivial branch, 1-cell, 2-cell, 3-cell, and some part of 4-cell branches of the steady states in terms of their energies.

The trivial branch ends on 1-cell branch and all other nontrivial n-cell branches end on $2n$-cell branches. From the figure it is obvious that there is a good resemblance among the nontrivial branches. The laminar state in Fig. 2.4 is represented by the horizontal axis, since it's energy is zero for any value of α. The bold solid line shows that the trivial branch is stable when $\sqrt{\alpha/4} < 1$ i.e., when $\alpha < 4$. The solid lines indicate the ranges of α in which the nontrivial branches are stable and the dotted lines indicate the ranges of α in which the nontrivial branches are unstable. These results are confirmed by the information of the eigenvalues as shown in the Fig. 2.5(a) and Fig. 2.5(b) of the linear stability matrix **J** (computed via (2.44)).

We have observed from Fig. 2.4 that 1-cell branch is stable in the interval $(4, 13)$ of α along the solid line and unstable on $[13, 16.125]$ along the dotted line. The 2-cell branch becomes unstable on $(16, 22.5]$, stable on $(22.5, 30.375)$, and then again unstable on $[30.375, 64.5]$. Similarly the 3-cell branch is unstable on $[36, 50.875]$, stable on $(50.875, 66.875)$, and again unstable on $[66.875, 144]$. As already mentioned that stability of the different solutions presented in Fig. 2.4 has been determined based on the data shown in Fig. 2.5. This figure presents the maximum real parts of the eigenvalues of the linearized

operator as a function of $\sqrt{\alpha/4}$. In fact, in the intervals redefined as stable the real parts of all the eigenvalues were very close to zero and a few of the eigenvalues has their real parts actually greater than zero. We believe that this is an artifact related to numerical calculation of the eigenvalues. However if we had considered these eigenvalues as zero, then the stability of the solutions that we have categorized here as stable would become inconclusive. This special problem requires further study of stability analysis which is beyond the scope of our thesis. Similar conclusions can be drawn for other branches of steady states. This confirms the results reported in (Hyman et al. [11]).

From the energy curves in Fig. 2.4 we have noticed that steady states of KSE are non unique. This means that for the same value of the parameter α we get different n-cell steady states. To address this issue we have chosen here some representative cases, for instance, when $\alpha = 16.1$, $\alpha = 37.75$, and $\alpha = 64.25$. Fig. 2.6(a) shows 1-cell and 2-cell steady states. Note that for $\alpha = 16.1$ there are three steady states, namely laminar state (trivial solution), 1-cell and 2-cell states. The laminar state is identical with the horizontal axis because its energy is zero. From the energy curve plotted in Fig. 2.4 or from the eigenvalue curve plotted in Fig. 2.5 we conclude that all the three states – laminar, 1-cell, and 2-cell, are unstable for $\alpha = 16.1$. In Fig. 2.6(a) the solid line represents 1-cell state and the dotted line represents 2-cell state. We have observed from the energy plot that 1-cell steady state ends at immediately after $\alpha = 16$ whereas the 2-cell steady state starts from $\alpha = 16$. Since 1-cell steady state is bifurcated to 2-cell steady state at $\alpha = 16$, therefore there is a competition between 1-cell and 2-cell steady states close to the bifurcation point. Hence the 1-cell steady state appears to be a 2-cell steady state near the bifurcation point. However there is a clear difference visible from the figure between the 1-cell and 2-cell steady states. This difference is reflected from the maxima and minima of the 1-cell and

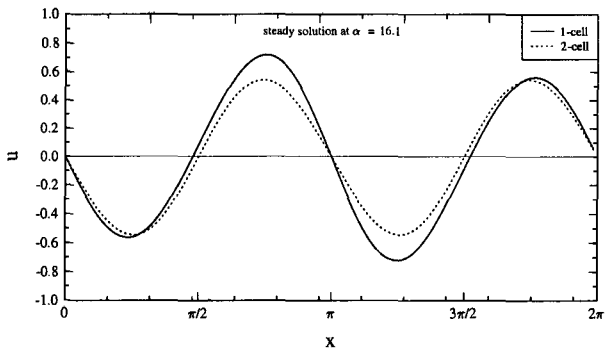

(a)

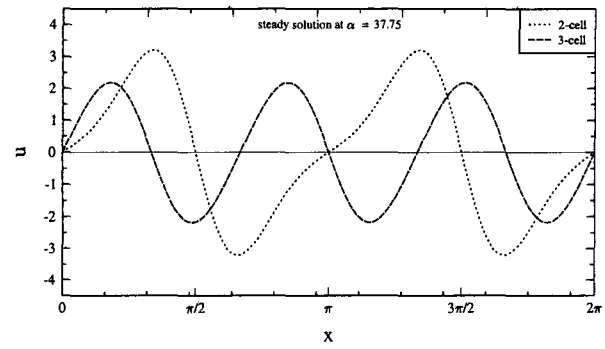

(b)

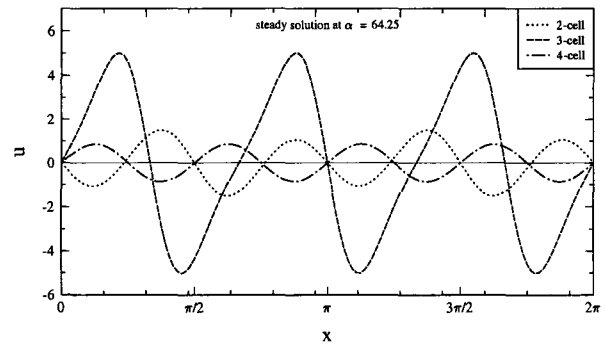

(c)

Figure 2.6: *Steady state u as a function of x. The laminar state is identical with horizontal axis. (a) Steady states at* $\alpha = 16.1$. *The solid line shows the 1-cell state and the dotted line shows the 2-cell state. (b) Steady states at* $\alpha = 37.75$. *The dotted line shows the 2-cell state. The dashed line shows the 3-cell state. (c) Steady states at* $\alpha = 64.25$. *The dotted line shows the 2-cell state. The dashed line shows the 3-cell state. The dashed dotted line shows the 4-cell state.*

2-cell steady states. Again in its domain a 2-cell steady state has 2-waves whereas a 1-cell steady state is dominated by 1-wave. Hence we may conclude that they are different steady states at the same value of the parameter.

2.6 Computational results for the unsteady state

From the study of steady state results of KSE we have observed that some states are stable for all time but some are not. These observations has tempted us to explore the properties of the unsteady KSE system. The unsteady KSE system is extensively studied by Hyman et al. [11]. They categorized alternating windows of α containing laminar behavior (fixed points) and windows of oscillatory and/or chaotic behavior of the unsteady solutions of KSE. As shown below we have reproduced different solutions as described in (Hyman et al. [11]). Now we define the L_2 norm of the solution as its energy E=E(t):

$$E = ||u(x,t)||_{L_2}^2 = \int_0^{2\pi} u^2(x,t)dx = \sum_{k=-N}^{N} |\hat{u}_k|^2,$$

where $\hat{u}_k(t)$ is the Fourier transform of $u(x,t)$.

We have discretized the unsteady KSE in space using spectral Galerkin method as described in section 2.3 and in time we have used a finite difference method. The time integration of the finite dimensional KSE has been done by Runge-Kutta-Wray (RKW) method because of its higher order accuracy compared to other time integration methods such as the Euler scheme. The resolution here we have taken is N = 128. As illustrated in the previous sections, the solutions of KSE are extremely sensitive to the initial conditions. Therefore special care has been taken to the right choice of initial condition. Here we have taken the initial condition $u_0(x) = \sin x$ of period 2π. This is a quite good choice for producing results of unsteady KSE having similar behavior to n-cell steady state solutions of KSE.

For numerical time integration we have taken 1.5×10^5 time steps. We have recalculated different solutions several times using different grid resolutions and got similar results.

We have systematically produced the attracting solution manifolds for the unsteady KSE. Here we have selected some representative values of α to analyze the corresponding unsteady solutions of KSE. For example, we have taken $\alpha = 10$ (where 1-cell steady state is stable), $\alpha = 14$ (where 1-cell steady state is unstable), and $\alpha = 37.75$ (where both 2-cell and 3-cell steady states are unstable) (details are discussed in Fig. 2.4). For the unsteady KSE if the solution trajectories are attracted as time evolves to some fixed points dominated by n full waves we call it n-modal solutions.

From the (x,t) contour plot drawn in Fig. 2.7(a) for $\alpha = 10$ it has been noticed that except for some transients at the beginning the unsteady solution of KSE is globally attracted to a unimodal fixed point. This is confirmed by the energy curve plotted in Fig. 2.7(b). This shows that after certain time at the beginning the energy of the unsteady solution remains the same. The initial condition here is chosen as $u_0(x) = \sin x$ to make sure that our attracting manifold becomes unimodal for $\alpha = 10$.

It is worthwhile to mention that if we choose the initial condition of unsteady KSE as $u_0(x) = \sin x$ for $\alpha = 10$ then after a transient the unsteady solution is attracted to a globally unimodal fixed point. However if we take the initial condition as a steady state, at the same value of α the unsteady solution remains on the 1-cell attractor without any transient change in the solution. This is evident from Fig. 2.8. Since 1-cell steady solution at $\alpha = 10$ is stable, so it remains steady and stable forever for the unsteady KSE.

Now we consider the unsteady KSE with initial condition taken as a 1-cell steady state solution for $\alpha = 14$ at which the steady state is unstable as we have illustrated before (see Fig. 2.4 and Fig. 2.5). This is a very interesting case from the view of the application of

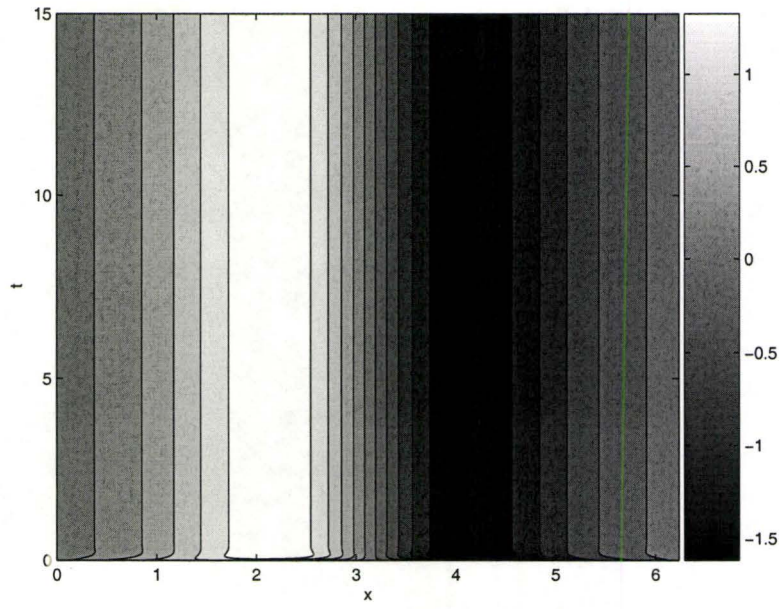

(a)

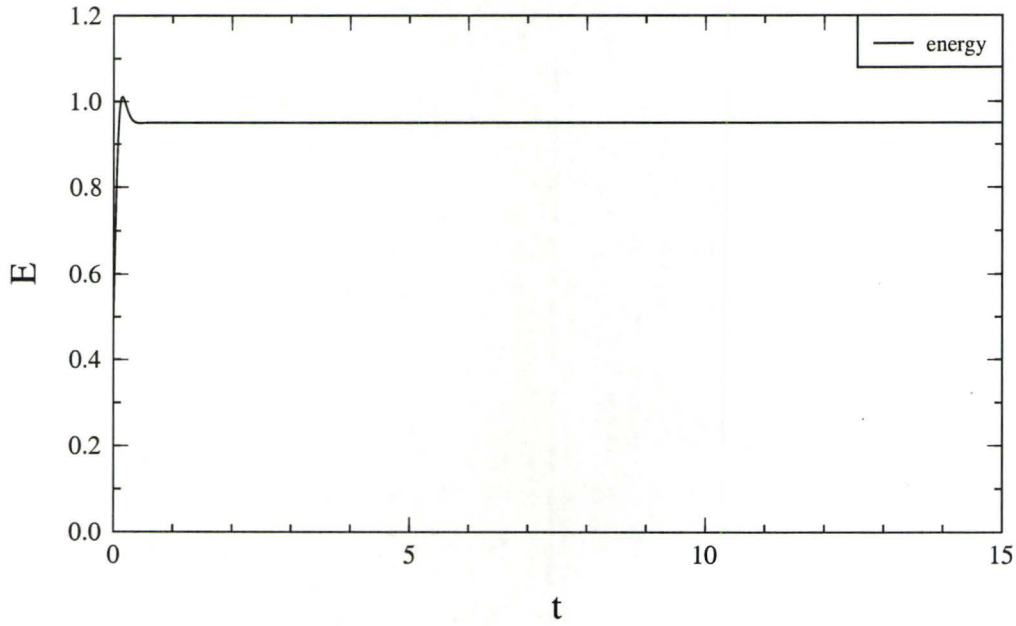

(b)

Figure 2.7: *Unsteady solution of KSE at* $\alpha = 10$ *with initial condition* $u_0(x) = \sin x$. *(a) The solution u is a function of space x and time t. The* (x,t) *contour plot of the solution of KSE shows that the solution is globally attracted to a unimodal fixed point. (b) Energy as a function of time t. The energy of the solution of KSE shows that the attracting manifold remains the same as time evolves.*

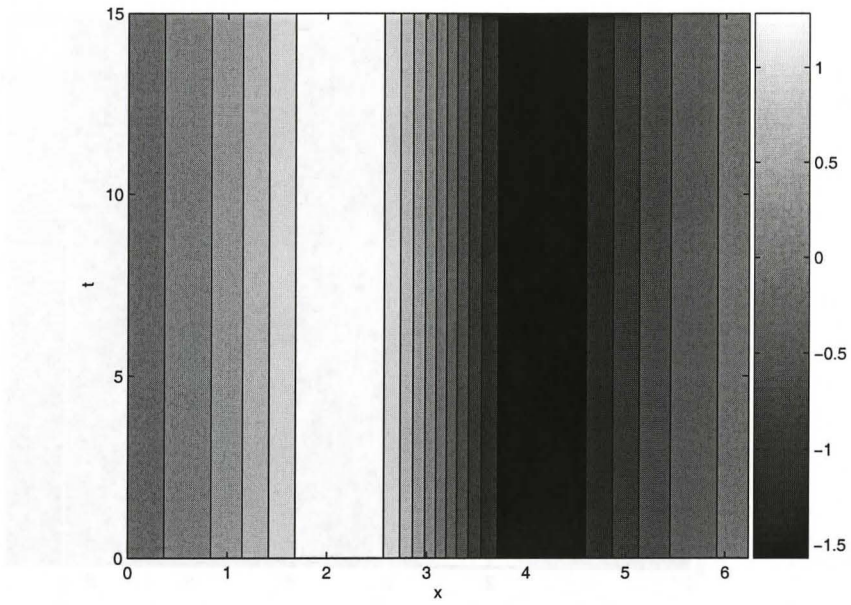

(a)

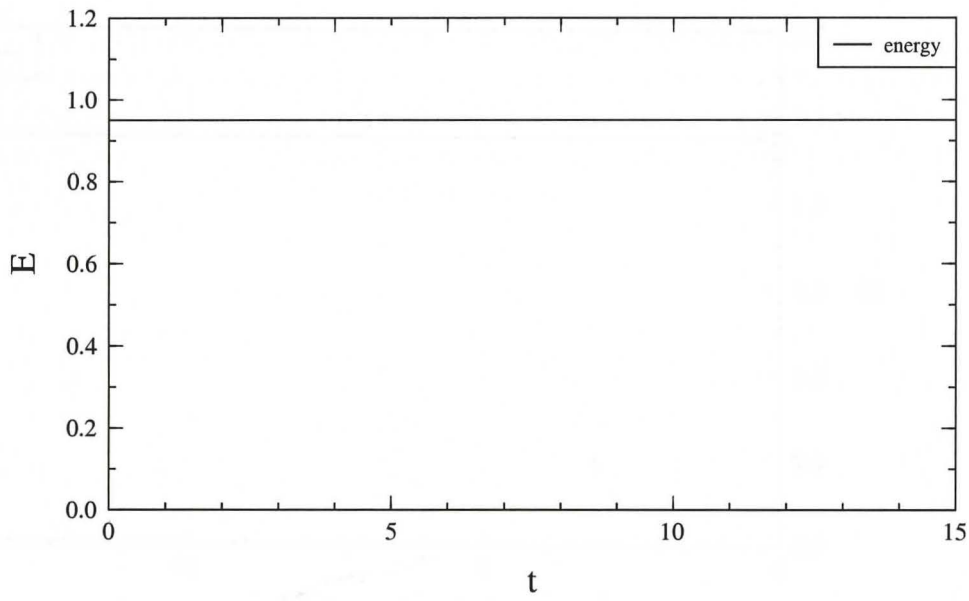

(b)

Figure 2.8. *Unsteady solution of KSE at* $\alpha = 10$ *with initial condition taken as the steady 1-cell solution at the same value of* α. *(a) Solution u as a function of space x and time t The* (x,t) *contour plot of the solution of KSE shows that the solution gets globally attracted to a unimodal fixed point. (b) Energy is a function of time t The energy of the solution of KSE shows that the solution stays on the attractor.*

control theory. Such issues become our primary concern throughout this project. From Fig. 2.9(a) we notice that the unsteady solution is locally attracted to a unimodal solution for certain time but soon after that the solution transitions to a traveling periodic wave regime. However, from the steady state results we have seen that at $\alpha = 14$ the solution is a 1-cell steady state but unstable. This means the unsteady trajectory is for some time ($t \leq 5$) attracted to the unstable 1-cell solution and before it transitions to a traveling periodic wave regime (see Fig. 2.9(a)). From the figure we see that for any time after $t = 5$ the unimodal solution is no longer seen since this is unstable. Fig. 2.9(b) shows that the energy E of the unsteady solution stabilizes at $E \approx 1.0$. The unstable unimodal solution that we have observed here is the type of solution we will try to stabilize below. It should be mentioned here that the characterization of bifurcations of the unstable n-cell steady state solution of KSE to new solutions requires calculation of the steady state traveling wave solutions of KSE. In our study we have simply ignored this case.

The next case for $\alpha = 37.75$ samples the oscillatory unsteady solution of KSE starting with same initial condition $u_0(x) = \sin x$. Note that the steady state solution of KSE at this value of α is unstable. From Fig. 2.10(a) we see that the unsteady solution of KSE gets attracted to oscillatory orbits. From Fig. 2.10(b) we see that the energy of the solution has periodic bursts. Here we are going to present one more result in Fig. 2.11 for unsteady KSE at $\alpha = 72$. At this value of α, we have seen that the 4-cell steady state is unstable (see Fig. 2.4). From Fig. 2.11(a) we notice that the trajectory of unsteady KSE gets attracted to chaotic orbits. Fig. 2.11(b) shows that there is a chaotic burst in the energy of the solution.

From practical point of view it is often advantageous to obtain solutions that are well-behaved (i.e., laminar, steady). Hence they need to be stabilized. Therefore the importance of stabilizing an unstable solution of KSE has further led us to study the control approach in

details. This requires a systematic study of control theory for the KSE system. In Chapter 3 first we will present the detailed control theoretic approach for KSE system starting from some basic materials in this subject. Later in that chapter we will provide some results of KSE for certain values of α after application of control approaches.

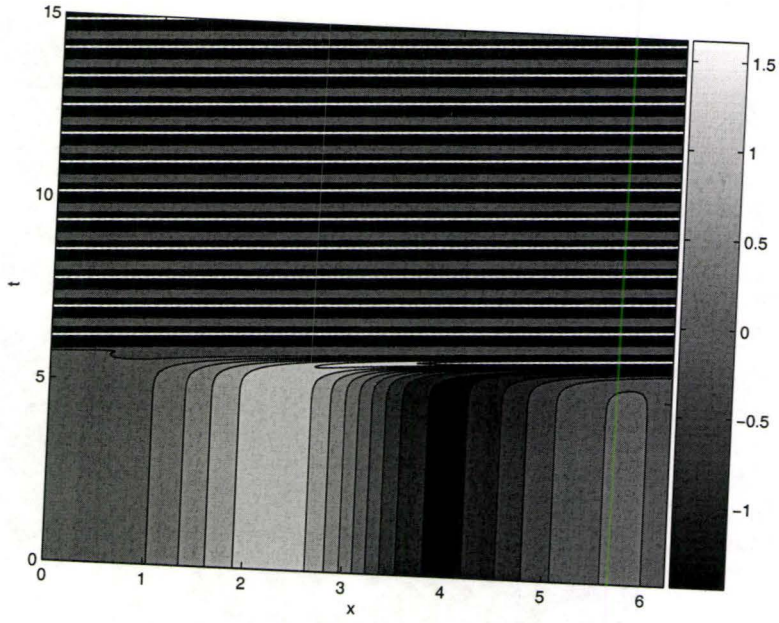

(a)

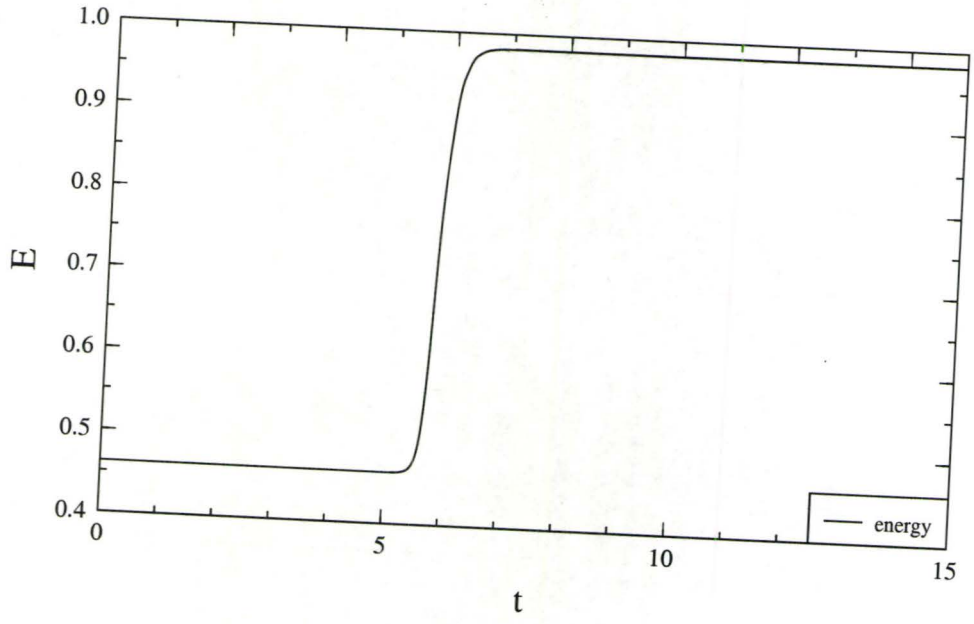

(b)

Figure 2.9: *Unsteady solution of KSE at* $\alpha = 14$ *with initial condition taken as a 1-cell steady state solution of KSE at the same value of* α. *(a) Solution* u *as a function of space* x *and time* t. *The* (x,t) *contour plot of the solution of KSE shows that the solution is attracted to a traveling periodic orbits. (b) Energy is a function of time* t. *The figure shows that energy* E *stabilizes on another attractor.*

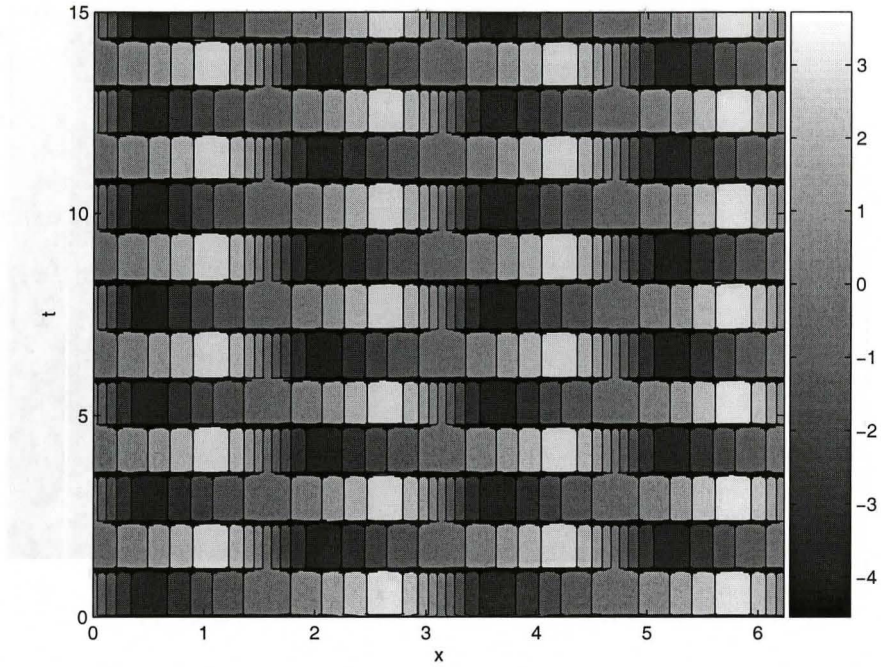

(a)

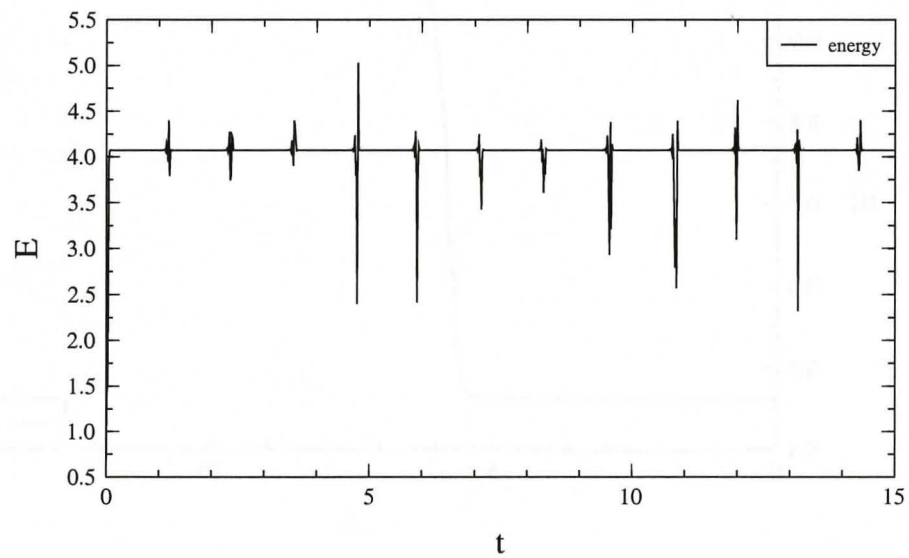

(b)

Figure 2.10: *Unsteady solution of KSE at* $\alpha = 37\ 75$ *with initial condition* $u_0(x) = \sin x$. *(a) Solution u as a function of space x and time t The* (x,t) *contour plot of the solution of KSE shows that the solution is attracted to the oscillatory orbits. (b) Energy is a function of time t This shows that the energy of the solution as time evolves remains the same except for transients when oscillation is observed.*

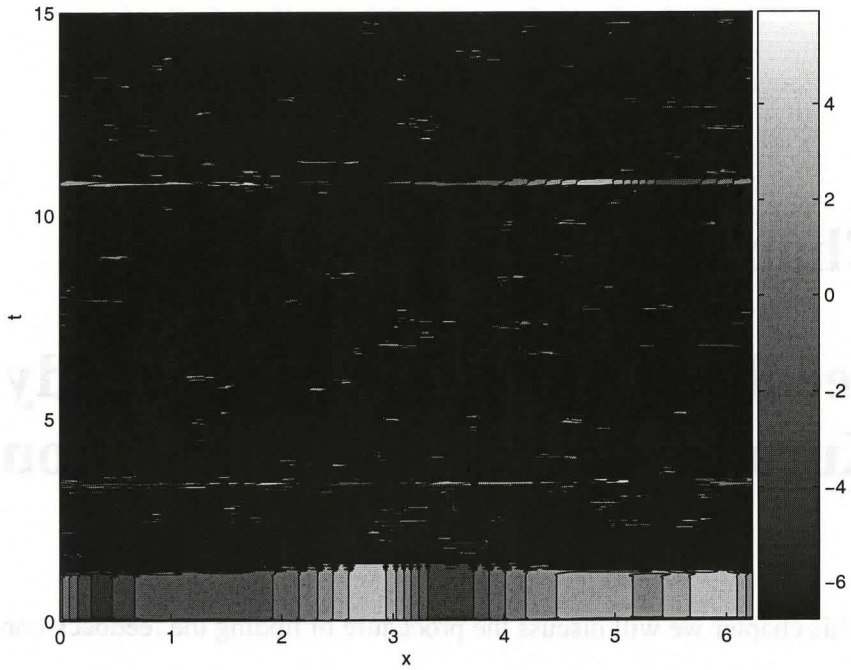

(a)

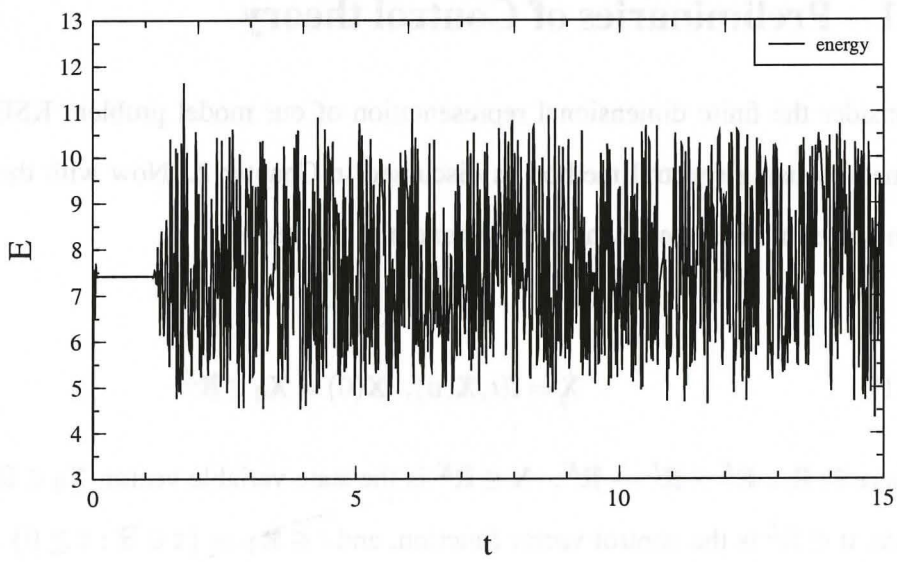

(b)

Figure 2.11 *Unsteady solution of KSE at* $\alpha = 72$ *with initial condition* $u_0(x) = \sin x$. *(a) Solution u as a function of space x and time t The* (x,t) *contour plot of the solution of KSE shows that the solution is attracted to the chaotic orbits. (b) Energy is a function of time t This shows that the energy of the solution as time evolves becomes more oscillatory*

Chapter 3

Feedback Stabilization of Steady Kuramoto-Sivashinsky Equation *KSE*

In this chapter we will discuss the procedure of finding the feedback control for our model system (KSE). We will present an approach known as the *Linear Quadratic Regulator (LQR).*

3.1 Preliminaries of Control theory

Consider the finite dimensional representation of our model problem KSE which is obtained by using spectral method as discussed in Chapter 2. Now with the addition of a control term this system can be more generally written as

$$\dot{\mathbf{X}} = \mathbf{f}(t, \mathbf{X}, \mathbf{u}), \ \ \mathbf{X}(0) = \mathbf{X}_0 \in \mathbb{R}^K, \tag{3.1}$$

where $\mathbf{f} : \mathbb{R} \times \mathbb{R}^K \times \mathbb{R}^L \rightarrow \mathbb{R}^K$, $\mathbf{X} \in \mathbb{R}^K$ is the state variable vector, $\mathbf{X}_0 \in \mathbb{R}^K$ is the initial state, $\mathbf{u} \in \mathbb{R}^L$ is the control vector function, and $t \in \mathbb{R}_+ = \{\tau \in \mathbb{R} : \tau \geq 0\}$ is the time. In control theory, it is common to complement this with an *output* equation, that is, a function

of the state of the system:

$$\mathbf{Y} = \mathbf{h}(t, \mathbf{X}, \mathbf{u})$$

Therefore, a more general nonlinear control system has the form

$$\dot{\mathbf{X}} = \mathbf{f}(t, \mathbf{X}, \mathbf{u}), \quad \mathbf{X}(0) = \mathbf{X}_0 \in \mathbb{R}^K, \tag{3.2a}$$

$$\mathbf{Y} = \mathbf{h}(t, \mathbf{X}, \mathbf{u}) \tag{3.2b}$$

After linearization of the above system about a fixed point we consider the following linear time-invariant system,

$$\dot{\mathbf{X}} = \mathbf{A}\mathbf{X} + \mathbf{B}\mathbf{u}, \quad \mathbf{X}(0) = \mathbf{X}_0 \in \mathbb{R}^K, \tag{3.3a}$$

$$\mathbf{Y} = \mathbf{C}\mathbf{X} + \mathbf{D}\mathbf{u} \tag{3.3b}$$

where $\mathbf{X} \in \mathbb{R}^K$, $\mathbf{Y} \in \mathbb{R}^M$, $\mathbf{u} \in \mathbb{R}^L$, $\mathbf{A} : \mathbb{R}^K \to \mathbb{R}^K$, $\mathbf{B} : \mathbb{R}^L \to \mathbb{R}^K$, $\mathbf{C} : \mathbb{R}^K \to \mathbb{R}^M$, and $\mathbf{D} : \mathbb{R}^L \to \mathbb{R}^M$. In control theory literature, the dimension L of $\mathbf{u}$ is called the *number of inputs*, and the dimension M of $\mathbf{Y}$ is called the *number of outputs.*

But we are interested only in state feedback control of KSE, therefore setting $\mathbf{C} = \mathbb{I}$, and $\mathbf{D} = \mathbf{0}$ we obtain the state feedback equation

$$\dot{\mathbf{X}} = \mathbf{A}\mathbf{X} + \mathbf{B}\mathbf{u}, \quad \mathbf{X}(0) = \mathbf{X}_0 \in \mathbb{R}^K, \tag{3.4}$$

As discussed earlier one distinguishes controls of two types: *open loop* and *closed loop*. An open loop control does not depend on the state of the system, whereas closed loop control does. Formally these two type of controls are defined as follows:

Open loop control: An *open loop control* is defined as an arbitrary function $\mathbf{u} : [0,\infty) \rightarrow \mathbb{R}^L$, for which the equation

$$\dot{\mathbf{X}} = \mathbf{f}(\mathbf{X},\mathbf{u},t), \ t \geq 0, \ \mathbf{X}(0) = \mathbf{X}_0 \in \mathbb{R}^K, \tag{3.5}$$

has a well defined solution. In open loop control $\mathbf{u}$ depends on the initial state and the system parameter if any.

Closed loop control: A *closed loop control*, however, can be identified with a mapping $\mathbf{k} : \mathbb{R}^K \rightarrow \mathbb{R}^L$, which may depend on $t \geq 0$, such that the equation

$$\dot{\mathbf{X}} = \mathbf{f}(\mathbf{X},\mathbf{k}(\mathbf{X}),t), \ t \geq 0, \ \mathbf{X}(0) = \mathbf{X}_0 \in \mathbb{R}^K, \tag{3.6}$$

has a well defined solution. The mapping $\mathbf{k}$ is called *feedback*. In closed loop control $\mathbf{k}$ depends on the current state, or the current output of the system. Controls are called *inputs*, and the corresponding solutions of equation (3.5) or (3.6) are *outputs* of the system.

One of the main aims of control theory is to find a control strategy such that the corresponding output has desired properties. Before this can be done, an appropriate characterization of the system in question is necessary. A system is *controllable* if it is possible to devise a control function $\mathbf{u}$ that will take it from one position in state space to another position in state space in a given time. A state $\mathbf{Z} \in \mathbb{R}^K$ for the system (3.4) is said to be *attainable or reachable* from a state $\mathbf{X}_0$ at time t_f if there exists a control $\mathbf{u}$ and a time $t_f > 0$ such that $\mathbf{X}_{t_f} = \mathbf{Z}$. We sometimes say that $\mathbf{X}_0$ can be steered to state $\mathbf{X}_{t_f}$ at time t_f, or that the control $\mathbf{u}$ transfers state $\mathbf{X}_0$ to state $\mathbf{X}_{t_f}$ at time t_f. In the special case we say that the system (3.4) is *controllable*, or that the pair $(\mathbf{A},\mathbf{B})$ is controllable, if an arbitrary state $\mathbf{X}_{t_f}$ is attainable from any state $\mathbf{X}_0$ at time t_f.

Problems that originate from controllability are those of *optimal control*, a control that is robust to perturbations of the system, and *finite horizon control*, a control reaching a state in minimal time, among other. An equally important issue is that of stabilizability. Assume that for some open loop control $\overline{\mathbf{u}}$ and some state $\mathbf{X}$, $\mathbf{f}(\overline{\mathbf{X}}, \overline{\mathbf{u}}) = 0$. A *stabilizing feedback* is a function $\mathbf{k} : \mathbb{R}^K \to \mathbb{R}^L$, with $\mathbf{k}(\overline{\mathbf{X}}) = \overline{\mathbf{u}}$, that is such that $\overline{\mathbf{X}}$ is a stable equilibrium for the closed loop control system. In many applications, one does not observe the state $\mathbf{X}$ of the system itself but the output $\mathbf{Y}$. In our present study we have considered the output $\mathbf{Y} = \mathbf{X}$. Observation is a dual problem to control. It can be posed as, knowing a control $\mathbf{u}$ and an output $\mathbf{Y}$, is it possible for one to determine the initial condition $\mathbf{X}_0$ uniquely, then the system is *observable*.

Now consider the nonhomogeneous linear differential equation with variable coefficients given below:

$$\dot{\mathbf{X}} = \mathbf{A}(t)\mathbf{X} + \mathbf{B}(t), \quad \mathbf{X}(t_0) = \mathbf{X}_0 \in \mathbb{R}^K, \tag{3.7}$$

Let the fundamental solution of the associated homogeneous equation $\dot{\mathbf{X}}(t) = \mathbf{A}(t)\mathbf{X}$ of (3.7) be $\mathbf{\Phi}_t$, then the matrix $\mathbf{R}(t, t_0)$ is said to be the resolvent set of (3.7) if $\mathbf{R}(t, t_0) = \mathbf{\Phi}_t \mathbf{\Phi}_{t_0}^{-1}$. Then we have the following theorem (J. Arino [18]):

Theorem 1 *If $\mathbf{R}(t, t_0)$ be the resolvent of the associated homogeneous equation $\dot{\mathbf{X}}(t) = \mathbf{A}(t)\mathbf{X}$, then the solution $\mathbf{X}$ to equation* (3.7) *is given by:*

$$\mathbf{X} = \mathbf{R}(t, t_0)\mathbf{X}_0 + \int_0^t \mathbf{R}(t, s)\mathbf{B}(s)ds$$

Denoting $\mathbf{R}(t, 0)$ by $\mathbf{R}(t)$, we define the *controllability matrix* for the system (3.4) as

$$\mathbf{Q}_t = \int_0^t \mathbf{R}(s)\mathbf{B}\mathbf{B}^T\mathbf{R}^T(s)ds$$

where $\mathbf{Q}_t$ is symmetric ($\mathbf{Q}_t^T = \mathbf{Q}_t$) and nonnegative definite (i.e., $\langle \mathbf{Q}_t\mathbf{X}, \mathbf{X}\rangle \geq 0$ for all $\mathbf{X} \in \mathbb{R}^K$ where $\langle .,. \rangle$ denotes the inner product of two vectors). Denote $[\mathbf{A}|\mathbf{B}]$ the matrix $[\mathbf{B}\ \mathbf{AB}\ \ldots\ \mathbf{A}^{K-1}\mathbf{B}]$ of size $K \times KL$ consisting of the columns of matrices $\mathbf{B}\ \mathbf{AB}\ \ldots\ \mathbf{A}^{K-1}\mathbf{B}$ written consecutively. Then we have the following result (J. Arino [18]):

Theorem 2 *The following conditions are equivalent.*

i) An arbitrary state $\mathbf{z} \in \mathbb{R}^K$ is attainable from $\mathbf{0}$.

ii) System (3.4) *is controllable (or that the pair $(\mathbf{A}, \mathbf{B})$ is controllable).*

iii) System (3.4) *is controllable at a given time $t_f > 0$.*

iv) The matrix $\mathbf{Q}_t$ is nonsingular for any $t > 0$.

v) rank $[\mathbf{A}|\mathbf{B}] = K$. (This is called Kalman rank condition, or simply the rank condition.)

vi) The matrix $[\mathbf{A} - \lambda\mathbb{I}\ \ \mathbf{B}]$ has full row rank at every eigenvalue λ of $\mathbf{A}$.

Note that condition (v) is very important. It gives a necessary and sufficient condition for system (3.4) to be controllable that is relatively easy to compute.

3.2 Linear Quadratic Regulator Problem

In this section our aim is to characterize the *Linear Quadratic Regulator Problem (LQR).* We want to find a control function $\mathbf{u}(t)$ defined on $[0, t_f]$, which can be a function of the state $\mathbf{X}$, such that the state $\mathbf{X}$ is driven to a neighborhood of origin at time t_f. This is called the *regulator problem.* An obvious question, however, may appear whether is it possible to construct such a controller for the regulator problem? The answer is positive, if the system (3.4) is completely controllable, i.e., if the control $\mathbf{u}$ drives any nonzero state $\mathbf{X}$ to zero as fast as possible. For practical engineering implementation, an upper bound is set on the magnitude of various variables in the system. One might ask if the state $\mathbf{X}_{t_f}$ is bounded, the control energy for $\mathbf{u}$, or the state $x(t)$ is bounded for any time $t \in [0, t_f]$ over which the

control is being exercised. This suggests that we have to impose certain measure on these variables. These sorts of measure can be defined in several ways; for example they are respectively,

- a measure for the final state $\mathbf{X}(t_f)$:

$$\mathbf{X}_{t_f}^T \mathbf{P}_0 \mathbf{X}_{t_f},$$

  where $\mathbf{P}_0$ is a symmetric positive semidefinite matrix.

- a measure for the magnitude of the control $\mathbf{u}(t)$:

$$\int_0^{t_f} ||\mathbf{u}||dt, \quad \int_0^{t_f} ||\mathbf{u}||^2 dt, \quad \sup_{t\in[0,t_f]} ||\mathbf{u}||;$$

  or, some weighted norm

$$\int_0^{t_f} ||W_{\mathbf{u}}\mathbf{u}||dt, \quad \int_0^{t_f} ||W_{\mathbf{u}}\mathbf{u}||^2 dt, \quad \sup_{t\in[0,t_f]} ||W_{\mathbf{u}}\mathbf{u}||$$

  for some constant weighting matrix $W_{\mathbf{u}}$.

- a measure for the transient state $\mathbf{X}(t)$:

$$\int_0^{t_f} ||W_{\mathbf{X}}\mathbf{X}||dt, \quad \int_0^{t_f} ||W_{\mathbf{X}}\mathbf{X}||^2 dt, \quad \sup_{t\in[0,t_f]} ||W_{\mathbf{X}}\mathbf{X}||$$

  for some weighting matrix $W_{\mathbf{X}}$

Typically we can take $W_1 = \frac{1}{2}\mathbf{X}_{t_f}^T \mathbf{P}_0 \mathbf{X}_{t_f}$ as a measure of the final state, $W_2 = \frac{1}{2}\int_0^{t_f} \mathbf{u}^T \mathbf{R}\mathbf{u}dt$ as a measure for the control $\mathbf{u}(t)$ where $\mathbf{R}$ is a symmetric positive definite matrix, and $W_3 = \frac{1}{2}\int_0^{t_f} \mathbf{X}^T \mathbf{Q}\mathbf{X}dt$ as a measure of the transient response $\mathbf{X}$ for $t \in [0,t_f]$ where $\mathbf{Q}$ is a symmetric positive semidefinite matrix.

Hence the regulator problem can be posed as an optimal control problem with certain combined performance index on $\mathbf{u}$ and $\mathbf{X}$. For our present problem we shall be concerned exclusively with quadratic performance problem. Moreover, we shall focus on the infinite time regulator problem (i.e., $t_f \rightarrow \infty$). In this case, our problem is as follows:

The *LQR* problem: Find a feedback control $\mathbf{u}(t)$ defined on $[0,\infty)$ such that the state $\mathbf{X}$ is driven to the origin as $t \rightarrow \infty$ and the following functional is minimized:

$$\mathcal{J} = W_1(\mathbf{X}(t_f), t_f) + \int_0^{t_f} \mathcal{L}(\mathbf{X}, \mathbf{u}(t), t)dt, \tag{3.8}$$

subject to:

$$\dot{\mathbf{X}} = \mathbf{A}\mathbf{X} + \mathbf{B}\mathbf{u}, \quad \mathbf{X}(0) = \mathbf{X}_0 \tag{3.9}$$

where the function

$$W_1 = \frac{1}{2}\mathbf{X}_{t_f}^T \mathbf{P}_0 \mathbf{X}_{t_f}$$

is the cost associated with the error in the terminal state at time t_f, and the function

$$\mathcal{L} = \frac{1}{2}\left(\mathbf{u}^T\mathbf{R}\mathbf{u} + \mathbf{X}^T\mathbf{Q}\mathbf{X}\right)$$

or (in the form that includes the cross-term $2\mathbf{u}^T\mathbf{S}\mathbf{X}$)

$$\mathcal{L} = \frac{1}{2}\left(\mathbf{u}^T\mathbf{R}\mathbf{u} + \mathbf{X}^T\mathbf{Q}\mathbf{X} + 2\mathbf{u}^T\mathbf{S}\mathbf{X})\right)$$

penalizes for transient state errors and control effort in which $\mathbf{P}_0$ and $\mathbf{Q}$ are symmetric and positive semidefinite, $\mathbf{R}$ is symmetric positive definite, and the dimension of $\mathbf{S}$ is compatible with $\mathbf{Q}$ and $\mathbf{R}$.

This problem is traditionally called a *Linear Quadratic Regulator* problem or, simply, an *LQR* problem, since our aim is to *control* or *regulate* the state vector $\mathbf{X}$ so that it goes to zero without any large control effort as fast as possible. In fact this LQR problem is an *optimal state regulator* problem. In a similar fashion one can formulate an *output regulator problem* for the control problem (3.3). In each case, the purpose of the quadratic form in $\mathbf{u}(t)$ is to ensure, by suitable choice of the elements of $\mathbf{R}$, that in satisfying the objective the control variable $\mathbf{u}(t)$ is not required to be impractically large. Since the terms in equation (3.8) are all quadratic forms, and since equation (3.8) can be thought of as a measure of the way in which the system behaves, $\mathcal{J}$ in equation (3.8) is usually called a *quadratic performance index* or *cost functional*. It should be admitted that the wide spread use of a *quadratic* performance index is due to the relative ease with which it can be handled mathematically and to the fact that it results in *linear* feedback (see [19], [20], and [21]).

3.3 Derivation of the Linear Quadratic Regulator Problem for KSE

Consider values of the parameter α in the time dependent KSE (1.15) for which the solution $u = u(x,t)$ is unstable. As shown before at every integer value of $\sqrt{\alpha/4}$ a cascade of bifurcations occur and the steady state solution changes qualitatively. It was also shown that for small perturbations some steady solutions are stable but others (e.g. $u \equiv 0$) are unstable. Later we will provide some quantitative data about this issue. For stabilizing the unstable solutions let us add some forcing $\phi(x,t)$ to the KSE :

$$\partial_t u + \alpha(\partial_x^2 + u\partial_x u) + 4\partial_x^4 u = \phi, \tag{3.10}$$

where $\phi = \phi(x,t)$. Here we have considered two possible forms of the forcing term

- localized in physical space:

$$\phi_P(x,t) \triangleq \phi(x,t) = \sum_{l=1}^{L} u_l(t)\delta(x-x_l) = \sum_{l\in\Pi_1}^{L} u_l\phi_l \tag{3.11}$$

where $\phi_l = \delta(x-x_l)$ is a Dirac-delta function, and Π_1 is an index set.

- localized in Fourier space

$$\phi_F(k,t) \triangleq \phi(k,t) = \sum_{l=1}^{L} u_l(t)\psi_l(k), \tag{3.12}$$

where

$$\psi_l(k) = \begin{cases} 1 & \text{if l =k and l, k} \in \Pi_l \\ 0 & \text{otherwise} \end{cases}$$

where Π_l is a nonempty index set specifying the Fourier modes that the control actuation u_l is acting on.

Here u with suffix l (i.e. u_l) is different from the solution $u = u(x,t)$ and indicates the l-th control actuator. The ways how the forcing function ϕ_P applied in physical space and ϕ_F applied in Fourier space are illustrated in the following Fig. 3.1 and Fig. 3.2 respectively.

Assuming the above structure of the control and that the perturbation of the stationary solutions are small, we want to derive and implement a feedback control strategy that will stabilize the stationary solutions. If we put

$$u = \tilde{u} + \varepsilon w, \tag{3.13}$$

in (3.10) where $u := \tilde{u}(x)$ is the steady solution that we want to stabilize, and $w := w(x,t)$ is the perturbation, then we obtain upon neglecting terms proportional to ε^2 the following linear perturbation equation

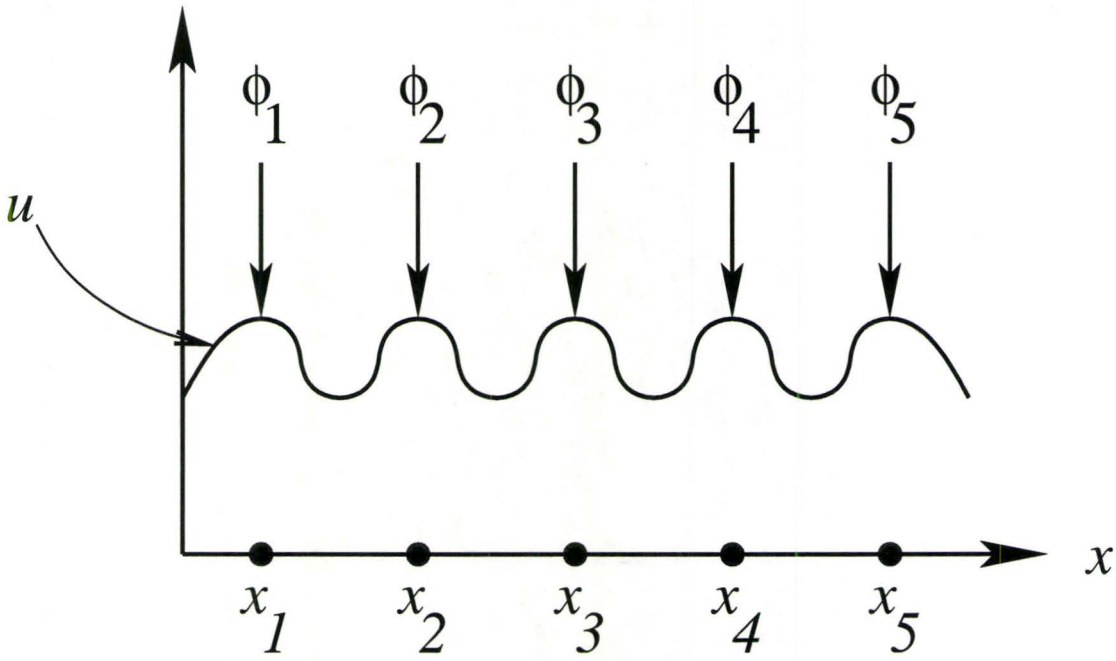

Figure 3.1: *Form of the Control function ϕ_P at some particular time $t = \tau$ implemented in physical space*

$$\begin{aligned} &\partial_t w + \alpha(\partial_x^2 w + \partial_x(\tilde{u}w)) + 4\partial_x^4 w = \phi \\ &w(x,0) = w_0 \end{aligned} \tag{3.14}$$

which describes evolution of perturbations w superimposed on the base state $\tilde{u}$. We search for a *feedback control*

$$\phi = -\mathcal{K}w,$$

where $\mathcal{K}$ is the *feedback* operator that will be determined so as to drive arbitrary perturbations w to zero, thereby stabilizing the state $\tilde{u}$.

Now considering the forcing $\tilde{\phi}_1$ in physical space defined by (3.11) we can write the controlled KSE as:

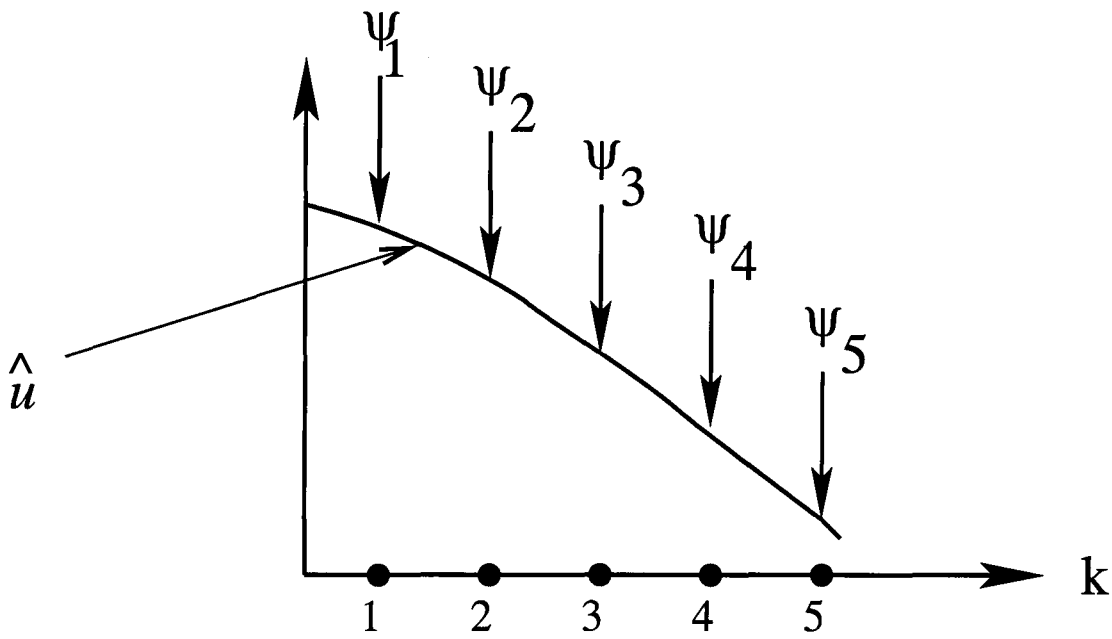

Figure 3.2: *Form of the Control function ϕ_F at some particular time $t = \tau$ implemented in Fourier space*

$$\partial_t w + \alpha(\partial_x^2 w + \partial_x(\tilde{u}w)) + 4\partial_x^4 w = \sum_{l=1}^{L} u_l(t)\phi_l(x) \tag{3.15}$$

subject to the periodic boundary conditions:

$$\partial_x^j w(0,t) = \partial_x^j w(2\pi,t), \;\; t \in [0,T], j = 0,\ldots,3, \tag{3.16}$$

and the initial condition

$$w(x,0) = w_0(x), \;\; x \in [0,2\pi] \tag{3.17}$$

L is the number of manipulated inputs (i.e., variables that can be manipulated externally to modify the dynamics of equation (3.15) in a desired fashion), $u_l(t)$ is the l-th manipulated

input, $\phi_l(x)$ is the actuator distribution function (i.e., $\phi_l(x)$ determines how the control action computed by the l-th control actuator, $u_l(t)$, is distributed in the spatial interval $[0,2\pi]$). We note that in the case of point actuation which influences the system at x_1 (i.e., $\phi_l(x) = \delta(x-x_1)$ where $\delta(.)$ is the standard Dirac function), we approximate the function $\delta(x-x_1)$ by the finite value $1/(2\varepsilon)$ in the interval $[x_1-\varepsilon, x_1+\varepsilon]$ (where $\varepsilon > 0$ is a small real number) and zero elsewhere in $[0,2\pi]$.

Now for spectral discretization let us approximate the solution $w(x,t)$ of the perturbation equation (3.15) by the truncated Fourier series

$$w_N(x,t) = \sum_{k=-N}^{N} \hat{u}_k(t) e^{ikx},$$

the actuator distribution function $\phi_l(x) = \delta(x-x_l)$ defined in (3.11) by the truncated Fourier series

$$\phi_l(x) = \sum_{k=-N}^{N} \hat{b}_k e^{ikx}$$

This truncated series represents a periodic sequence of δ-functions with period 2π. Note that after taking the Fourier transform of the control term in (3.15) with respect to x, we have

$$\mathcal{F}_x\left(\sum_{l=1}^{L} \phi_l(x) u_l(t)\right) = \sum_{l=1}^{L} \mathcal{F}_x(\phi_l(x)) u_l(t)$$

where

$$\mathcal{F}_x(\phi_l(x)) = \hat{b}_k = \frac{1}{2\pi}\int_0^{2\pi} \delta(x-x_l) e^{-ikx} dx = \frac{1}{2\pi} e^{-ikx_l}$$

Using the spectral Galerkin technique as illustrated in section 2.3 together with the substitution $\hat{u}_k = \xi_k + i\eta_k$, $k = 1,2,\ldots,M = N-1$, the above controlled KSE (3.15) yields the following form:

$$\frac{d}{dt}\mathbf{X} = \mathbf{A}\mathbf{X} + \mathbf{B}\mathbf{u}$$
$$\mathbf{X}(0) = \mathbf{X}_0 \tag{3.18}$$

where $\mathbf{X} \in \mathbb{R}^K$, $\mathbf{A} : \mathbb{R}^K \to \mathbb{R}^K$, $\mathbf{B} : \mathbb{R}^L \to \mathbb{R}^K$, and $\mathbf{u} \in \mathbb{R}^L$ with $K = 2M$ such that the state vector $\mathbf{X}$ in Fourier coordinates can be represented as

$$\mathbf{X} = \begin{bmatrix} \xi_1 \\ \xi_2 \\ \vdots \\ \xi_M \\ \eta_1 \\ \eta_2 \\ \vdots \\ \eta_M \end{bmatrix},$$

the system matrix $\mathbf{A}$ is given by

$$\mathbf{A} = -\begin{bmatrix} \frac{\partial \mathbf{F}_k^r}{\partial \xi_q} & \frac{\partial \mathbf{F}_k^r}{\partial \eta_q} \\ \frac{\partial \mathbf{F}_k^i}{\partial \xi_q} & \frac{\partial \mathbf{F}_k^i}{\partial \eta_q} \end{bmatrix} \qquad p,q,k = 1,2,\ldots,M$$

computed at the stationary solution $\tilde{u}$ in Fourier coordinates, the control matrix $\mathbf{B}$ (localized in physical space) is given by

$$\mathbf{B} = \frac{1}{2\pi}\begin{bmatrix} \cos(kx_l) \\ -\sin(kx_l) \end{bmatrix} \qquad k = 1,2,\ldots,M \qquad l = 1,2,\ldots,L$$

with $x_l = 2\pi l/(2N+1)$, and finally the control $u(t)$ is given by

$$\mathbf{u} = \begin{bmatrix} u_1(t) \\ u_2(t) \\ \vdots \\ u_L(t) \end{bmatrix}$$

It is interesting to mention that the straightforward calculation of system matrix **A** for the system (3.18) is difficult due to the presence of the term $\tilde{u}(x)$ in (3.15). However, the system matrix **A** corresponding to the homogeneous system of (3.18) is the same as the Jacobian matrix **J** calculated in (2.44) for the linearized system of (2.41) with a change of sign. Therefore, without any loss of generality we can adopt this Jacobian as our system matrix **A** for (3.18) with a change of sign, provided that **A** is calculated at the stationary solution $\tilde{u}(x)$ while **J** is calculated at every Newton iteration. This greatly simplifies the amount of computations required.

A stabilizing linear *feedback control* $\mathbf{u} = -\mathcal{K}\mathbf{X}$ can be found by solving a *Linear Quadratic Regulator* problem (**LQR**) where $\mathcal{K} : \mathbb{R}^K \to \mathbb{R}^L$. Note that substitution of $\mathbf{u} = -\mathcal{K}\mathbf{X}$ in the system (3.18) gives

$$\dot{\mathbf{X}} = (\mathbf{A} - \mathbf{B}\mathcal{K})\mathbf{X}, \quad \mathbf{X}(0) = \mathbf{X}_0 \tag{3.19}$$

Hence our final *LQR* problem can be read as follows: (see [3], [20], and [21])

The LQR problem for KSE: Find the control $\mathbf{u}(t) = -\mathcal{K}\mathbf{X}$ on $[0, t_f]$ such that the state **X** is driven to the origin as $t \to t_f$ and the following cost functional is minimized:

$$\mathcal{J}(\mathbf{u}) = \frac{1}{2}\mathbf{X}_{t_f}^T \mathbf{P}_0 \mathbf{X}_{t_f} + \frac{1}{2}\int_0^{t_f} \left(\mathbf{X}^T \mathbf{Q}\mathbf{X} + \mathbf{u}^T \mathbf{R}\mathbf{u}\right) dt \tag{3.20}$$

subject to:

$$\dot{\mathbf{X}} = (\mathbf{A} - \mathbf{B}\mathcal{K})\mathbf{X}, \quad \mathbf{X}(0) = \mathbf{X}_0 \tag{3.21}$$

where the term $\frac{1}{2}\mathbf{X}_{t_f}^T \mathbf{P}_0 \mathbf{X}_{t_f}$ is the cost associated with the error in the terminal state at time t_f, the term $\frac{1}{2}\left(\mathbf{X}^T\mathbf{Q}\mathbf{X} + \mathbf{u}^T\mathbf{R}\mathbf{u}\right)$ penalizes for transient state errors and control effort, $\mathbf{P}_0$ is a nonnegative definite matrix, $\mathbf{Q}$ is symmetric nonnegative definite matrix, $\mathbf{R}$ is symmetric positive definite matrix and all are having real constant entries. This is a classical and well understood problem as will be discussed in next section 3.4.

Enforcing the constraints, construct the Lagrangian (i.e., the augmented functional)

$$\begin{aligned} \mathcal{L}(\mathbf{X},\mathbf{u},\boldsymbol{\lambda}) &= \mathcal{J}(\mathbf{u}) + \int_0^{t_f} \boldsymbol{\lambda}^T \left(\dot{\mathbf{X}} - \mathbf{A}\mathbf{X} - \mathbf{B}\mathbf{u}\right) dt \\ &= \frac{1}{2}\mathbf{X}_{t_f}^T \mathbf{P}_0 \mathbf{X}_{t_f} + \int_o^{t_f} \left[\frac{1}{2}\mathbf{X}^T\mathbf{Q}\mathbf{X} + \frac{1}{2}\mathbf{u}^T\mathbf{R}\mathbf{u} + \boldsymbol{\lambda}^T(\dot{\mathbf{X}} - \mathbf{A}\mathbf{X} - \mathbf{B}\mathbf{u})\right] dt, \end{aligned}$$

where $\boldsymbol{\lambda}$ is the Lagrangian multiplier ("adjoint variable"). The optimality conditions which minimizes the cost functional in problem (3.20) are:

$$\begin{cases} \dfrac{\partial \mathcal{L}}{\partial \boldsymbol{\lambda}} = 0 \\ \dfrac{\partial \mathcal{L}}{\partial \mathbf{X}} = 0 \\ \dfrac{\partial \mathcal{L}}{\partial \mathbf{u}} = 0 \end{cases} \tag{3.22}$$

which together imply the following equations

(3.23a) $$\dot{\mathbf{X}} = \mathbf{A}\mathbf{X} + \mathbf{B}\mathbf{u}, \quad \mathbf{X}(0) = \mathbf{X}_0$$

(3.23b) $$-\dot{\boldsymbol{\lambda}} = \mathbf{A}^T\mathbf{X} + \mathbf{Q}\mathbf{X}, \ \boldsymbol{\lambda}(t_f) = \mathbf{P}_0\mathbf{X}_{t_f}$$

(3.23c) $$\mathbf{R}\mathbf{u} = \mathbf{B}^T\boldsymbol{\lambda}$$

Using equation (3.23c) we can express the optimal control as:

$$\mathbf{u} = -\mathbf{R}^{-1}\mathbf{B}^T\boldsymbol{\lambda}$$

Then putting together (3.23a) and (3.23b) we have

(3.24a) $$\frac{d}{dt}\begin{bmatrix}\mathbf{X}\\ \boldsymbol{\lambda}\end{bmatrix} = \begin{bmatrix}\mathbf{A} & -\mathbf{B}\mathbf{R}^{-1}\mathbf{B}^T\\ -\mathbf{Q} & -\mathbf{A}^T\end{bmatrix}\begin{bmatrix}\mathbf{X}\\ \boldsymbol{\lambda}\end{bmatrix}\begin{bmatrix}\mathbf{X}(0)\\ \boldsymbol{\lambda}(t_f)\end{bmatrix} = \begin{bmatrix}\mathbf{X}_0\\ \mathbf{P}_0\mathbf{X}_{t_f}\end{bmatrix}$$

This is a two-point boundary value problem and is very difficult to solve. It can be considerably simplified by expressing the terminal conditions

$$\boldsymbol{\lambda}(t_f) = \mathbf{P}_0\mathbf{X}_{t_f}$$

for the whole time interval $[0, t_f]$, i.e., we obtain the following "ansatz"(i.e. there exists a matrix $\mathbf{P}(t)$ such that)

$$\boldsymbol{\lambda} = \mathbf{P}\mathbf{X}.$$

Thus the control is given as

$$\mathbf{u} = -\mathbf{R}^{-1}\mathbf{B}^T\boldsymbol{\lambda} = -\mathbf{R}^{-1}\mathbf{B}^T\mathbf{P}(t)\mathbf{X} = -\mathcal{K}\mathbf{X}$$

which immediately gives

(3.25) $$\mathcal{K} = \mathbf{R}^{-1}\mathbf{B}^T\mathbf{P}(t)$$

An equation characterizing $\mathbf{P}(t)$ is obtained as follows: Differentiating the equation

$$\boldsymbol{\lambda} = \mathbf{P}(t)\mathbf{X}$$

with respect to time t, we have

$$\begin{aligned} \dot{\mathbf{P}}\mathbf{X} &= \dot{\boldsymbol{\lambda}} - \mathbf{P}\dot{\mathbf{X}} \\ &= -\mathbf{Q}\mathbf{X} - \mathbf{A}^T\boldsymbol{\lambda} - \mathbf{P}(\mathbf{A}\mathbf{X} - \mathbf{B}\mathbf{R}^{-1}\mathbf{B}^T\boldsymbol{\lambda}) \\ &= (-\mathbf{Q} - \mathbf{A}^T\mathbf{P} - \mathbf{P}\mathbf{A} + \mathbf{P}\mathbf{B}\mathbf{R}^{-1}\mathbf{B}^T\mathbf{P})\mathbf{X} \end{aligned} \tag{3.26}$$

which after simplification gives

$$\begin{aligned} \dot{\mathbf{P}} &= -\mathbf{Q} - \mathbf{A}^T\mathbf{P} - \mathbf{P}\mathbf{A} + \mathbf{P}\mathbf{B}\mathbf{R}^{-1}\mathbf{B}^T\mathbf{P} \\ \mathbf{P}(t_f) &= \mathbf{P}_0 \end{aligned} \tag{3.27}$$

Equation (3.27) is called *the matrix differential Riccati equation* for the matrix $\mathbf{P}(t)$. Considering the infinite time horizon ($t_f \to \infty$), we get the following *algebraic Riccati equation*

$$-\mathbf{Q} - \mathbf{A}^T\mathbf{P} - \mathbf{P}\mathbf{A} + \mathbf{P}\mathbf{B}\mathbf{R}^{-1}\mathbf{B}^T\mathbf{P} = 0 \tag{3.28}$$

where now $\mathbf{P}$ is independent of time t. It should be worthwhile to mention that in this setting $\mathbf{X}_{t_f}^T\mathbf{P}_0\mathbf{X}_{t_f}$ is irrelevant. Since all of $\mathbf{A}$, $\mathbf{B}$, $\mathbf{Q}$, and $\mathbf{R}$ are real constant matrices, therefore the solution $\mathbf{P}$ of equation (3.28) is constant as well and hence from (3.25) we obtain a constant feedback operator $\mathcal{K}$.

3.4 Solutions of the Riccati Equation

The well-known scalar Riccati equation is given by

$$\dot{w} = ew^2 + fw + g,$$

where e, f, and g are scalar functions of t. Analogously, the matrix Riccati equation is defined as:

$$\dot{\mathbf{W}}(t) = \mathbf{W}(t)\mathbf{E}(t)\mathbf{W}(t) + \mathbf{D}(t)\mathbf{W}(t) + \mathbf{W}(t)\mathbf{F}(t) + \mathbf{G}(t), \tag{3.29}$$

where $\mathbf{D}(t)$, $\mathbf{E}(t)$, $\mathbf{F}(t)$, and $\mathbf{G}(t)$ are given $n \times n$ matrices the elements of which are real continuous functions of the real variable t on some interval $[t_0, t_f]$.

It is well known (see E. D. Sontag [3] and S. Barnett [20]) that the solution to the problem described by (3.8) and (3.9) (assuming $\mathbf{S}(t) = 0$, for simplicity) is given by the linear feedback control

$$\mathbf{u} = -R^{-1}(t)\mathbf{B}^T(t)\mathbf{P}(t)\mathbf{X}, \tag{3.30}$$

where $\mathbf{P}(t)$ is the symmetric matrix which satisfies

$$\dot{\mathbf{P}}(t) = \mathbf{P}(t)\mathbf{B}(t)\mathbf{R}^{-1}(t)\mathbf{P}(t) - \mathbf{A}^T(t)\mathbf{P}(t) - \mathbf{P}(t)\mathbf{A}(t) - \mathbf{Q}(t) \tag{3.31}$$

subject to $\mathbf{P}(t_f) = \mathbf{P}_0$. Clearly equation (3.31) is a special case of equation (3.29) and represents $\frac{1}{2}n(n+1)$ scalar equations for the $\frac{1}{2}n(n+1)$ unknown entries of $\mathbf{P}(t)$. Notice that even if $\mathbf{A}$, $\mathbf{B}$, $\mathbf{Q}$ and $\mathbf{R}$ are all independent of t, the matrix $\mathbf{P}$ will still be a function of time, so that the optimal control (3.30), although linear in $\mathbf{X}$, will be time-varying. The unique solution of the nonhomogeneous equation (3.31) is given by the following theorem (see S. Barnett [20]):

Theorem 3 *There exists a unique symmetric solution $\Pi(t)$, defined for $t \in [0, t_f]$, satisfying equation* (3.31) *subject to $\Pi(t_f) = \mathbf{P}_0$. Further, the minimum value of* (3.8) *is $\frac{1}{2}\mathbf{X}_0^T\Pi(0)\mathbf{X}_0$.*

Riccati algebraic equations

Riccati algebraic equations for the LQR problem (3.8)- (3.9) are obtained by considering $t_f \to \infty$. In this case the term W_1 in (3.8) is irrelevant, since our aim is to make $\mathbf{X}$ approach zero as $t \to \infty$, it no longer makes sense to include a terminal expression in the performance index, so we simply set $\mathbf{P}_0 = 0$ in (3.8) to get rid of the W_1 term and hence we obtain the following important result (see S. Barnett [20]):

Theorem 4 *If* (3.9) *is controllable and* $\mathbf{P}_0 = \mathbf{0}$, *then in Theorem 3* $\lim_{t_f \to \infty} \Pi(t, t_f) = \hat{\mathbf{P}}(t)$ *exists for all t and is a solution of the Riccati equation* (3.31).

Now if we consider the matrices in equations (3.8) and (3.9) to be real and constant (i.e., independent of t), so that the optimization problem becomes (letting $\mathbf{S} = 0$) the following:

LQR problem: Choose $\mathbf{u}$ so as to minimize

$$\mathcal{J} = \frac{1}{2}\int_0^\infty \left(\mathbf{X}^T\mathbf{Q}\mathbf{X} + \mathbf{u}^T\mathbf{R}\mathbf{u}\right)dt, \tag{3.32}$$

subject to:

$$\dot{\mathbf{X}} = \mathbf{A}\mathbf{X} + \mathbf{B}\mathbf{u}, \quad \mathbf{X}(0) = \mathbf{X}_0. \tag{3.33}$$

Since $\mathbf{Q}$ and $\mathbf{R}$ are symmetric positive definite constant matrices, so the limiting matrix $\hat{\mathbf{P}}(t)$ in Theorem 4 is constant. Therefore, we obtain the following theorem (see S. Barnett [20]):

Theorem 5 *The solution to the problem* (3.32) *and* (3.33) *is given by*

$$\mathbf{u} = -\mathbf{R}^{-1}\mathbf{B}^T\mathbf{P}\mathbf{X}, \tag{3.34}$$

where, if the pair $[\mathbf{A}, \mathbf{B}]$ *is controllable, the constant symmetric matrix* $\mathbf{P}$ *is the unique positive definite solution of the algebraic matrix Riccati equation*

$$\mathbf{P}\mathbf{B}\mathbf{R}^{-1}\mathbf{P} - \mathbf{A}^T\mathbf{P} - \mathbf{P}\mathbf{A} - \mathbf{Q} = 0, \tag{3.35}$$

and the minimum value of (3.32) *is* $\frac{1}{2}\mathbf{X}_0^T\mathbf{P}\mathbf{X}_0$.

Since the solution **P** of (3.35) is the limiting solution of the corresponding differential equation, so (3.35) is sometimes called as the *"steady state"* Riccati equation. Now for ensuring that the solution to (3.35) is positive definite, and hence unique, we need to impose the controllability criterion. The resulting optimal system when (3.34) is applied to (3.33) is

$$\dot{\mathbf{X}} = \left(\mathbf{A} - \mathbf{B}\mathbf{R}^{-1}\mathbf{B}^T\mathbf{P}\right)\mathbf{X}, \tag{3.36}$$

and therefore we have following very useful result:

Theorem 6 *The closed loop system* (3.36)*, where* **P** *is given by Theorem 5, is asymptotically stable.*

Therefore, we have observed that the equation (3.35) is the same as (3.28) which we want to solve for **P** in order to compute the optimal control **u**. However, we have established the existence and uniqueness of the solution of (3.35) and hence of (3.28). We can solve the quadratic equation (3.28) using linear matrix algebra (the more detailed discussion can be found in [20]).

3.5 Computational results of unsteady KSE obtained applying control technique

In this chapter we have developed control strategies for stabilizing the unstable solutions of KSE using the standard linear control theory. In section 2.5 we have presented results for steady state KSE and in section 2.6 we have presented some results for unsteady KSE. There we have noticed that some steady state solutions of KSE are unstable and bifurcate to more complicated regimes. Since these steady laminar solutions are in many cases more

interesting, therefore we want to stabilize them by applying the control tools developed earlier. Here we have produced the results using control forces applied in physical space. The control forces are applied at points uniformly distributed over the one dimensional periodic domain $\Omega = [0, 2\pi]$. We have found that if a steady state is stable for some α then it remains stable for all time whether we apply the control technique or not. However when a steady state is unstable we need to apply controls in order to stabilize it. There are many control laws for application of control as discussed in Chapter 1 but we have considered only linear state feedback law due to its simplicity. For calculation of control we have solved a linear quadratic regulator problem (LQR). In order to compute feedback operator we have solved a matrix differential Riccati equation in infinite time horizon as discussed in section 3.3.

In this section we want to present the feedback control results for the selected values of $\alpha = 14$, $\alpha = 37.75$, and $\alpha = 72$ where the steady states of KSE are unstable as presented in Fig. 2.4. At $\alpha = 14$ we have seen from Fig. 2.9 that the unsteady solution get attracted to a periodic orbit and therefore 1-cell steady state becomes unstable. For stabilizing this unstable solution we obtain the feedback gain, $\mathcal{K}$, using only one actuator placed localized at a point x_0 in the physical space. It was observed in our calculation that one actuator is sufficient for stabilizing this unstable 1-cell steady state.

In order to investigate how the control acts in time, we have studied cases when control is switched on at different time levels when we were integrating the unsteady KSE in time. For $\alpha = 14$ we have applied the control forcing at time $t \geq 5$, and $t \geq 10$. For the sake of comparison we have presented the control results together with uncontrolled results. We have portrayed the contour plot of uncontrolled KSE system with an initial condition $u_0(x) = \sin x$ in Fig. 2.9. This again displayed in Fig. 3.3(a). The contour plot of controlled

unsteady KSE at time $t = 5$ is displayed in Fig. 3.3(b). The initial condition for controlled unsteady KSE is taken as a 1-cell steady state solution of KSE. From Fig. 3.3(a) we see that the instabilities of the unsteady solution are developing mildly from time $t = 0$ and then become worse after time $t = 5$.

After applying the control to the unsteady KSE system we expect that the control force will act against the development of instabilities of the unsteady solution. This would reduce the perturbation $w(x,t)$ as defined via equation (3.13) to zero and thereby stabilize the system to the steady state $\tilde{u}(x)$. At the same time we also expect that it will take less control effort if we apply the control authority when the instabilities are not so strong. These results are reflected in following figures. From Fig. 3.3 we observe that the instabilities grow severely after time $t = 5$. Therefore it will take less control effort if we apply the control forcing at $t = 5$. For comparing the results we have provided uncontrolled solution of KSE in Fig. 3.3(a) and controlled solution of KSE in Fig. 3.3(b).

The energy of the solution of uncontrolled and controlled KSE are plotted as function of time t in Fig. 3.4. From Fig. 3.4(a) it is noticed that apart from some oscillations at the beginning the energy remains constant for some time but later it is increasing with time and hence instabilities result. But from Fig. 3.4(b) we see that energy is is increasing before applying the control at time $t = 5$ but diminishing with time after control forcing is taken into action at time $t = 5$. The figures Fig. 3.5(a) and Fig. 3.5(b) account for the behavior of control forcing c_f (defined in section 3.3) and perturbation energy E_p (defined as $E_p := ||u(x,t) - \tilde{u}(x)||_{L_2}$ where $u(x,t)$ and $\tilde{u}(x)$ are unsteady and steady solutions of KSE respectively) with time after applying the control forcing. These two phenomena behave quite in the same manner as we expected. Fig. 3.5(a) shows that we need more control efforts at the beginning of the application of control forcing to tackle the instabilities but

less control efforts for later time. Fig. 3.5(b) shows that the perturbation energy E_p is diminishing with time t and hence the solution of KSE system is tending towards its steady states.

Similar interpretation of the results drawn in Fig. 3.6-Fig. 3.8 of controlled KSE hold for when we apply the control forcing at time $t = 10$. The only exception in this case is that there is change of phase shift in the stabilized steady states as visible if we compare Fig. 3.3(b) and Fig. 3.6(b). However to check that the stabilized steady states is indeed a 1-cell steady state we have calculated the energy of perturbation solution $w(x,t)$ in Fig. 3.8(b) which shows that E_p is diminishing to zero after time $t = 10$ where control forcing is applied. This shows the same results as we obtained for control forcing applied at time $t = 5$.

Now we would like to present some more interesting results when $\alpha = 37.75$. For this value of α two nontrivial steady states, namely 2-cell and 3-cell steady states, exist but are unstable. These solutions have been sketched in Fig. 2.6(b). The unsteady solution of KSE for $\alpha = 37.75$ is attracted to oscillatory orbits and was presented in Fig. 2.10. Note that 2-cell steady state was obtained using the initial guess $u^0(x) = 3\sin x$ and 3-cell steady state was obtained using the initial guess $u^0(x) = 5\sin 2x$. We have computationally observed that stabilization of a 2-cell steady states requires only one actuator placed at a point in the physical space for $\alpha = 37.75$. However this is not the case for stabilizing a 3-cell steady state for the same value of α. In this case we have noticed that this requires two actuators placed at points uniformly distributed over the domain in the physical space. Stabilization results for unstable 2-cell steady state are presented in Fig. 3.9-Fig. 3.11 and unstable 3-cell steady states are presented in Fig. 3.12- Fig. 3.14

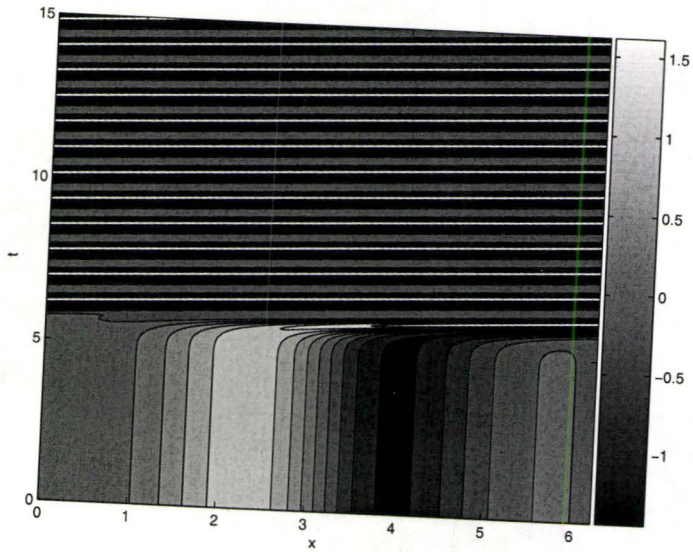

(a)

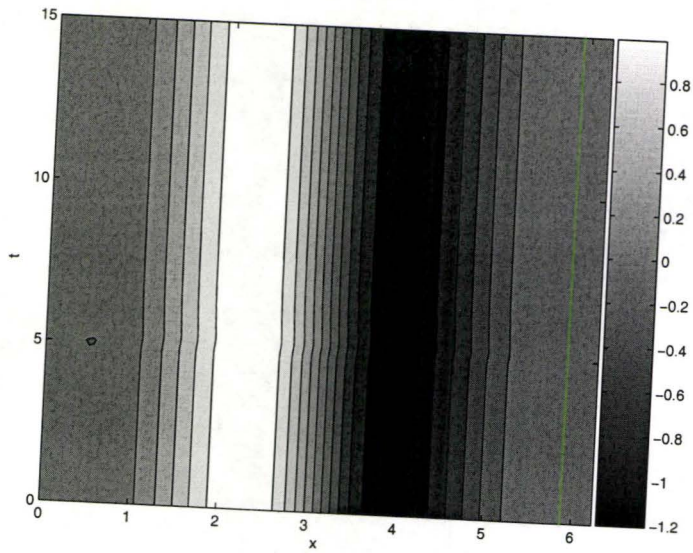

(b)

Figure 3.3: *Unsteady solution of KSE at* $\alpha = 14$ *with initial condition taken as a 1-cell steady state solution of KSE at the same value of* α *after the control forcing applied at* $t \geq 5$. *(a) Uncontrolled* (x,t) *contour plot. (b) Controlled* (x,t) *contour plot.*

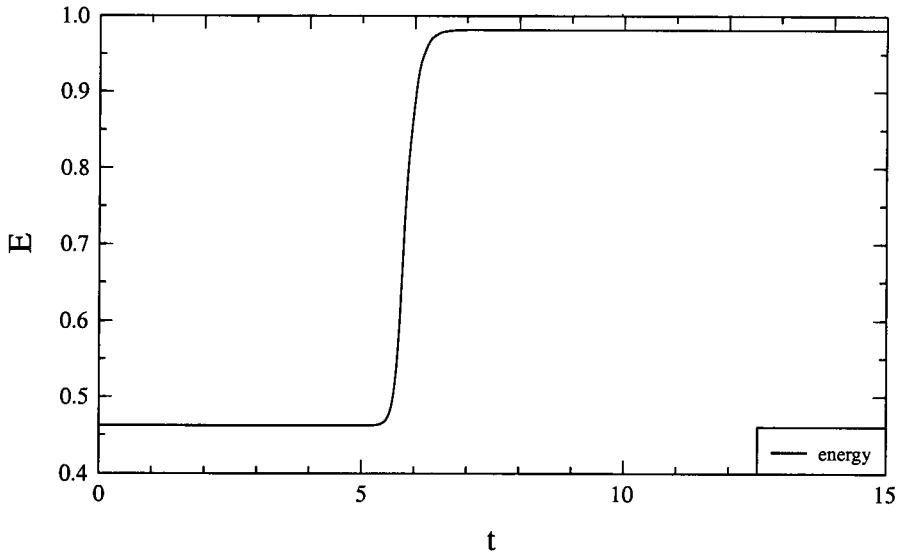

(a)

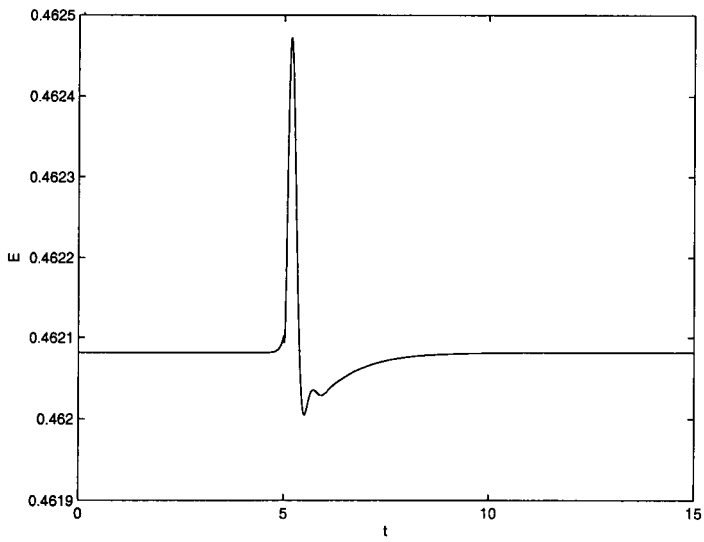

(b)

Figure 3.4: *Energy E as a function of time t for unsteady solution of KSE at* $\alpha = 14$ *with initial condition taken as a 1-cell steady state solution of KSE at the same value of* α *after the control forcing applied at* $t \geq 5$. *(a) Energy for uncontrolled KSE. This shows that the instabilities are developing as time evolves. (b) Energy for controlled KSE. This shows that after execution of control forcing the energy of the system is reducing and therefore no instabilities develop further.*

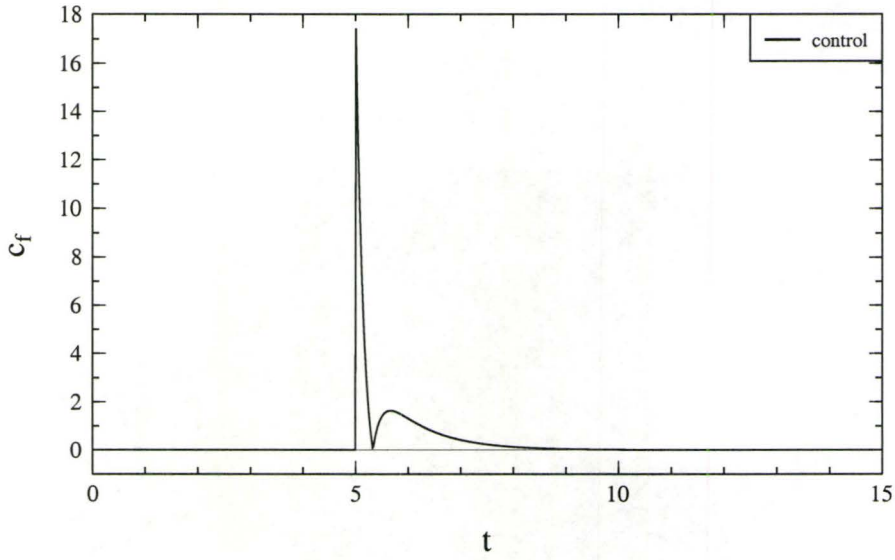

(a)

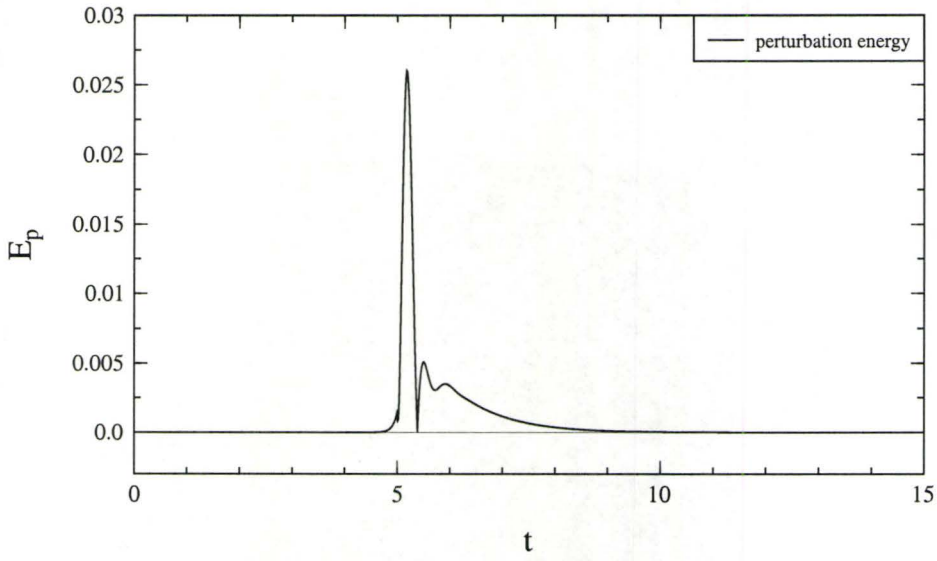

(b)

Figure 3.5: *Unsteady solution of KSE at* $\alpha = 14$ *with initial condition taken as a 1-cell steady state solution of KSE at the same value of* α *after the control forcing applied at* $t \geq 5$. *(a) Control forcing* c_f *as a function of time t. This shows that initially we need more control efforts for stabilization. (b) Energy* E_p *of the perturbation solution of KSE as a function of time t. This indicates that the perturbation energy is decreasing with time soon after the control forcing is applied at time* $t = 5$.

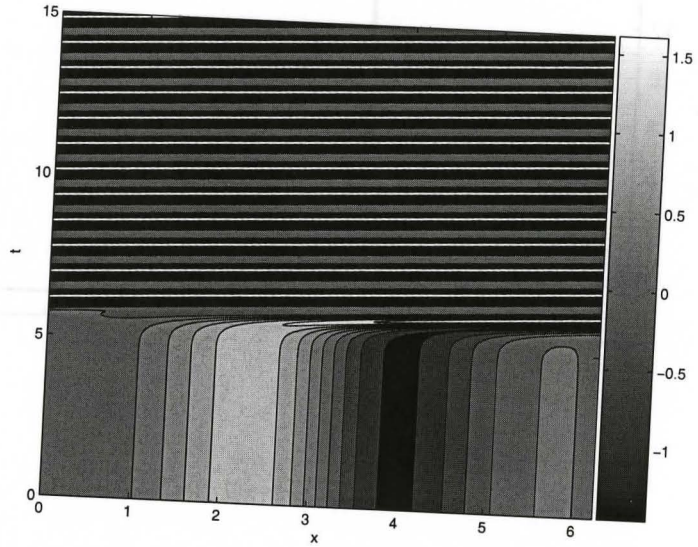

(a)

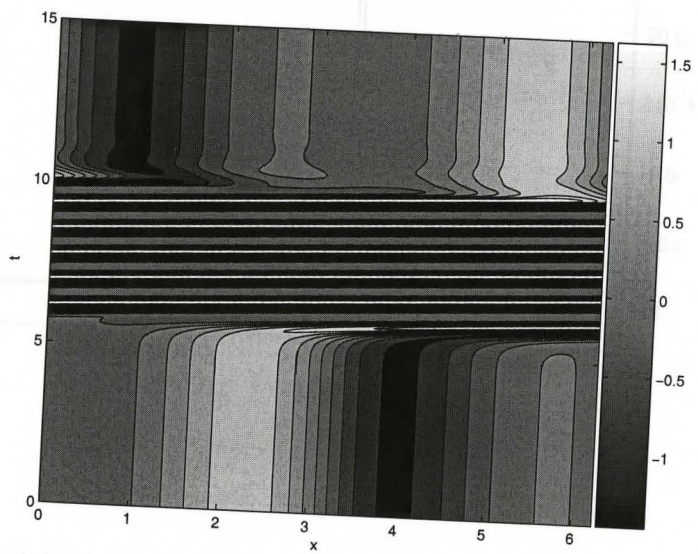

(b)

Figure 3.6: *Unsteady solution of KSE at* $\alpha = 14$ *with initial condition taken as a 1-cell steady state solution of KSE at the same value of* α *after the control forcing applied at* $t \geq 10$. *(a) Uncontrolled* (x,t) *contour plot. (b) Controlled* (x,t) *contour plot.*

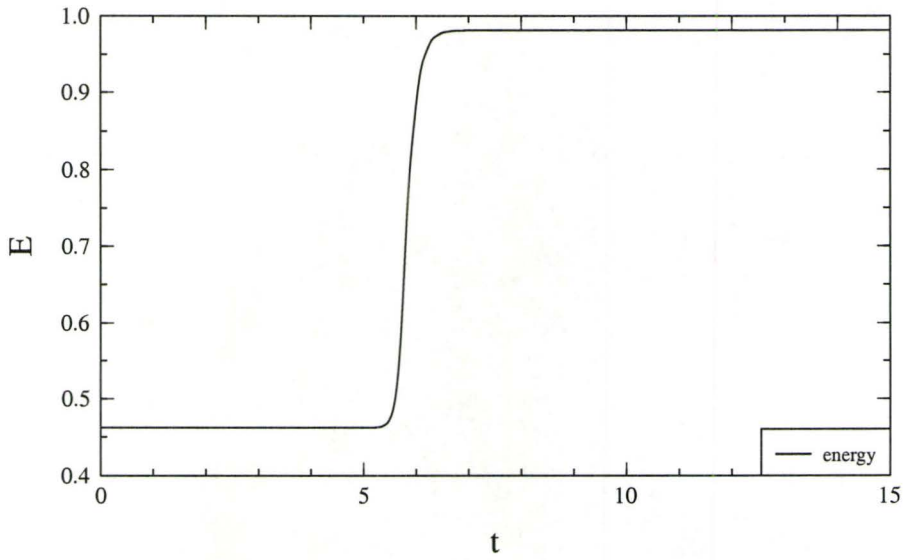

(a)

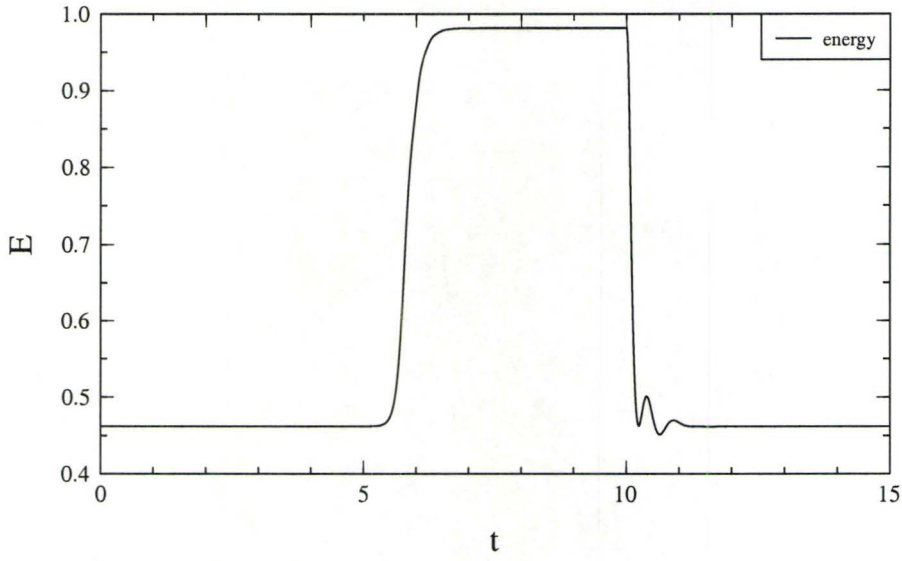

(b)

Figure 3.7: *Energy E as a function of time t for unsteady solution of KSE at* $\alpha = 14$ *with initial condition taken as a 1-cell steady state solution of KSE at the same value of* α *after the control forcing applied at* $t \geq 10$. *(a) Energy for uncontrolled KSE. This shows that the instabilities are developing as time evolves. (b) Energy for controlled KSE. This shows that the instabilities are developing until the control is applied at time* $t \geq 10$. *When the control is applied at time* $t \geq 10$ *the energy of the control is reducing to the energy of steady state and thereby stabilizing the system. Henceforth no instabilities develop further.*

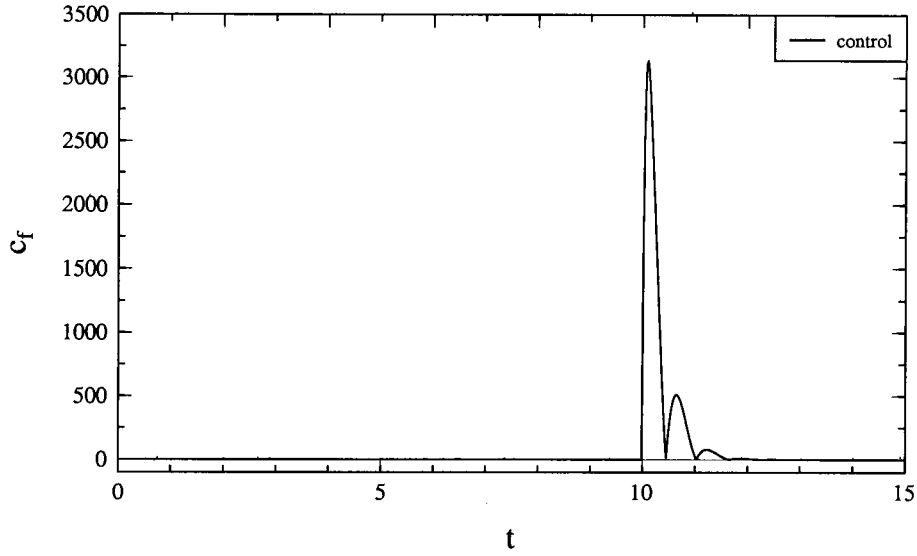

(a)

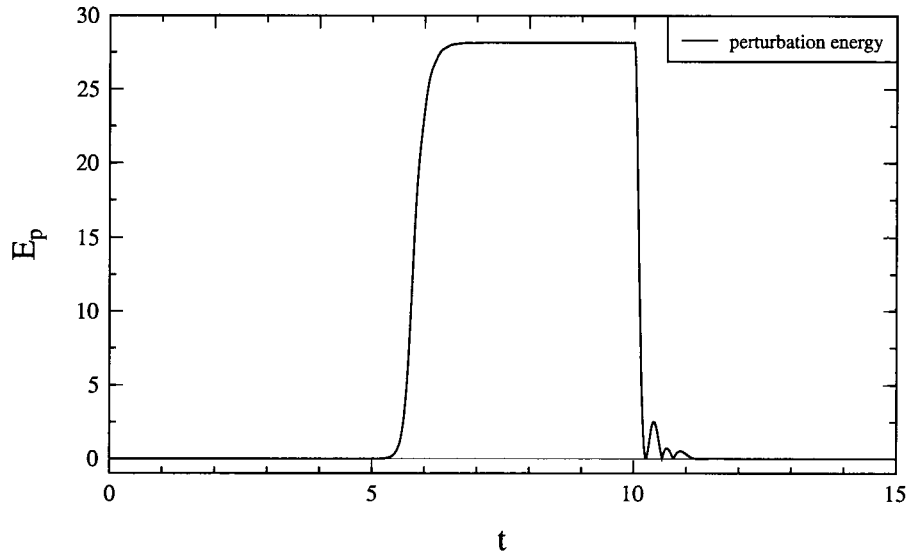

(b)

Figure 3.8: *Unsteady solution of KSE at* $\alpha = 14$ *with initial condition taken as a 1-cell steady state solution of KSE at the same value of* α *after the control forcing applied at* $t \geq 10$. *(a) Control forcing* c_f *as a function of time t. This shows that initially we need more control efforts for stabilization. (b) Energy* E_p *of the perturbation solution of KSE as a function of time t. This indicates that the perturbation energy is decreasing with time soon after the control forcing is applied at time* $t = 10$.

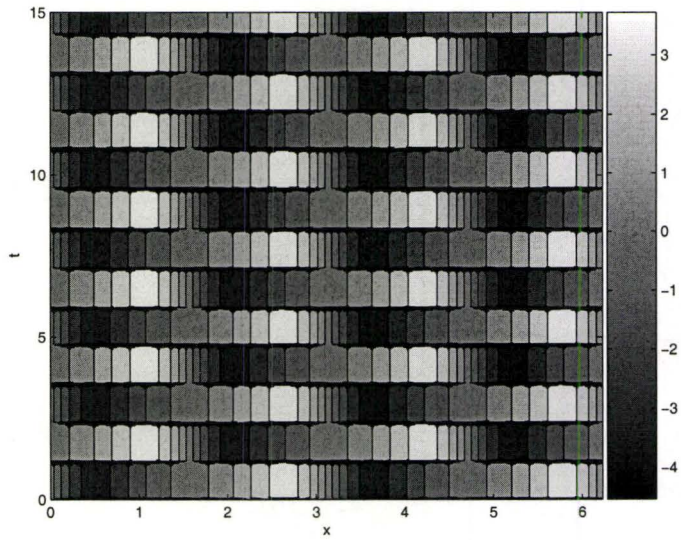

(a)

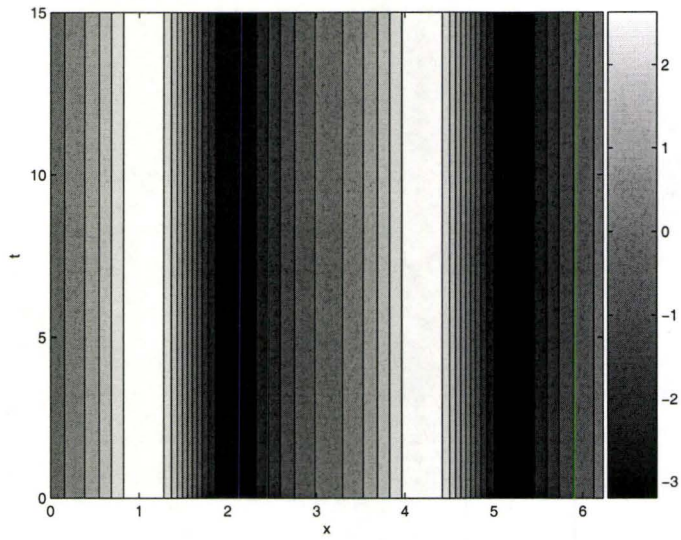

(b)

Figure 3.9: *Unsteady solution of KSE at* $\alpha = 37.75$. *(a) Uncontrolled* (x,t) *contour plot with initial condition is* $u_0(x) = \sin x$. *(b) Controlled* (x,t) *contour plot with initial condition taken as a 2-cell steady state solution of KSE at the same value of* α

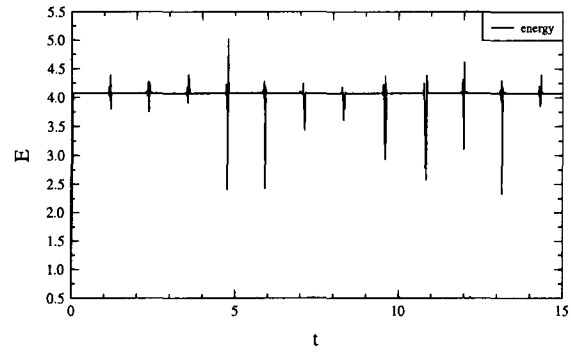

(a)

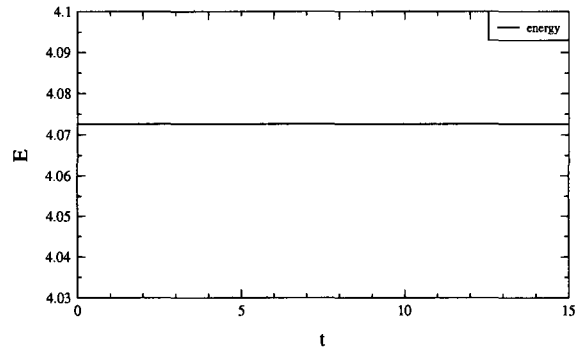

(b)

Figure 3.10: *Energy for unsteady solution of KSE at* $\alpha = 37.75$ *(a) Uncontrolled energy shows periodic bursts with initial condition is* $u_0(x) = \sin x$. *(b) Controlled energy without any periodic bursts with initial condition taken as a 2-cell steady state solution of KSE at the same value of* α. *This shows that the energy is reduced to that of the initial 1-cell steady state solution for all time.*

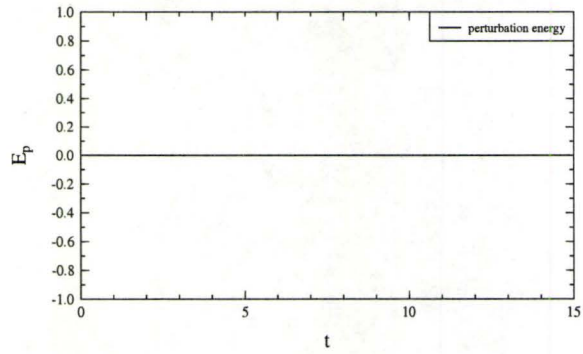

(a)

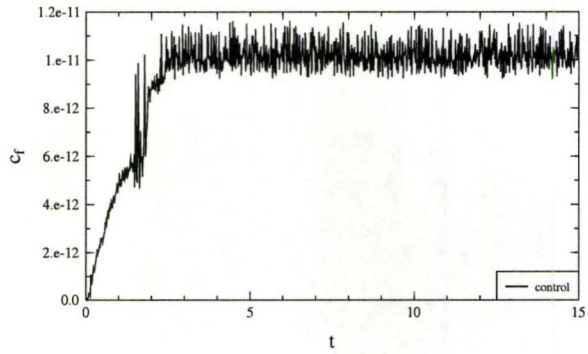

(b)

Figure 3.11: *For controlled unsteady solution of KSE at* $\alpha = 37.75$ *with initial condition taken as a 2-cell steady state solution of KSE at the same value of* α. *(a) Energy of perturbation solution . It shows that perturbation energy is reduced with time and hence drives the system to the steady state regime. (b) Control force responsible for stabilization is oscillating with time but with magnitude close to zero.*

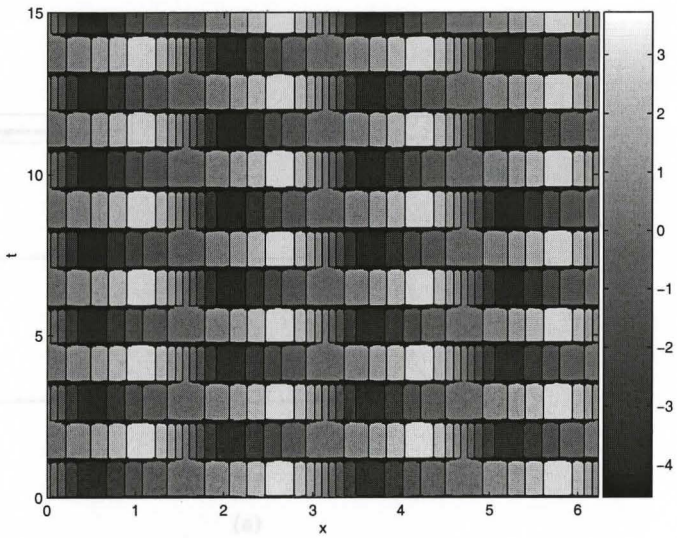

(a)

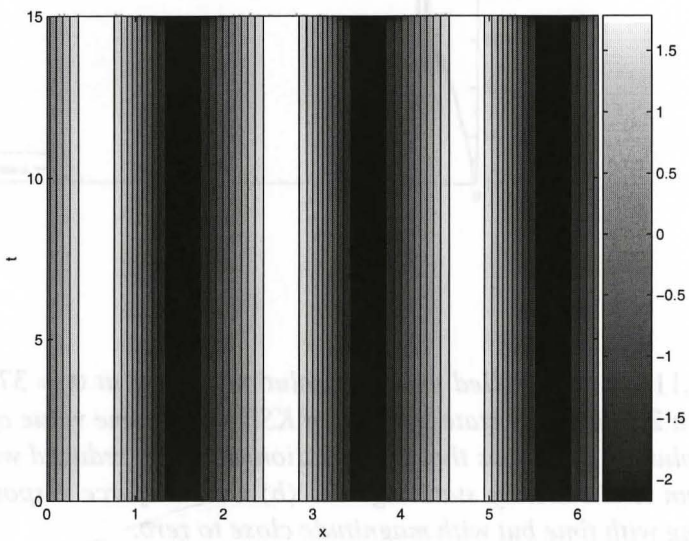

(b)

Figure 3.12. *Unsteady solution of KSE at* $\alpha = 37\ 75$. *(a) Uncontrolled* (x,t) *contour plot obtained with initial condition* $u_0(x) = \sin x$. *(b) Controlled* (x,t) *contour plot obtained with initial condition taken as a 3-cell steady state solution of KSE at the same value of* α.

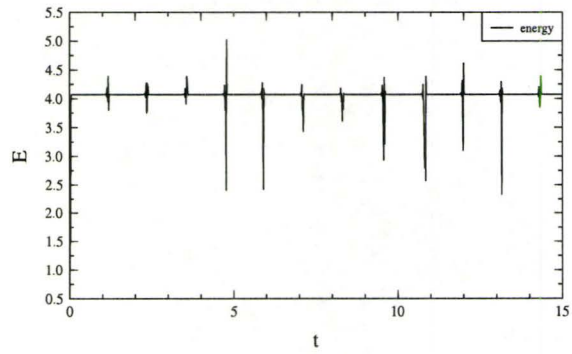

(a)

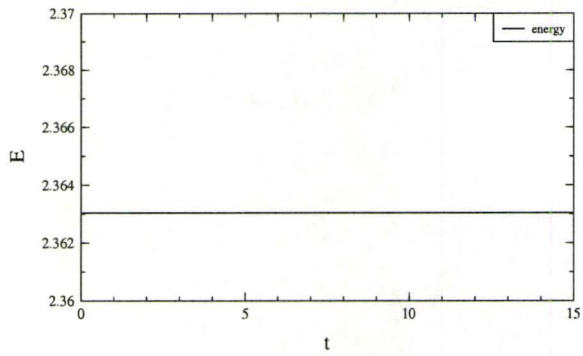

(b)

Figure 3.13: *Energy for unsteady solution of KSE at* $\alpha = 37.75$. *(a) Uncontrolled energy obtained for solution of KSE with initial condition* $u_0(x) = \sin x$. *This shows there are periodic bursts in the energy. (b) Controlled energy obtained for the solution of KSE with initial condition taken as a 3-cell steady state solution of KSE at the same value of* α. *This shows that there is no chaotic bursts observed in the energy of the controlled system.*

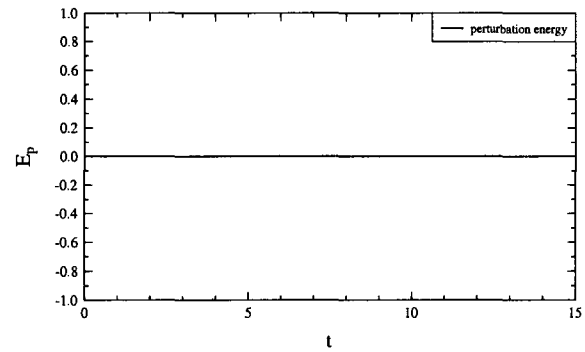

(a)

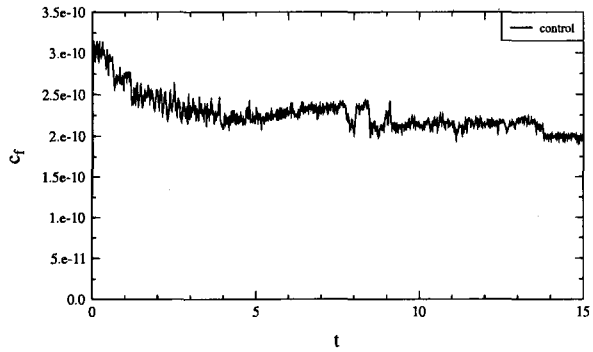

(b)

Figure 3.14: *For controlled unsteady solution of KSE at* $\alpha = 37.75$ *with initial condition taken as a 3-cell steady state solution of KSE at the same value of* α. *(a) Energy of perturbation solution. It shows that perturbation energy is reduced with time and hence drives the system to the steady state regime. (b) Control force responsible for stabilization is oscillating with time but its magnitude approaches to zero with time.*

Chapter 4

Conclusions

4.1 Discussion

In this dissertation we have presented the necessary mathematical basis for an extensive study of Kuramoto-Sivashinsky Equation (KSE). Our main achievements in this work can be arranged as follows:

- Development of efficient numerical method for the study of steady, unsteady, and controlled KSE. The three problems, including the control problem, were solved in Fourier space.

- Numerical study of the bifurcations of steady KSE, and presence of cells and their stabilizing confirm results for the literatures. These give a validation of our approaches.

- Algorithm for efficient stabilization of unstable steady solutions of KSE. Even though the control we have applied is linear, it also works for significant magnitudes of the perturbation. This confirms robustness of the approaches.

4.2 Future Directions

While working with this problem we have not resolved some of the important issues. For the moment we have left them as open problems. They can be studied for further understanding of the dynamics of KSE. Resolving these problems may provide some new directions of work concerning KSE. The new problems can be presented below:

- loss of controllability for increasing values of the parameter α of KSE
- need for a larger number of actuators for stabilizations
- numerical analysis of the convergence of the feedback kernels as the resolution is refined
- investigation of the forcing term localized in Fourier space, and
- properties of the linear feedback operator

Bibliography

[1] A. Armaou, P. D. Christofides, "Feedback control of the Kuramot-Sivashinsky equation", *Physica D*, (137), 49-61, (2000)

[2] P. D. Christofides, A. Armaou, "Global stabilization of the Kuramot-Sivashinsky equation via distributed output feedback" *control, System & Control Letters*, (39), 283-294, (2000).

[3] E. D. Sontag, "Mathematical Control Theory", *Springer-Verlag, New York*, (1990).

[4] W. L. Brogan, "Modern Control Theory", *Prentice-Hall*, Englewood Cliffs, New Jersy, (1991).

[5] K. T. Lee, "Lectures on Dynamical Systems, Structural Stability and their Applications", *World Scientific Publishing Co. Pte. Ltd.*, (1992).

[6] M. M. Denn, "Optimization by Variational Methods", *McGraw-Hill Book Company*, (1969).

[7] Ganti Prasada Rao, "Elements of control systems" International Centre for Water and Energy Systems, PO Box 2623, Abu Dhabi, UAE

[8] J. L. Lions, "Optimal control of systems governed by partial differential equations" *Springer-Verlag, New York*, (1971).

[9] E. Zuazua, "Propagation, Observation, and Control of Waves Approximated by Finite Difference Methods" *SIAM Review*, Vol.47, No.2, pp.197-243

[10] E. Lauga, & T. R. Bewley, "The decay of stabilizability with Reynolds number in a linear model of spatially developing flows", *The Proc. R. Soc. Lond.*, A (2003) 459, 2077-2095

[11] J. M. Hyman and B. Nicolaenko, "The Kuramoto-Sivashinsky Equation: A bridge between pde's and dynamical systems", *Physica* 18D, 113-126, (1986).

[12] J. M. Greene and J. S. Kim, "The steady states of the Kuramoto-Sivashinsky equation", *Physica D*, (33), 99-120, (1988).

[13] I. G. Kevrekidis, B. Nicolaenko, & J. C. Scovel, "Back in the saddle again: A computer assisted study of the Kuramoto-Sivashinsky equation", *SIAM J. APPL. MATH. Vol. 50*, (3), 760-790, (1990).

[14] B. Protas, T. Bewley, & G. Hagen, "A computational frame work for the regularization of adjoint analysis in multiscale systems", *J. of Comp. Phy.*, 195(1), 49-89, (2004).

[15] R. Peyret, "Spectral Methods for Incompressible Viscous Flow", *Springer-Verlag, New York*, (2002)

[16] R. Temam, " Infinite-dimensional Dynamical Systems in Mechanics and Physics", *Springer-Verlag, New York*, (1997)

[17] S. Wiggins, "Global bifurcations and chaos : analytical methods" *Springer-Verlag,New York*, (1988).

[18] J. Arino, "Lecture notes for Dynamical Systems", McMaster University, Canada.

[19] K. Zhou, & J. C. Doyle, " Essentials of Robust Control", *Prentice-Hall, Inc.*, (1998)

[20] S. Barnett, " Matrices in Control Theory with application to linear programming" *Van Nostrand Reinhold Company, London*, Great Britain, (1971)

[21] B. D. O. Anderson, & J. B. Moore, " Linear Optimal Control", *Prentice-Hall*, Englewood Cliffs, New Jersy, (1971).